A structural analysis of the Orielton anticline Pembrokeshire

Hancock, P. L.

A STRUCTURAL ANALYSIS OF THE ORIELTON ANTICLINE, PEMBROKESHIRE

P.L.Hancock, B.Sc. (Dunelm), F.G.S.

A thesis presented for the degree of Doctor of Philosophy in the University of Durham

1963

University College,

Durham.

Frontispiece

Abstract

A structural analysis of the Orielton anticline, Pembrokeshire.

The results of a detailed investigation into the relationships between folds, faults and joints in the Orielton anticline are presented. The study continues the early structural work of Dixon (1921) and the stress analysis of the area made by Anderson (1951).

The Orielton anticline is a compound and faulted Armorican fold largely affecting Upper Palaeozoic rocks. The structural pattern of the anticline developed during two major deformation phases: the first essentially corresponding to a period of folding and thrusting, the second to a period of wrench faulting.

Within each phase, which is divisible, faulting occurred before jointing with joint sets not necessarily lying parallel to equivalent faults. The attitudes of both faults and joints depend on fold geometries. Faults are oriented relative to fold axial planes and axes, whilst joint attitudes are largely controlled by bedding dip and the plunge of the bedding - fracture cleavage intersection. It is tentatively suggested that the dependence of fracture attitudes upon fold geometries is due to the operation of residual stress systems.

The dihedral angle between complementary shear planes has been investigated and shown to be consistently low, usually less than 50°. Regional tension joints appear to be absent.

Joint orientations in collapsed blocks of Carboniferous Limestone enclosed in Triassic breccias show that all phases of the deformation belong to the Armorican orogeny.

Acknowledgments

This research topic arose out of a casual visit to South Pembrokeshire made in the summer of 1958 when I was attracted by the striking and superficially simple structural pattern. Since then many people have encouraged me to inquire more deeply into that structural pattern. In particular I should like to thank Professor K. C. Dunham for allowing me to pursue the topic in his department, and especially for him giving me the opportunity to talk about my work at the British Association (1961) meeting in Norwich.

To Dr. Martin Bott, my supervisor, I owe a very great debt of thanks, especially for his patience when explaining to me the importance of previous experimental and theoretical studies.

For the use of a computer programme I should like to thank Dr. R. Girdler, and for help in operating the programme I must thank the staff of the Kings College computing laboratory in Newcastle.

To the other members of the Durham Colleges Geology Department staff, especially Dr. M. R. House and Dr. C. H. Emeleus, and to the research school I am grateful for many stimulating ideas and for friendship.

I was able to visit freely all parts of the Castlemartin RAC Range and All Arms Target Area due to the kind co-operation of Range Officers, Capts. Squire and Paice, for their cutting of 'red tape' I am very grateful.

During my visits to Pembrokeshire I was also considerably encouraged by the kindness of Mr. and Mrs. J. Thomas with whom I stayed for most of the time.

Finally, I should like to thank the Council of the Durham Colleges for awarding me a Durham Colleges Research Studentship.

Conventions and symbols adopted in this thesis

1. All structural measurements are given in terms of dip (inclination) and azimuth (declination). Dips are quoted as angles measured down from the horizontal, inverted dips being recorded as angles greater than 90°. Declinations are recorded around a 360° compass. Inclinations values are placed before declination values, so that 75°.185° implies a dip of 75° along a bearing of 185°.
   Structural lines are recorded in the same way as planes, 75°.185° implying a line plunging at 75° along a bearing of 185°, the line being assumed to lie in a plane striking at right angles to its plunge.

2. Most structural values quoted in the text or the Appendices are mean values (either angular or arithmetic) given to the nearest degree.

3. Each field station has been given a number and the same number applies to the stereographic plot of the structural readings from that station. It is always a four figure number, the first digit indicating the relevant field zone, according to the following scheme:-

2000's	Lydstep
3000's	Freshwater East
4000's	Greenala
5000's	Stackpole
6000's	Bullslaughter
7000's	Freshwater West
8000's	Angle Cliffs
9000's	West Angle Bay

The approximate location of each of the 90 analysed field stations is shown on Fig. 1.2, the precise location of each station being given as an eight figure grid reference in Appendix IV.

4. All stereographic diagrams have been constructed and drawn using an equal area (Lambert), equatorial projection stereographic net of radius 10 cms. A tick at the top of a figured diagram indicates the north.

5. Stress axes

Geometrical equivalent relative to two complementary shear planes	Stress	Symbol
acute bisectrix	max. principal pressure direction	σ_x
line of intersection between shears	int. principal pressure direction	σ_y
obtuse bisectrix	min. principal pressure direction	σ_z

6. θ - the angle between a shear plane and σ_x. 2θ sometimes being referred to as the dihedral angle.

7. Wavelength - λ Used mainly in fold description.

Amplitude - a

CONTENTS

Contents

Contents

Contents

Chapter 5 (Cont.)

Contents

Contents

List of Text Figures

List of plates

CHAPTER 1 INTRODUCTION

I GENERAL STATEMENT

The Orielton anticline is a compound uplift, affecting Palaeozoic rocks, within the Armorican fold belt of south Pembrokeshire. The purpose of studying the anticline has been to describe its structural pattern and to reconstruct its stress history. The most important aspect of the problem has been to investigate the geometrical and kinematical relationships between the folds, faults and joints of the anticline. The Orielton anticline is a particularly suitable structure for studying these relationships since it was formed at a high level in the earth's crust, where folding closely controls later fracturing.

The first detailed structural account of the anticline was given by Dixon for the Geological Survey in 1921. Since then no new structural work has been undertaken in the area, although Sullivan (1960) in a study of the Mid-Dinantian stratigraphy emphasised the important part the Ritec fault is considered to have played in the geological history of the region since earliest Carboniferous times. In "The Dynamics of Faulting", Anderson (1951) made an interpretative stress analysis of the area which he regarded as an almost perfect example of the association of folding, thrusting and complementary wrench faulting: one of the objects of the present research is to make a similar interpretation using minor as well as major structures.

II GEOLOGICAL SETTING OF SOUTH PEMBROKESHIRE

Pembrokeshire lies at the meeting point of the Caledonian and Armorican mountain chains. The northern half of the county is underlain by E.-W. Caledonian structures formed after the Silurian but before the deposition of the Old Red Sandstone. The southern half corresponds to WNW.-ESE. Armorican structures of post-Carboniferous but pre-late Triassic age. It is difficult to assess the effect the later Armorican movements had on the earlier Caledonian trends, which north of Pembrokeshire become NE.-SW., the characteristic British Caledonian strike direction. The close parallelism of the two fold belts in Pembrokeshire may be due to either an original swing in the Caledonian geosyncline at this point, or to the effect of the later Armorican movements. The Armorican structures of Pembrokeshire are part of a much longer frontal fold belt running in a broad arc from southern Ireland, through Pembrokeshire, the Gower and then beneath a Mesozoic cover in south-east England to crop out again in Belgium. Folds of the same age affecting similar rocks in south central Pembrokeshire, the Vale of Glamorgan and near Bristol cannot be regarded as belonging to the true Armorican fold belt as they are both less intense, and trend ENE.-WSW. Their direction is probably controlled by the grain of the underlying Caledonian structures. However, they were probably formed at the same time as the Armorican fold belt and by the same principal pressures.

III STRUCTURAL DIVISIONS OF ARMORICAN PEMBROKESHIRE

The material in this section is based on the accounts given in the Geological Survey memoirs for sheets 244-245, 226-227 and 228. (Memoirs of the Geological Survey, The Geology of the South Wales Coalfield, Parts XI, XII and XIII).

Although all the Armorican folds of South Pembrokeshire are essentially wrinkles on the limbs of the coalfield syncline this simple pattern masks a number of distinct structural zones cutting the WNW.-ESE. trend of the basin (Fig.1.1). A line joining Amroth, Begelly and the fork in the Cleddau separates a northern area of structures controlled by the underlying Caledonian grain, from a southern area of structures of characteristic Armorican trend.

The northern area (Region 1.) is divisible into -

(1A) A wedge shaped strip of country about 2.5 miles wide in the east and narrowing westwards until it disappears in the region of the eastern Cleddau. It consists of relatively undisturbed strata dipping gently south.

(1B) The area east of the Eastern Cleddau where folds and strike faults trend ENE.-WSW. These structures downthrow the Upper Palaeozoic rocks to the north.

(1C) The area east of the Eastern Cleddau and north of the Johnston thrust consisting of E.-W. folds and faults which again downthrow the rocks to the north. This region corresponds to the meeting point of the two directions of fold trend seen in the Upper Palaeozoic sediments.

South of Region (1) fold and thrust structures trend WNW.-ESE., the underlying Caledonian direction being no longer apparent. Region 2 is divisible into -

(2A) A wedge of Pre-Cambrian and Lower Palaeozoic rocks bounded to the north by the Johnston thrust and to the south by the Benton fault. Both these faults have had long and complicated histories, this zone possibly representing a long established line of weakness which has moved many times since it was first formed. It may have corresponded to the southern limit of the Lower Palaeozoic geosyncline in this part of Wales.

(2B) A broad zone of folds north of the Ritec thrust corresponding to most of the southern limb of the coalfield syncline, and to the Winsle-Carew anticline.

(2C) An area south of the Ritec thrust consisting of tight but relatively simple folds cut and displaced by complementary wrench faults. The major fold of this area is the Orielton anticline.

IV STRATIGRAPHY OF THE ROCKS IN THE ORIELTON ANTICLINE

Except for the work of Sullivan (1960) this summary is based on the accounts given in the Geological Survey Memoirs.

(a) Table of Formations

PERMO-TRIASSIC		- Cave breccias
CARBONIFEROUS	Namurian	- Shales and thin sandstones
	Dinantian	Main limestone (Z - D zones)
		Lower Limestone shales (K)
DEVONIAN	Upper O.R.S.	- Skrinkle sandstones
	Lower O.R.S.	Ridgeway conglomerate
		Red marls and basement beds
SILURIAN	Ludlovian	- Mudstones, sandstones and shales
	Wenlockian	- Mudstones
ORDOVICAN	Llanvirnian	- Shales

(Fig 1.2 illustrates the simplified geological outcrop pattern).

(b) Lower Palaeozoic

Exposed in the core of the Orielton anticline are the oldest rocks seen in the area, these are Llanvirnian graptolitic shales largely of the *Didymograptus bifidus* zone, with a few feet of *D.murchisoni* shales in one small area. They are soft grey laminated shales containing a few thin sandstone bands towards the top. Their total thickness which is probably great, is unknown because of repeated folding and poor exposure. Where the Ordovician-Silurian contact is exposed it is a disconformity.

Wenlockian strata are only exposed at Freshwater East where they consist of 30 feet of unlaminated mudstones. Ludlovian rocks are more widely exposed in the core of the anticline, where the sequence consists of 250 feet of sandstones with alternations of shale and decalcified limestone.

(c) Old Red Sandstone

Although in the field the Old Red Sandstone succeeds the Ludlovian without a structural break a time gap separates the two formations. Erosion prior to the deposition of the Old Red Sandstone had been sufficient in some cases to allow the Old Red Sandstone to rest directly on the Ordovician.

The Red marls and Basement beds comprise of, at the base 20 feet of conglomerate, followed by red and green marls, cornstones, felspathic grits and sandstones. The succession which is 1460 feet thick at Freshwater West thickens northwards until it is about 3260 feet thick on the Ridgeway. The higher division of the Lower Old Red Sandstone (The Ridgeway Conglomerate) is 1200 feet thick on the Ridgeway, although almost non-existent on the southern limb of the Orielton anticline, except at Freshwater West where it is 800 feet thick. It consists of interdigitations of thick conglomerate bands in a red marly succession. The conglomerates are formed of well rounded pebbles of Lower Palaeozoic sediments enclosed by red and purple marls and sandstones.

Although in this part of Wales no structural break, at any exposure, can be detected between the Upper and the Lower Old Red Sandstone, its position is marked by a palaeontological gap. Over a wide area the upper division transgresses over the lower. In contrast to the Lower Old Red Sandstone, the Upper thickens northwards, a characteristic it shares with the overlying Carboniferous. Lithologically the rocks of the Upper division are similar to those of the Lower although breccias predominate over conglomerates, millet seed sandstones are more common and the rocks generally are of a more brick red hue. Towards the top of the succession there are intercalations of marine horizons in an otherwise continental sequence. These marine horizons consist of shales, mudstones, thin bedded limestones and red sandstones, all containing undoubted marine fossils. In general the thickness of marine strata increases towards both the south and west, until the great thickness of rocks of Lower Limestone shale facies at Freshwater West probably includes strata belonging to both the Upper Devonian and the K zone of the Carboniferous. Continental rocks are therefore absent in the highest parts of the Old Red Sandstone sequence of Freshwater West. Elsewhere although the rocks at the boundary of the two systems may not be of the same facies the junction between the Old Red Sandstone and the Carboniferous is a passage.

(d) Carboniferous

In broad outline the Carboniferous Limestone sequence is simple. The basal rocks are K zonal Lower Limestone Shales, 450-550 feet thick, consisting mainly of shales with a few thin limestone and sandstone bands. The shales are succeeded by the Main Limestone succession over 4300 feet thick in the south, and 2200 feet thick in the north. This succession consists of pure and argillaceous limestones, oolites, dolomites and a few thin mudstone bands. In detail the stratigraphy is complicated and has been more fully described by Dixon (1921) and Sullivan (1960) .

Sullivan's recent work has shown the importance the Ritec fault line played during Dinantian times in controlling sedimentation. South of the old St. George's Land shore line was a shelf sea deepening southwards and across this shelf a hinge line, corresponding to the present position of the Ritec fault, separated a deeper southern sea area from the shallow in-shore sea area. South of the hinge the sea floor subsided faster than to the north of it and this produced marked thickness and facies changes within the Dinantian Limestones. North of the hinge the succession is thin (<2200 feet) and characterised by oolites, lagoonal phase limestones, rapid changes of facies, evidence of contemporaneous erosion and a general indication of shallow water conditions. South of the hinge the succession is thicker (2200-4300 feet), complete and characterised by Zaphrentid phase and bio-clastic limestones. The pre-Tournasian shore line must have lain close to the fault since to the north of it Tournasian rocks rest directly on the Old Red Sandstone. The same was probably true of the pre-Visean and pre-Seminulan shore lines.*

All these north to south changes Sullivan believes reflect incipient stages of the Armorican orogeny and from this the implication is that the Ritec overthrust developed along a line of pre-existing weakness.

Namurian shales are exposed in two small outliers, one near Bosherton, the other near Lydstep. At both places the rocks are poorly exposed and they have not been examined in the course of this study.

(e) Permo-Triassic

New Red Sandstone rocks are represented by breccias contained within Visean limestones. The breccias were caused by the collapse and consequent infilling of old solution caves in the limestone. The matrix surrounding the limestone blocks is largely red marl and stalactitic calcite. These breccias are especially important to this study since they can be used to date the age of the deformation. The age of the breccias themselves is a complex problem and will be discussed later.

(f) Younger Rocks

Rocks younger than the Permo-Triassic lie outside the scope of this study, they are, however, few being limited to isolated patches

* The zonal positions of limestones quoted in this thesis are based on Dixon's work.

of Tertiary clay and quartz gravels. Recent rocks comprise raised beach deposits, a little glacial gravel, extensive sand dunes and valley alluvium.

V TOPOGRAPHY

South Pembrokeshire is part of a much larger marine peneplain now uplifted to about 250 feet. Despite the complicated geological structure which underlies the plain the platform cuts almost evenly across all rock types. At the coast the platform ends abruptly in steep cliffs 100-200 feet high.

In detail the relief does pick out the geological structure. Areas underlain by Old Red Sandstone rocks form the highest ground at about 250 feet, Carboniferous Limestone tracts have generally been eroded to give 'flats' at about 100 feet and the more easily weathered Lower Palaeozoic shales correspond to the deeper valleys. Outcrops of Namurian shales and sandstones give rise to areas of slightly higher ground within the limestone 'flats'. Because the outcrop of the Lower Limestone Shales is thin it does not correspond to any well marked relief feature, although in places a narrow strip of depressed ground occurs between the Old Red Sandstone uplands and the limestone 'flats'.

The shape of the coastline reflects even more closely the geological structure, since not only does relative rock hardness have an effect but individual structure planes may be eroded out. In general the Old Red Sandstone rocks form headlands whilst shales form bays. Limestones are eroded to bays if they are surrounded by harder sandstones and stand out as headlands if they are flanked by shales. On the smallest scale the precise shape of the coastline is controlled by the direction of faults, bedding planes and joints. Most of the very narrow inlets along the coast correspond to either near vertical bedding planes or faults.

To the geologist the topographic style of southern Pembrokeshire implies almost continuous coastal sections but few natural inland exposures.

VI HISTORY OF STRUCTURAL RESEARCH

(a) General Remarks

Both the rocks and structures of south Pembrokeshire have for long attracted the attention of geologists. In the 16th Century George Owen recognised that the various strata were different from one another and that they ran in veins; a particularly valid analogy since over much of the area the rocks are vertical.

At the beginning of the modern era of scientific geology both De la Beche and Murchison visited the area and recognised what formations were present and drew profiles to illustrate the structure.

The detailed mapping of the area by the Geological Survey on a scale of 6 inches to the mile was begun before the first World War although publication was delayed until 1921. Dixon mapped all the present region and his results were incorporated in the Memoirs for sheets 244 (Linney head), 245 (Tenby) and parts of sheets 228 (Haverfordwest) and 227 (Milford).

Anderson (1951) using Dixon's observations made an interpretative stress analysis of the region basing it upon his theory of faulting. No further detailed work was then attempted until Sullivan (1960) made a close study of the Mid-Dinantian statigraphy.

(b) Dixon's Work

The principal folds and faults are shown in Fig.3.1. In general Dixon's nomenclature has been followed although a few new names have been added where necessary.

Dixon restricted the term 'Orielton anticline' to the Lower Palaeozoic and Old Red Sandstone parts of the fold, regarding the Carboniferous rocks as belonging to the adjacent synclines. In this study, however, the limits of the fold are taken to lie in the outer limbs of the Pembroke and Bullslaughter synclines.

In the Geological Survey Memoir, Dixon (1921, p. 176-179) describes all the principal folds, their outcrops, dips, axes and axial planes. In his synthesis he stresses the persistence of fold axis trends and the outward fan of axial planes. He emphasises that whilst most folds trend WNW.-ESE., thrusts strike more truly E-W.

Dixon mapped, described and tabulated (p. 181-185) all the important cross faults and he recognised that in plan they were symmetrical about the axial direction and that they showed essentially horizontal displacements. Although Dixon recorded fault dips he did not draw any conclusions about their departures from the vertical. The cross faults he thought were due to the same stresses as the folds but were formed after them, in many cases before the New Red Sandstone. Dixon (p.182-183) also describes wrench faults curving into thrusts.

Dixon (p.185-186) did not distinguish between slaty and fracture cleavage although he described the cleavage in the K_2 shales of West Angle Bay as being more perfect than elsewhere. He also noted the now accepted idea that where beds are inverted cleavage dips are less than, but in the same direction as, bedding dips. In shales he observed that cleavage planes were closer spaced and at more acute angles to the bedding than they were in sandstones and limestones.

Dixon (p.185) recorded little about joints, however, because of their importance in this study his remarks are summarised below.

1. The relations between joints and Triassic breccias show that some joints are pre-Triassic, others later. The two common strike directions of joints not affecting the Trias are NNE. and NNW., as, however, they show no constant differences in direction it is impossible to classify those joints whose relations with the Trias are not exposed.

2. A broad classification into strike and dip joints at right angles to the bedding is applicable.

3. Joints vary considerably in development, direction and dip and are often most noticeable in thick bedded homogeneous limestones.

(c) Anderson's Stress Interpretation

In the "Dynamics of Faulting" (1951) Anderson developed his theory of rock fracture. Using the theory Anderson then interpreted many British fault patterns including the Armorican system of South Pembrokeshire which he regarded as an almost perfect instance of the association of folding, thrusting and complementary wrench faulting.

Both the folds and the low angle thrusts were considered by Anderson to have been formed when the maximum principal pressure (σ_x) was oriented horizontally along NNE.-SSW., the intermediate principal pressure (σ_y) horizontally along WNW.-ESE. and the minimum principal pressure (σ_z) vertically. The wrench faults Anderson regarded as having formed during the action of a subsequent stress field of the same gross orientation, except that σ_y corresponded to the vertical load and σ_z to the WNW.-ESE. fold axial direction.

Anderson regarded the dominantly southward dipping thrusts as indicating a movement picture of southward underthrusting rather than overthrusting to the north. The smaller north dipping thrusts were not considered necessarily to be the complements of the larger south dipping ones. The dihedral angle of 50° between the complementary wrench faults Anderson regarded as good field confirmation of the Navier principle of fracture.

Anderson's interpretation suggests that in south Pembrokeshire there exists a complementary pair of low-angle thrust faults cut by a complementary pair of vertical wrench faults. Genetically associated faults and joints are commonly regarded as lying parallel to one another, therefore in south Pembrokeshire it was expected that faults would be accompanied by parallel joints. Neither of the above suppositions, however, has been shown to be entirely true although the expectation of finding that structural pattern hindered for a long time an understanding of the real situation. Briefly, low-angle thrusts are rare, although strike shear joints at low angles to the bedding planes are common. Wrench faults depart systematically from the vertical, their orientation depending on the attitudes of the axial plane and axis of the folds which they cut. Wrench faults are accompanied by few parallel joints but a system of joints acting as wrench shears relative to bedding planes is common. In addition other tectonic sub-phases not detected by Dixon's earlier survey have been found.

CHAPTER 2 METHODS

I GENERAL REMARKS

The problem of sampling the structures of the area has been approached by selecting sets of stations around the coast and recording from them all structural information. The stations have been sited in relation to the major structures so that a representative picture of the total pattern will be gained. Minor structure observations have then been simplified for each station and stress directions calculated. Since major structures frequently extend beyond individual stations they have been given, in some instances, a broader treatment. Summary diagrams for both major and minor structures have then been even further simplified.

II FIELD PROCEDURE

The eight field zones (Fig.1.2) have been sub-divided into stations from which all structural data have been recorded. The number of stations within a zone varies with its size, most stations, however, extend between 100-300 feet along the cliffs and, except where adjacent, have been spaced at about 100 yard intervals.

The only instrument used in the field was the Brunton compass clinometer corrected for magnetic declination. Structural attitudes have been recorded as the number of degrees of dip from the horizontal, followed by the direction of this dip around a 360° compass. The position and extent of the stations together with the pattern of the major structures were plotted on 25 inch Ordnance Survey maps, copies of the Geological Survey 6 inch sheets being used to give the necessary geological control. Some of this information was transferred from the 6 inch sheets onto the 25 inch sheets so that as little field time as possible was lost locating the exact positions of folds and faults.

In addition to the attitudes of structural planes and lines the characters of these structures were also recorded, the following list being a summary of those most commonly noted.

1. Lithology. Stratigraphical position and lithology which a structure cuts, together with any structural variations due to these.

2. Surface characters. Including, smoothness and surface markings.

3. Regularity, persistence and spacing. Including, the extent of a fracture along its strike and dip across bedding planes, whether the fractures of a particular set are precisely parallel and the spacing of fractures. Spacing has been measured in two ways: either as planar frequency for a unit distance normal to the fractures or as the average distance apart of the fractures. The first method is most useful for closely spaced planes, the second for widely spaced planes.

4. Veining. Including, the mineral species and its megascopic characters, the presence or absence of voids, mineral alignment and the thickness, spacing and extent of veins.

5. Cross cutting relationships. Including, whether a plane cross cuts, distorts or displaces earlier structures and when there are two sets of vein infillings cutting one another which vein set is the older.

III LABORATORY PROCEDURE

Three stages are involved in the structural interpretation of the field observations -

(a) Data reduction

(b) Analysis

(c) Synthesis

(a) Data reduction

For each field station and for the major structures point diagrams were constructed, using the equatorial projection of the Lambert Equal Area stereographic net of radius 10 cms. All planes were plotted as poles except when cyclographic traces were required for subsequent calculations. The pattern of poles obtained on the point diagram usually suggested a natural grouping of the fractures. In order to simplify the readings in each group to average values which could be used for analysis three data reduction procedures were tried.

1. Contouring.

2. Calculation of an angular mean together with a 95% circle of confidence.

3. Calculation of an arithmetic mean.

i) Contouring

Methods of contouring stereograms have been discussed by Knopf and Ingerson (1938), Fairbairn (1949), Billings (1954), Phillips (1954) and many others. All the procedures are essentially similar, differing only in detail and accuracy. During this study the method of contouring described by Phillips (1954) has been followed except that in a few cases a graticule of 0.5 cm. squares was used instead of a graticule of standard 1 cm. squares. The most commonly adopted contour intervals have been 1% and 2%, the 2% probably being the preferable interval since the resulting diagram is simpler. Fig.2. A illustrates a contoured diagram for two stations combined, the poles from which the diagram was constructed being given on Fig.2. B.

ii) Angular mean and 95% Circle of Confidence

In order to calculate the angular mean and the 95% circle of confidence a ready written computer programme for Fisher's statistics, kindly supplied by Dr. R: Girdler of the Durham Colleges, was used. The computer employed was the Ferranti Pegasus Computor housed at Kings College, Newcastle. The mathematical principles and limitations involved in calculating the mean and the circle of confidence are discussed by Fisher (1953), Watson and Irving (1957) and Cox and Doell (1960).

The angular mean differs from the arithmetic mean of the inclinations and declinations by allowing for the mutually modifying effects upon one another of declination and inclination. The circle of confidence represents in degrees the radius of a circle which can be drawn around the mean, within which there is a 95% probability of the true angular mean lying. It is, however, only meaningful if the poles making up the mean have a circular distribution on the stereogram and since this condition is rarely fulfilled in the case of the present diagrams the circle of confidence can be regarded only as an empirical estimate. In general, if the poles making up a mean are few, wide scattered or eccentrically distributed about the mean the circle of confidence value is high (i.e. $>10°$). Conversely a close and even cluster of poles, or a large number of readings yields a low circle of confidence value. About seven poles lying close to the mean are considered to give a reliable estimate of the true mean.

On the stereographic plots both the angular means and circles of confidence have been plotted to the nearest degree, the computer yielding values correct to one decimal place of a degree. Due to the distorting effect of the equal area net the circle of confidence does not plot as a circle except in the centre of the stereogram, elsewhere it plots as an ellipse: the ellipticity being greatest near the perimeter, with the long axis of the ellipse parallel to a great circle. In addition to plotting the angular mean and the circle of confidence the limit of the poles used for calculating these values have also been indicated on the stereographic diagrams.

The computer programme also calculated a kappa value to describe the dispersion of poles within a group, this value has, however, not been used.

iii) Arithmetic mean

The mean inclination and declination of a group of poles can be found by calculating their separate arithmetic means. This mean can then be plotted on a stereogram together with a line limiting the poles making up the mean.

To find either an angular or an arithmetic mean poles to structural planes have to be grouped into related sets. A disadvantage arises here since on point diagrams adjacent groups of poles frequently coalesce and, therefore, the grouping of poles common to both maxima has occasionally to be arbitrary. In addition if the poles to structural planes from a large number of adjacent stations are all plotted on one diagram the various groups coalesce, it has therefore been necessary to treat each station separately.

iv) Comparison of data reduction methods

Each of the data reduction methods outlined above has certain advantages, those of calculating a meanvalue rather than contouring are listed below.

1. The grouping of fractures into related sets achieves a partial analysis at an early stage in the laboratory procedure.

2. The effect of readings which lie distant from or eccentric about the mean are allowed for during the reduction procedure. A contoured maximum always corresponds to the area of greatest concentration of poles and this area may not be a representative maximum for the group as a whole.

3. In order to differentiate between rotation joints in different lithologies overlapping contours would have to be drawn, these would be both confusing to look at and difficult to construct.

4. Calculating a mean provides a single value for the attitude of a structure, and this value can then be used for further calculations. Over a large area of maximum concentration of poles the highest contour would enclose a large area within which a point would still remain to be chosen as the mean.

5. Two distinct groups of readings the end members of which coalesce may contour as a single maximum, alternatively a single maximum may contain several close clusters of poles which would result in several contour maxima. In either case the mean would remain to be chosen arbitrarily.

6. The calculation of an arithmetic mean compared with contouring is quick.

The principal disadvantage of calculating a mean value is the subjective grouping of related readings which is required in the early stage, however, to obtain a useable mean value from a contoured diagram also frequently requires such a subjective choice.

It is now pertinent to compare the calculation of an angular mean and circle of confidence with the calculation of an arithmetic mean. The two advantages of the former are:-

1. Accuracy

2. The calculation of a circle of confidence.

The results of calculating the mean by the two methods are shown in Table 2.1. The example chosen is the stereogram illustrated on Fig.2.1B.

The conclusion which can be drawn from the Table is that the arithmetic mean is a sufficiently close approximation to the angular mean, the introduced error being less than the observational error. Possible observational errors include both the irregularity of the geological structures being measured and the limit of accuracy to which the Brunton compass may be read, this being about one degree.

The preparation of the computer tapes is in addition very time consuming and frequently impractical when many later regroupings are required. To calculate the angular means and the circles of confidence in the normal manner using logarithmic tables would be even more tedious. Therefore, the result of calculating an angular mean and circle of confidence to represent the average attitude of a group of planes, is to go against the scientific principle of economy of accuracy, a falsely accurate answer being obtained after a disproportionately great amount of time has been spent calculating it.

TABLE 2.1

Angular and arithmetic means compared

N	Angular	Arithmetic	Diff.I	Diff.D
9	80.4 at 008.3	80.4 at 008.3	0.0	0.0
13	21.7 " 010.7	22.1 " 010.7	0.4	0.0
7	30.6 " 272.2	30.7 " 272.4	0.1	0.2
7	30.3 " 059.2	30.4 " 059.6	0.1	0.4
3	77.8 " 185.7	78.0 " 186.7	0.2	0.0
22	61.9 " 278.8	62.1 " 278.6	0.2	0.2
23	60.3 " 102.4	60.8 " 101.7	0.5	0.7

Note. N. number of readings, Diff.I. difference in inclinations, Diff.D. difference in declinations. Attitudes given to the nearest degree, inclination preceding declination.

(b) Analysis

i) Rock fracture

Despite a wide literature covering the theoretical and experimental aspects of rock deformation few assumptions have to be made in order to deduce a possible sequence of stress axis orientations from a fracture pattern. Some of these are discussed below. Initially, it must be taken that the observed deformation pattern reflects the changing stress fields which acted upon the group of rocks.

Rocks are capable of deforming by both flow and rupture, rupture occurring on either tension (extension) or shear (compression) fractures. Two theories of rupture have dominated geological literature, the strain theory and the stress theory, both so named by Wilson (1946).

1. Strain theory. This theory of rupture was first given prominence by Becker (1893), and was then subsequently developed and applied to geological problems by Bucher (1920), Swanson (1927), Lovering (1928), Griggs (1935) and Leith (1937). More recently Wilson (1946) has summarised the conclusions of these and other earlier writers and applied the theory to the solution of field observations. However, the strain theory is now regarded as being discredited and in a recent paper Wilson (1961) has also abandoned the theory.

The principal geological application of the strain theory was to account for the attitudes and origin of fracture cleavage planes, most writers agreeing that other shear planes were probably best explained in terms of the stress theory. Fracture cleavage was considered to be caused by bedding-slip during folding setting up shearing stresses across a bedding unit so that as the strata were progressively deformed the two circular sections (the planes of maximum strain) of the ellipsoid came to lie at increasingly acute angles to one another. Such an explanation accounted for fracture cleavage planes in incompetent strata subtending smaller acute angles with the bedding than in competent strata, incompetent strata being capable of greater plastic deformation before rupture. The strain theory implies that the acute angle between a fracture cleavage plane and the bedding faces the direction of tectonic transport, whilst the intersection of the cleavage on the bedding traces a line normal to this direction. Despite the theory being discredited the geological application of these implications has been found to be widely valid for respectively determining, facing directions of strata and the approximate attitudes of fold axes (See Wilson 1946 and 1961).

In his recent paper Wilson (1961, p.473) gives the following account of the origin of fracture cleavage - "Fracture cleavage, formed during the folding of a series of strata, results from the transverse shearing stresses which are developed by the bending of the beds, combining with those which are induced by the slip of the beds upwards towards the anticlinal hinges." If such an account is accepted the geological applications which have just been discussed will still be valid as Wilson shows by considering field examples.

2. Stress theory. This theory of fracture accounts for the attitudes of shear and tension fractures which develop in brittle rocks, suffering no plastic deformation before rupture. It is based on the Navier principle of shear fracture. Anderson (1951, p.3) regards Navier's principle as being based on the earlier work of Coulomb in 1775, work which was generalised and expanded in 1900 by Mohr. In geological literature, however, the rule for deciding stress directions has become known as Hartmann's Law. The maximum principal pressure direction (σ_x) bisects the acute angle between complementary shear planes, whilst the minimum principal pressure direction (σ_z) bisects the obtuse angle between the shear planes. Hartmann's Law was extended by Bucher (1921), who added that the line of intersection between complementary shear planes marked the intermediate principle pressure direction (σ_y). Later Anderson (1951) using the Coulomb-Mohr-Navier principle of fracture applied these rules to the classification of faults. Using his theory of faulting Anderson (1951) then proceeded to make a stress interpretation of many British fracture patterns.

Hartmann's Law applies to isotropic bodies. Jaeger (1959 and 1960) and Donath (1961) have considered the effect on the development of shear planes of pre-existing planar anisotropies and have as a result of their considerations added certain limiting conditions. Donath (1961) has shown that no new shear plane need be formed if a pre-existing plane lies up to 60° from the direction of σ_x. Hafner (1951) has also slightly modified Anderson's ideas by considering what possible deviations of the stress axis orientations, from the horizontal or vertical, might occur when two stress systems interact upon one another. More recently, Muehlberger (1961) has considered possible explanations for the unexpectedly small dihedral angles frequently observed between complementary shears, Anderson (1951) having predicted angles of approximately 60° between complementary shears.

From two complementary shear fractures the three principal stress directions can be deduced knowing that

the acute bisectrix marks σ_x,

the line of intersection marks σ_y,

the obtuse bisectrix marks σ_z.

In addition it is known that a tension fracture always lies normal to σ_z, its plane containing σ_x and σ_y. Tension fractures form only when one of the principal pressures is negative. A shear fracture intersects a related tension fracture along σ_y. Therefore, provided that there are two complementary shear planes or a shear plane and a related tension fracture the directions of σ_x, σ_y and σ_z can be calculated.

ii) Station analysis procedure

The point diagram for a station should suggest various possible geometrical relationships between structural planes and lines and from the pattern a natural grouping of structures should be obvious.

The procedure for analysing a station is illustrated using an ideal example (Figs. 2C and D), which represents most of the common structures encountered on a fold limb. The principal deductions which can be made are summarised below.

FOLDING PHASE (Fig. 2.1C)

1. The fold axis. The fold axis can be calculated from -

(A) Direct observation of the fold or its congruous buckles and ripples.

(B) The intersection of the cyclographic traces of average fold limb dips at various points. This is the β diagram of Sander.

(C) The pole at 90° from the great circle girdle of poles representing the bedding from the two fold limbs. This is the π diagram of Sander.

(D) The intersection of bedding with fracture cleavage planes, rotation joints, slaty cleavage or related tension cracks. This direction has been called the local fold axis. These intersections are most simply found by calculating the attitude of the pole lying at 90° to the fracture-bedding great circle. The same procedure can, of course, be adopted for finding the intersection between any two planes.

e.g. bedding-fracture cleavage = 10°.115° (point A)

bedding-rotation joints = 10°.115° "

bedding-tension joints related to bedding-slip = 10°.115° "

(E) Slickensides on the bedding which form parallel to the sense of slip during folding and therefore lie at 90° from the fold axis in the plane of the bedding.

e.g. 1st set bedding plane slickensides plunge 58°.213° therefore 90° from them in the plane of the bedding is 10°.115°.

(F) Slickensides on fracture cleavage planes or rotation joints, which also lie at 90° from the fold axis within the plane of the fracture.

e.g. Slickensides on rotation joints plunge 39°.007°, therefore at 90° to the lineation in the plane of the fracture is 10°.115°.

2. The axial plane. The axial plane can be calculated by bisecting the modal dips of the fold limbs.

3. The inverse axis. The inverse axis is defined as the line corresponding to the intersection of the bedding with a second set of fracture cleavage planes (close joints), called inverse rotation joints. These fractures are strike joints, whose attitudes are symmetrically about the bedding strike, the inverse of rotation joints (See Fig. 4.3B). The inverse axis can be calculated from -

(A) The trace of the intersection between the bedding and an inverse rotation joint.

e.g. bedding-inverse rotation joint = 10°.267° (point 1A)

(B) A possible 2nd set of bedding plane slickensides which lie at 90° in the plane of the bedding from the inverse axis.

e.g. 2nd set of bedding slickensides plunges 58°.167°, therefore, the inverse axis plunges at 10°.267°.

4. Axial symmetry. During the analysis it was found useful to calculate the following two relationships.

(A) The angle between the axis and the inverse axis, measured within the bedding plane about its strike.

e.g. Axis onto inverse axis about bedding strike = 24°

(B) The angle between the bedding plane dip direction and both the axis and the inverse axis.

e.g. Bedding plane dip direction onto axis = 78°.

Bedding plane dip direction onto inverse axis = 78°.

5. Relative lithogical distortion. The amount a unit thickness of a bed has thinned on a fold limb can be calculated from -

(A) Measurement of distorted structures whose original shape was known.

(B) The acute angle between fracture cleavage planes, rotation joints or inverse rotation joints and the bedding, measured about a common great circle.

e.g. bedding onto rotation joints = 80°

bedding onto fracture cleavage = 60°

bedding onto inverse rotation joints = 86°

6. Strike shear joints, miscellaneous strike joints and thrusts.

(A) Applying Hartmann's Law to the illustrative pair of of complementary strike shear joints yields -

$$\sigma_x = 58°.209°, \ \sigma_y = 10°.102°, \ \sigma_z = 30°.006°.$$

The angle ϑ (between σ_x and one of the shears) is stereographically the angle between σ_z and one of the shears measured along a great circle common to both points.

e.g. σ_z onto the strike joint dipping at 36°.178°, is 25°.

(B) Frequently only one of the two possible complementary strike shear joints is developed, nevertheless some estimate of stress directions can be made assuming that σ_y is parallel to the shear-bedding intersection and that σ_x lies at 90° from σ_y in the plane of the bedding.

e.g. The strike shear joint dipping 36°.178° is assumed to be the only one developed. Therefore σ_y^1 = 14°.107°, σ_x^1 = 56°.210°, and σ_z^1 = 30°.010°.

(C) Any slickensides on strike shear joints should be parallel to the actual or potential direction of tectonic transport, and hence at 90° in the shear plane from σ_y.

e.g. Slickensides on the strike joint dipping at 36°.178° plunge at 35°.199°, therefore σ_y plunges at 10°.102°.

(D) From less systematic strike joints the angle between the fracture and the bedding and the plunge of the bedding - fracture intersection can be calculated.

e.g. The thrust dipping at 47°.034° intersects the bedding along a line plunging at 15°.109° and subtends an angle of 76° with the bedding. If the thrust dip is assumed to be independent of the bedding dip other stress directions can be estimated assuming σ_z to have been near vertical and σ_x to have been near horizontal and at right angles to the strike of the thrust.

7. Down dip drag zones. From the attitudes of these structures it is possible to calculate the angles which they make with the bedding and the plunges of their intersections with the bedding.

e.g. The drag zone dipping at 65°.344° intersects the bedding along 15°.109° and subtends an acute angle of 40° with the bedding.

LATE FRACTURE PHASE (Fig.2.1D)

1. Primary fractures. Wrench faults, shear zones parallel to faults and diagonal but later formed shear joints characterise this phase. To any pair of these complementary shear planes Hartmann's Law can be applied in order to calculate the causative stress axis orientations. In addition ϑ can be measured since it is the angle between σ_x and a shear plane, stereographically this angle is, however, determined by measuring the angle between σ_z and one of the shear planes along a common great circle.

(A) e.g. For the two wrench faults dipping at 86°.262° and at 76°.311°, σ_x^1 = 10°.199°, σ_y^1 = 76°.033°, σ_z^1 = 10°.107° and ϑ = 25°.

(B) e.g. For the two primary diagonal shear joint sets dipping at 79°.097° and at 59°.304°, σ_x^2 = 57°.216°, σ_y^2 = 32°.014°, σ_z^2 = 10°.110° and ϑ = 25°.

(C) Slickensides should lie at 90° in the plane of a shear from σ_y.

e.g. On the second set of dip shear joints slickensides plunge 43°.248° and therefore σ_y^2 = 32°.014°.

(D) En-echelon tension lenses within a shear zone may not bisect the angle between the complementary shear planes, therefore these lenses, which are assumed to have lain normal to σ_z, must have been rotated within the shear zone. This rotation can be calculated by comparing the orientation of σ_z derived from the normal to the lenses with the 'regional' orientation of σ_z deduced from the complementary shear planes.

e.g. The lenses in the belt parallel to the 1st set of dip joints dip at 68°.298°, therefore locally within the shear σ_z must have lain at 22°.118°, since regionally σ_z was oriented at 10°.110° the lenses must have been rotated 15° clockwise about an axis normal to the bedding.

The lenses in the belt parallel to the 2nd set of dip joints dip at 86°.102°, therefore locally σ_z must have lain at 04°.282°, since σ_z was again regionally oriented at 10°.110° the lenses of the 2nd belt must have been rotated 15° anticlockwise. The intersection between the lenses and their shear belts gives an estimate of σ_y.

2. Secondary fractures. Secondary shear fractures should intersect related primary shear fractures parallel to σ_y, calculated from the primary shears. In addition to calculating this intersection the angle between a primary shear and a secondary shear can also be determined and compared with predicted values (See McKinstry (1953) and Moody and Hill (1956)).

iii) <u>The possible effect of incorrectly grouping poles</u>

Frequently the groups of poles representing the maxima for the two diagonal dip shear joints (wrench-joints) merge so that the intermediate readings have to be distributed arbitrarily between the maxima. If this distribution is made evenly it is unlikely that the deduced stress axis orientations will be adversely affected. The angle θ. however, may be reduced since it is possible (although there is no positive field evidence) that some of the intermediate joints represent a bisecting regional tension joint set.

(c) Synthesis

The stage of synthesis consisted of correlating one structural feature with another in order to determine whether there were any systematic variations. It was found that deduced stress axis orientations frequently depended upon certain fold structure attitudes in addition to regional stress field orientations.

In all cases the plunge of a fold axis (or local fold axis) influenced later stress field attitudes. Wrench faulting stress fields were in addition oriented relative to the axial plane of the fold which the faults cut. Strike joint and wrench-joint stress fields on fold limbs were oriented relative to the dip of the bedding in addition to the plunge of the local fold axis. Wrench-joint stress fields at fold crests, however, were found to be oriented relative only to the plunge of the fold axis which the joints crossed. Such randomly oriented stress fields were obviously related to regional stress fields.

In order to reconstruct the regional stress fields the local orientations of the stress axes were rotated with the various modifying elements of the fold geometries to the horizontal (fold axes and bedding), or vertical (axial planes).

Therefore, local wrench fault stress field orientations were resolved by rotating the stress axes with the fold axis to the horizontal and then with the axial plane to the vertical.

Local orientations of strike joint and wrench-joint stress fields on fold limbs were resolved by rotating the stress axes with local fold axes to the horizontal, and then with the re-oriented bedding poles to the horizontal. The latter movement was always performed so that after rotation the bedding lay in its correct stratigraphical position.

Wrench-joint stress axis orientations at fold crests were resolved by rotating the stress axes with the host fold axis to the horizontal.

CHAPTER 3 FOLDING

I GENERAL REMARKS

The purpose of this chapter is to describe the style of folding within the Orielton anticline rather than to describe the shape and outcrop of each individual fold, this aspect having been fully covered by Dixon (1921).

Undoubtedly the greatest effect of the Armorican earth movements was the formation of a series of asymmetric and occasionally overturned folds trending WNW. and generally plunging gently east. The Lower and Upper Palaeozoic rocks affected are unmetamorphosed, only in the K_2 shales of West Angle Bay was slaty cleavage developed, elsewhere the rocks failed by fracture cleavage.

The folds are essentially a series of periclines and elongate basins replacing one another in importance along the strike.

Figs.3.1. and 3.2. illustrate in map and section the principal folds.

II AGE OF THE FOLDING

Dixon (1921), using stratigraphical evidence, showed the presence of several unconformities which in the field cannot be detected by structural discordance.

These occur between the :-

Llanvirnian and Wenlockian

Ludlovian and Lower Old Red Sandstone

Lower and Upper Old Red Sandstone

Lower and Upper Dinantian

Dinantian and Namurian

These disconformities indicate minor earth movements and emergence and erosion, probably involving no more than gentle tilting. Certainly no minor structures are seen in older rocks which are not present in younger ones. Dixon describes one fold, near Corston, which he believed to be earlier than Armorican, which has a NE.-SW. trend and brings up the Ordovician astride the Silurian. The evidence for this fold is, however, slight and its location is based on the outcrop of a patch of wet clay ground.

Beds, from the Nolton-Newgale coalfield, belonging to the Anthraconia tenuis zone of the uppermost Westphalian (Jenkins 1962) are the youngest rocks in Pembrokeshire affected by the Armorican folding. Gash-breccias ascribed to the Permo-Triassic are the oldest rocks unaffected by the Armorican movements.

III CLASSIFICATION OF FOLDS

(a) Basis of Classification

The folds of the area can be classified according to their size (i.e. on the basis of lateral extent of the axis, wavelength and amplitude). This classification although useful for the purposes of description masks the continuous gradation of a fold of one size into that of another, for example, a small buckle may grow in size until it becomes a minor or even a major fold. The wavelength of a fold is taken as the horizontal distance separating the two axes bounding it on either side, and the amplitude as the vertical distance separating the crests of an adjacent anticline and syncline. Since a fold may be asymmetrical its crest is not necessarily precisely half way between the two adjacent fold axes and therefore it may possess two 'half' wavelengths of different dimensions. Similarly the two limbs of a fold may be of different length resulting in two possible amplitudes with adjacent fold axes. Nevertheless the idea of wavelengths and amplitudes remains useful for description.

Fold wavelengths are easy to measure on a map but amplitudes are more difficult, due to the tentative projection of beds above and below ground and marked changes in stratigraphical thickness. Amplitudes are often best described by the stratigraphical range of the beds the fold involves at the surface, allowing for the greater range expected in a fold of long wavelength.

The four classes are:-

1. Major Folds
2. Minor Folds
3. Buckles
4. Ripples

(b) Major Folds

The principal fold of the area is the Orielton anticline and its most important components are the major folds.

Major fold dimensions are: wavelengths greater than 1 mile, amplitudes 1000-7000 feet and exposed lateral extents of more than 6 miles. (Table 3.1.)

The Orielton uplift consists of two major anticlines, mutually replacing one another in importance along their strikes and separated by a shallow synclinal sag. In the east the westerly plunging Freshwater East anticline is the dominant element, whilst in the west its importance is replaced by the easterly plunging Castle-martin Corse anticline.

The Orielton syncline, separating the two anticlines, is in the east broad (1.2 miles), compound and easterly plunging. In the west it is narrow (0.3 miles), simple and westerly plunging. There, it is no more than a buckle on the northern limb of the Castlemartin Corse fold. This is reflected by the beds involved, in the east Lower Palaeozoic and Lower Old Red Sandstone rocks, in the west only Old Red Sandstone rocks.

TABLE 3.1.

MAJOR FOLDS	MAXIMUM DIMENSIONS			
Name	Axial extent (miles)	λ (miles)	α (feet)	Horizons at Surface
Pembroke syncline	>16	2.5	3000	Ordovician-Namurian
Angle syncline	5.8 * 3	1.4	2500	L.O.R.S.-L.Dinantian
Freshwater East Anticline	>11 * 8	2.4	5000	Ordovician-Namurian
Orielton syncline	>10.5	1.2	1500	Ordovician-L.O.R.S.
Castlemartin Corse Anticline	>7.5 * 3	2.6	7000	Ordovician-Namurian
Bullslaughter Syncline	>6.2	>2.5	7000	Ordovician-Namurian
ORIELTON ANTICLINE	>19 * 3	4.3	7000	Ordovician-Namurian

N:B. > after a value indicates that since the fold shows no signs of dying away it must at one time have extended beyond the present coast-line.

* indicates that the fold extends beyond the exposed limit of its axis but only one limb is present.

The Orielton anticline is bounded to the north and south by major synclines. To the north the easterly plunging Pembroke syncline preserves Dinantian and Namurian rocks in its core, but its structural analogue the boat shaped Angle syncline, preserves only lowermost Dinantian rocks. The Angle syncline starts as a small limb buckle on the northern flank of the Freshwater East anticline, westwards its wavelength and amplitude increase until the Pembroke syncline has been replaced. The two folds overlap for 3 miles.

The southerly bounding Bullslaughter Bay syncline persists across the entire area as an inwardly plunging fold. Due to flattening of the limbs near Linney the fold has almost disappeared on the western coast. The greater part of the outcrop of the fold is in Carboniferous rocks, near Newton, Dixon (1921, p.157) records shales, perhaps representing a Namurian core to the fold.

(c) Minor Folds

Developed on the limbs of the major folds are smaller folds whose wavelengths are usually less than 1 mile (often less than 1/2 mile), and whose amplitudes are usually less than 1000 feet.

The axial extents of these folds are rarely traceable for more than 2 miles. At the surface a minor fold is usually exposed in only one major stratigraphical subdivision. Major folds may pass laterally into minor folds and when this happens the whole fold has been regarded as belonging to the major class. Minor folds are best developed in the eastern part of the Orielton syncline and in the Carboniferous rocks south of Stackpole. Due to poor exposure in the Orielton syncline only the Stackpole folds have been measured in detail, they are listed in Table 3.2.

TABLE 3.2.

MINOR FOLDS	MAXIMUM MEASURABLE DIMENSIONS			
Name	Axial extent feet	λ feet	α feet	HORIZONS at surface
Murchison syncline	3520	$.5\lambda=612$ *2	485	$K-C_2S_1$
Stackpole Quay anticline	3520	2380	750	C_2S_1-D
Barafundle syncline	5280 *1	3430	1750	$C_2S_1-D_1$
Stackpole Warren anticline	5280	$.5\lambda=1940$ *3	1050	S_2-D_1
Lily Ponds anticline	8800	$.5\lambda=790$ *4	250	$C_2S_1-S_2$
Broadhaven syncline	3520	1580	250	$C_2S_1-S_2$
Broadhaven anticline	4400	2380	600	S_2-D_1
New Quay anticline	2600	>3260	550	S_2-D_1

N.B. *1 Another 10,000' possible west of Stackpole Warren cross fault
*2 Between Murchison syncline and Stackpole Quay anticline axes
*3 Between Stackpole Warren anticline and Barafundle syncline axes
*4 Between Lily Ponds anticline and Broadhaven syncline axes

In most cases the $1/2\lambda$ representing the distance between any axis and the adjacent axis across the steeper limb (usually the northern) is less than the $1/2\lambda$ across the shallower limb by an average ratio of 1:2. Similarly of the two possible amplitudes which can be measured the greatest is that between any axis and the one immediately north of it. This is the value quoted in Table 3.2.

Minor folds are illustrated in map and section on Figs.3.3. and 3.4. and Plate 3.1.

(d) Buckles

i) General characters

The average dimensions of these even smaller wrinkles on the principal folds are:- wavelengths 6-150 feet, amplitudes 10-150 feet and lateral extents of less than 2500 feet. Their presence can only be detected if exposure is good. They are mostly too small to be shown individually on 1" maps and often too small for clear representation on the 6" scale.

There is a general correlation between the frequency of buckles and thick incompetent horizons, for example, near Stackpole Quay and at West Angle Bay where shaly beds at the base of the Carboniferous have wide surface outcrops, buckles are particularly common.

Buckles can be classified into two groups on the basis of their geometry and position in the host fold.

(i) Limb buckles

(ii) Axial buckles

ii) Limb buckles

Limb buckles consist of an associated anticline and syncline which, for a short distance, interrupt the otherwise uniform dip of beds on a fold limb. They can be compared directly with congruous drag folds, although only a few parts of a large fold limb will be buckled. (Fig. 3.5C).

Limb buckles are illustrated on the maps and sections of Figs. 3.3 and 3.6 and on Plates 3.2 and 3.3.

TABLE 3.3.

LIMB BUCKLES	DIMENSIONS			
Name or position	Traceable axial extent (feet)	$1/2\lambda$ *1 (feet)	a *1 (feet)	Horizon
Stackpole Quay quarry buckle	230	20	15	C_2
Buckle south of Stackpole Quay anticline	84	30	15	C_2
Buckle south of Bullslaughter syncline, eastern end	2532	105	126	D_1D_2
Buckle south of Bullslaughter syncline, western end		127	105	D_1

Nb. (*1) Measured from anticline to syncline axis.

The essential geometry of a limb buckle (Fig.3.5C) is equally applicable to two adjacent minor folds on the limb of a major fold. By increasing its wavelength and amplitude a limb buckle can become a major fold, for example, the Angle syncline starts as a buckle on the northern flank of the Freshwater East anticline increasing gradually in size until it has structurally replaced the Pembroke syncline.

A limb buckle with an almost horizontal middle limb will form a structural terrace. Fig. 3.7 illustrates the visible western limits of the Freshwater East anticline, and the Orielton syncline reduced in scale to minor folds. In the west the northern limb of the syncline is complicated by two structural terraces apparently separated by a monocline.

The axes and axial planes of limb buckles reflect those of surrounding larger folds. (See Figs. 3.5A and C).

iii) Axial buckles

Axial buckles are restricted to the cores of large folds, being commonest in incompetent horizons (Fig. 3.5D). Within the field zones studied in detail axial buckles are found on the following folds: the Pembroke syncline at Lydstep (not seen), the Stackpole Quay anticline (Fig. 3.3), the Orielton anticline at Greenala Point (Fig. 3.8A and Plate 3.4) and the Angle syncline at West Angle Bay (Fig. 3.10 and Plates 3.5 and 3.6). Many of these buckles are accompanied by thrusts.

The axes and axial planes of axial buckles do not necessarily reflect those of the larger host fold. (See Figs. 3.5B and D).

(e) Ripples

The smallest scale of folding recognisable is a rippling of bedding planes which usually involves no reversals in steep dips, although it produces "b" lineations reflecting the axis of the host fold. In size ripples are variable, wavelengths being in the range 1-15 feet and amplitudes 2 inches - 2 feet. The acute angle the axial plane of a ripple makes with the dominant dip faces the direction of tectonic transport.

Ripples are common everywhere especially in alternating successions of competent and incompetent strata. (E.g. Fig. 3.9 and Plate 3.7).

Just south of Great Furzenip in steeply dipping marine Devonian shales is a 20 feet wide belt of intensely contorted strata. Individual fold wavelengths vary from 1-15 feet and amplitudes from

1/2-6 feet. Axial planes and axes are not systematically related to the major fold. In scale the folds are more akin to ripples but since dip reversals are the rule they can be thought of as unsystematic limb buckles. If individually these folds are unsystematic the two average modal dips of all limbs give on a diagram an overall axial direction of 10°.015° and an axial plane dip of 83°.006°. These attitudes compare closely with those of the major fold, the Castlemartin Corse anticline (Fig.3.11C).

IV DIPS AND FOLD SHAPE

Bedding dips vary from horizontal through vertical to inversion by 40°. The two most common ranges of dips 65°-100° and 35°-45° reflect the degree of fold asymmetry.

Inverted strata occur in the region of Stackpole Quay (inversion by 40°) and to a more limited extent on the southern limb of the Pembroke syncline east of Pembroke where inversion rarely exceeds 10°.

Most folds have straight limbs and in some instances there is an approach to the geometry of box folding. The outer parts of the Orielton syncline limbs are steep but on the inner sides of two hinges dips are much shallower (See sections $F-F^1$, $G-G^1$, $H-H^1$ of Fig.3.2). The western end of the same syncline also shows this effect although it is four times less wide (Section $B-B^1$ of Fig. 3.7). The Stackpole Warren anticline, of which only the northern limb is completely exposed (Section $A-A^1$ of Fig. 3.4) is a further possible example . The outer part of the limb dips north at 75° but south of a hinge, complicated by a thrust, the dip flattens out so that for 160 yards north of the anticlinal axis it is less than 10° (Plate 3.8). The southern part of section B-B[1] of Fig. 3.4 also illustrates another possible example of a box fold.

Most fold limbs are of unequal length, the Orielton anticline outer limbs, for example, being longer by a ratio of 3:1 than the inwardly dipping limbs of the adjacent major synclines. However, despite unequal limb lengths and fold asymmetry, nowhere is there a rachet style of folding. Neither is there an overall younging of beds to the north or south, each fold or group of folds stratigraphically compensating for the effect of adjacent ones. In addition the style of folding is harmonic. The folds south of the Ritec thrust therefore contrast with those north of the thrust where disharmonic folds and rachet profiles are common (Plate III, p.160 Strahan et al 1914).

Many of the differences in style are probably due to the dominantly incompetent succession of the Coalfield basin and the dominantly competent succession south of the Ritec thrust.

The style of folding within the Orielton uplift is neither entirely concentric nor similar, showing features of both. Where arch bends are exposed they are acute and a projection of beds above and below surface on a structure section results in a profile of folds which retain their form at depth. This characteristic would classify them with the similar group. Bedding slickensides and fracture cleavage planes, however, indicate that bedding-slip was outwards from synclinal fold cores in the stratigraphically higher beds; a characteristic of concentric folding. Exposed fold cores rarely show marked thickening of the crestal regions at the expense of the limbs. The fold style can be most closely compared with the Appalachian type of Willis (1893).

V FOLD AXES AND AXIAL PLANES

(a) Axes

All the principal folds of the area trend WNW.-ESE. and they generally plunge east. The exceptions to the general easterly plunge are the eastern part of the Angle syncline, the Freshwater East anticline, the western part of the Orielton syncline, the New Quay anticline and the eastern part of the Bullslaughter syncline. All these folds or parts of folds plunge west. The Orielton anticline has no overall plunge.

Average plunge inclinations are in the range of 5-15°, a plunge of 20° rarely being exceeded except on some of the axial buckles of West Angle Bay. Between north Freshwater West and West Pickard Bay the trace of fracture cleavage on bedding indicates a fold plunge of 20-35°, this lineation may, however, reflect a local direction of bedding-slip since where the fold plunge is exposed further west it does not exceed 15°.

(b) Axial Planes

Dixon (1921, p. 176) first noted the inwardly leaning fan of axial planes in the Orielton anticline relative to the centre line of the anticline, east of Pembroke, axial planes north of the Orielton syncline dipping south and everywhere south of the syncline dipping north. West of Pembroke, the Pembroke syncline is, however, a symmetrical fold, whilst the axial plane of its structural analogue the Angle syncline dips north at 80°. The axial plane of the Orielton syncline separating the outwardly leaning planes is nearly vertical.

Although most folds are asymmetric average axial plane dips are high, being from 65-85°.

Figs.3.11 and 3.5A-B depict stereographically the orientations of fold axes and axial planes for the various field zones, the general constancy of these directions across the area being readily appreciable.

CHAPTER 4 SUMMARY OF TECTONIC SEQUENCE AND STRUCTURES OF THE FOLD PHASE

I SUMMARY OF TECTONIC SEQUENCE

The minor structures can be placed in sequence and dated relative to one another by piecing together the evidence of cross cutting relationships. If one structure cuts cleanly across, distorts or displaces another it must be the younger. Veined structures are of less use in this respect since the vein may infill an early formed structural plane.

The structures of the Orielton anticline were produced during a sequence of tectonic sub-phases (outlined below) the order of which has been built up by correlating the evidence of age relationships collected from over the area. This sequence is being introduced at this point in order that the importance and significance of the detailed structural descriptions of Chapters 4 and 5 can be appreciated more readily.

FOLD PHASE

Sub-Phase 1. Folding. Structures produced comtemporaneously with and as a result of the folding

a) Slaty cleavage

b) Fracture cleavage and rotation joints

c) Inverse rotation joints

d) Bedding slickensides

e) Tension fractures related to bedding-slip

f) Radial tension joints at fold crests

g) Lenses in fold crests

h) Thrusts
i) Distorted sedimentary structures

Sub-Phase 2. Plastic flow and associated shearing

a) Distorted 'race' rods and curved irregular strike shears

Sub-Phase 3. Thrusting

a) Thrusts and thrust movements on pre-existing planes

b) Complementary strike shear joints

c) Miscellaneous strike joints

Sub-Phase 4. Shearing on down dip drag zones

a) Joints, joint-drags and downward facing drag folds

LATE FRACTURE PHASE

Sub-Phase 5. Wrench faulting

a) Wrench faults

b) Shear joints antithetic to wrench faults

c) Joint-shears

d) Lens belts and joint-drags

Sub-Phase 6. 'Wrench-jointing'

a) Lens belts and joint-drags

b) Primary and secondary shear joints

Sub-Phase 7. Veining and accentuation of earlier structures

Sub-Phase 8. Final adjustments

The two major phases are each divisible into four sub-phases and within each sub-phase all structures are probably of the same age.

Not all structures are present everywhere or equally developed in all lithologies.

II SUB-PHASE I: STRUCTURES ASSOCIATED WITH THE FOLDING

(a) Slaty cleavage

Slaty cleavage is present only in some of the K_2 calcareous shales of West Angle Bay (Plate 3.7). It was first noticed by Salter (1863, p.477) who compared the shales with the Carboniferous Slate of Southern Ireland.

In thin section slaty minerals are clearly aligned and the fissility is due to their parallelism rather than to very close spaced fractures.

Fig. 4.1A is a plot of cleavages from both limbs of the Angle syncline at West Angle Bay. It shows that cleavage attitude is largely unaffected by bedding dip; there being an anticlinal fan of cleavage planes about the axial plane. Cleavage planes which cut a small structural terrace on the north side of the bay (9007) do not vary their attitudes with the changes of bedding dip. Two of the cleavage attitudes (9021) on the southern limb of the syncline dip more gently north than the axial plane of the fold, their unusual attitudes may be due to the action of shearing stress rotating the planes during folding.

The line of intersection between bedding and cleavage planes is parallel to the axis of the Angle syncline (Fig.4.1A).

(b) Fracture cleavage and rotation joints

For the purposes of description Wilson's (1946 and 1961) accounts of fracture cleavage will be accepted since these accounts are distillations of many earlier ideas.

Fracture cleavage planes and rotation joints are equivalent structures, the term fracture cleavage being usually restricted to the close spaced fractures of incompetent rocks and the term rotation joints being applied to the wider spaced fractures of competent rocks (C.f. de Sitter 1956, p.100). Fracture cleavage planes usually make smaller angles with the bedding than do rotation joints. There is, of course, a complete graduation between the two types of fracture. However, in this account the term fracture cleavage will be used for both types unless the distinction is necessary.

Fracture cleavage occurs in all rock types and is equally developed on fold limbs and over fold crests.

Individual planes are usually restricted to a single bedding unit, although occasional prominent joints cut several bedding planes. Laterally their extent, as seen on bedding surfaces, is short, rarely more than 20 feet, usually being less than 10 feet.

It is difficult to generalise about the spacing of these fractures; in shales, mudstones and marls they are usually close spaced (1-5 m.m.), but since individual planes are often irregular they may intersect and split the rock into phacoids (Plate 4.1).

In thick-bedded limestones the fractures are wider spaced (1 inch-3 feet), frequently occurring in localised swarms of slabby joints, varying considerably in regularity. In thinner bedded or argillaceous limestones the planes are usually more closely spaced (1 inch-1 foot) although often irregular.

Rotation joints in sandstones may be closely spaced (1-6 inches) and regular if the rock is soft or marly (Plate 4.2). In harder sandstones they are usually wider spaced and more irregular. In very hard well-lithified conglomerates the planes are often spaced half an inch apart, cutting evenly through both pebbles and matrix. Those in less well lithified conglomerates may be spaced 2-4 feet apart.

At most stations a few planes are prominent and between them minor ones may be more closely spaced. For a given lithology cleavage planes are equally developed on fold limbs or at fold crests.

TABLE 4.1.

Frequency of fracture cleavage planes. Lower Old Red Sandstone rocks, Angle cliffs. Average frequency per foot.

Rock type	F	Rock type	F
Marl	19	Laminated sandstone	7
Marl	13	Fine-grained sandstone	7
Marl with 'race'	19	Medium-grained sandstone	9
Marly sandstone	17	Sandstone	9
Fine-grained marly sandstone	4	Sandstone	8
Thinly laminated hard sandstone	4	Hard sandstone	7

The lithological descriptions are, of course, partly subjective but the table shows the general although not universal correlation between competency and spacing.

Occasionally marls contain only a few wide spaced (6+ feet) rotation joints (Plate 4.3), usually planes which are continuations of prominent ones in adjacent competent bands. Possibly in plastic beds, such as these marls, any early formed fracture cleavage planes healed as the rock progressively deformed and only at a late stage when the rock, perhaps, was behaving more rigidly, did a final set of rotation joints form by projection from adjacent competent beds.

The smoothest and most regular planes are not necessarily confined to the incompetent rock types, homogeneity probably being a more important factor controlling the smoothness of the fractures. Since, however, most shales are homogeneous their fracture cleavage planes are usually smooth. Many marls, though, contain calcareous concretions and around these 'race' blebs the cleavage planes tend to break. In other marls intersecting cleavage planes split the rock into small diamond shaped phacoids. The smoothest planes recorded occur in a hard, fine grained siliceous sandstone of the Lower Old Red Sandstone (8002). Quartzites often contain many individually smooth planes occuring in irregular sets. In general rotation joints are more irregular than fracture cleavage planes. Rotation joints are at their most irregular in thin-bedded limestones, especially when the limestones are intercalated with mudstones, rocks of this type being common in the Z and C sub-zones. In many moderate to steeply dipping S_2 and D_1 limestones the gently dipping rotation joints frequently occur as swarms of slabby fractures. Each swarm is usually restricted to one bedding unit, across a bedding plane or laterally along the strike they may be entirely absent, and their place taken by a similar swarm of inverse rotation joints.

The surfaces of many rotation joints are coated with calcite, when they cut limestones, and more rarely with quartz when they cut sandstones. Occasionally the vein material is slickensided or striated, the lineation lying perpendicularly in the plane of the fracture from the local fold axis (Fig. 4.1B).

Fracture cleavage planes in the axial buckle belt on the north side of West Angle Bay are frequently so irregular in strike that they enclose between them long diamond shaped units of limestone. The resulting rock resembles a breccia.

There was some thrust movement along a few fracture cleavage planes. Each fracture plane may show a small amount of movement (1/8-1 inch) or a single plane may show all the displacement which may be up to 20 feet (Plates 4.3 and 4.5). The smaller movements probably occurred as the cleavage formed but the larger displacements on isolated planes possibly belong to a later thrust phase.

The angle between a fracture plane and the bedding (γ) depends on both lithology and the position of the rocks in a fold. In general γ is lower in incompetent rocks than in competent rocks providing they occupy equivalent structural positions. Tables 4.2. - 4.3. illustrate γ values for different rock types occurring in areas of similar structure.

TABLE 4.2.

γ, Lower Old Red Sandstone rocks North limb, Castlemartin anticline. Angle cliffs.

Rock type	γ	Rock type	γ
Basal conglomerate	97°*	Marly sandstone	87°
Sandstone	86°	Marly sandstone	72°
Sandstone	82°	Marly sandstone with 'race'	76°
Sandstone	73°	Marl with 'race'	82°
Sandstone	68°	Marl with 'race'	74°
Sandstone	66°	Marl with 'race'	62°
Hard sandstone	77°	Marl	73°
Fine Sandstone	54°	Marl	56°

* γ values greater than 90° probably indicate insufficient sampling of irregular structures.

TABLE 4.3.

γ, Dinantian rocks From fold limbs of similar dip. Stackpole

Rock type	γ	Rock type	γ
S_1 mudstone	65°	S_2 thick-bedded limestone	95°
S_1 mudstone	41°	S_2 thick-bedded limestone	89°
S_1 thin-bedded limestone	83°	S_2 thick-bedded limestone	74°
S_1 thin-bedded limestone	81°	D_1 thick-bedded limestone	85°
S_1 thick-bedded limestone	87°	D_1 thick-bedded limestone	73°

The relationship between γ and bedding dip is not so simple. However, where the dip is less than 10°, γ usually approaches 90° for all rock types.

TABLE 4.4.

γ, rocks from areas of less than 10° dip

Rock type	γ	Rock type	γ
Marl	80°	Sandstone	77°
Marl with 'race'	88°	S_2 thick-bedded limestone	88°
Soft sandstone	88°	D_1 thick-bedded limestone	101°
Sandstone	72°	D_1 thick-bedded limestone	84°

For steeper dips γ does not necessarily decrease with increasing dip as Table 4.5 shows.

TABLE 4.5

γ, marls on the limbs of the Freshwater East anticline Freshwater East Bay

N.limb. Dip 82°.007°		S.limb. Dip 69°.209°	
Rock type	γ	Rock type	γ
Marl	82°	Marl	54°
Marl	78°	Marl	32°
Marl	75°	Marl with 'race'	41°
Marl with 'race'	77°	Marl with 'race'	37°

Sandstones from the two limbs show no marked differences in γ but the incompetent marls illustrate well the possible differences which can occur.

Fracture cleavage planes in Silurian rocks are similar to those in equivalent rock types of the Old Red Sandstone. On the north side of Freshwater East rotation joints in the Ludlovian pass without deflection into the basal conglomerate of the Old Red Sandstone.

Ordovician shales are only well exposed at Freshwater West. There, Dixon (1921 p.11) records both repeated folding and steep cleavage planes, neither of which have been found during the course of the present research. Perhaps this was due to Dixon being able to examine an unusually large foreshore outcrop which had been cleared of its sand cover during a storm.

The acute angle a fracture cleavage plane makes with the stratigraphically higher bed is commonly regarded as pointing in the direction of tectonic transport (Wilson 1946 p.277). Fracture cleavage planes in inverted strata dip in the same direction as the bedding but less steeply (Fig. 4.2A), unless the amount of inversion is small and γ is high ($90-\gamma$, < inversion), when the acute angle faces downwards on the undersides of exposed bedding planes (Fig. 4.2B).

Because, as is being accepted here, a fracture cleavage plane develops perpendicularly to the direction of bedding-slip during folding, it follows that the bedding-cleavage intersection should trace the fold axis (Wilson 1946 p.278) (Fig. 4.3B and Plate 4.6). Any fold limb is, however, shared between two adjacent axes, and if these axes have slightly different trends and plunges the trace of the fracture on the bedding is therefore not necessarily parallel to either. It should, nevertheless, be perpendicular to the local direction of tectonic transport. Here, this direction will be referred to as the local fold axis. Figs. 4.1 D-F illustrate axial directions and cleavage-bedding intersections.

(c) Inverse rotation joints

The characters of inverse rotation joints are similar to those of rotation joints although they are less common, being present in only 43% of the analysed stations. They intersect the bedding along a line which, symmetrically about the bedding strike, is the inverse of the local fold axis (See Figs. 4.3B and 4.1D and Plate 4.7). A second but unnamed fracture cleavage set figured by Voll (1961, p.549, Fig. 18a) from a monoclinal fold in St. Brides Bay, Pembrokeshire, undoubtedly belongs to this class of fracture.

Inverse rotation joints are present only on the limbs of folds. They are absent at fold crests.

Details of the symmetry of inverse and local fold axes are given in Appendix III. Although the Table shows that the angle between the axes about the bedding strike is not constant, $37^\circ \pm 11^\circ$ is a representative mean value. This angle does not vary systematically with the position of the fractures on the fold limb, bedding dip, lithology or fold plunge. In only a few cases are the inverse and fold axes perfectly symmetrical about the bedding strike, one axis usually plunging 10° more steeply than the other. This variation is also unsystematic.

The angle γ can be measured for these fractures in the same way as for rotation joints, and Table 4.7 compares characteristic average γ values for rotation and inverse rotation joints.

γ values differ little for the two types of fractures, perhaps in general being higher for inverse rotation joints. However, it is not possible to compare them directly since inverse rotation joints are restricted to competent horizons where the bedding dip exceeds 50°.

In Old Red Sandstone rocks inverse rotation joints are more common in thin sandstone bands intercalated between marly rocks. On the north side of Freshwater East the inverse rotation joints are unusual since they are large planes, only between six and four fractures being present in each station. Inverse rotation joints are absent where slaty cleavage is developed.

TABLE 4.7.

rotation and inverse rotation joints

Structural position	Lithology	γ(R)	γ(IR)
N.limb Pembroke syncline	S_2 limestone	84°	83°
S.limb Pembroke syncline	S_2 limestone	85°	85°
S.limb Broadhaven syncline	S_2 limestone	74°	93°
N.limb Broadhaven syncline	S_2 limestone	89°	90°
N.limb Bullslaughter syncline	S_2 limestone	95°	90°
S.limb Bullslaughter syncline	D_1 limestone	83°	73°
S.limb Bullslaughter syncline	D_1 limestone	76°	86°
S.limb Castlemartin anticline	Upper ORS.	89°	100°
N.limb Angle syncline	Lower ORS.	86°	105°
N.limb Angle syncline	Z limestone	87°	89°
S.limb Angle syncline	Lower ORS.	84°	100°

Inverse rotation joints are spaced at the same intervals as rotation joints in those lithologies such as sandstones and limestones where they are equally developed.

Although inverse rotation joints may be veined by calcite or quartz up to 1/4 inch thick they are never slickensided, neither have displacements across inverse rotation joints been recorded. At one station (5212) inverse rotation joints have been distorted by bedding-slip and their distortion indicates upwards slip of the stratigraphically higher beds out of the synclinal core.

(d) Bedding slickensides

Bedding slickensides or striations are developed only in vein materials occurring as veneers on bedding planes. Bedding planes in limestones are coated with calcite and in sandstones with quartz. Although slickensided bedding plane veins are uncommon they characteristically consist of alternating fine laminae of vein material and rock, the average thickness of most laminae being 1 mm.

Usually there is a single lineation lying perpendicular to the fold axis. At station 2006 a single set of slickensides is related in a similar way to the inverse axis.

At two stations (6001 and 600 feet south of 4011) two bedding slickenside directions occur, one set of slickensides being related to the fold axis, the other to the inverse axis (Fig. 4.3A and 4.3C and Plate 4.8). The lower layers are always related to the fold axis, and the upper layers to the inverse axis.

Of two sets of slickensides in calcite at station 2011, the stratigraphically higher set is related to the inverse axis, whilst the lower set is parallel to the inverse axis.

(e) Tension fractures related to bedding-slip

Wilson (1946, p.287) has shown that tension fractures can be produced by the action of a bedding-couple during folding. In this part of Pembrokeshire such tension fractures are uncommon joints. They are most frequently found where distorted fracture cleavage planes indicate continued bedding-slip and forced deformation (Wilson 1946, p.279) of the fracture cleavage. Generally these tension fractures lie at 30° to the bedding and are thus easily confused with strike shear joints. They extend only for short distances from bedding planes, often in belts of sygmoidal en-echelon lenses (Plate 4.1). Unfilled tension joints may also be sygmoidally deformed in the same sense as the fracture cleavage (Fig. 3.8B).

Tension joints due to bedding-slip should intersect the bedding along fold axis traces, they are, however, too rare for this hypothesis to be rigorously tested.

(f) Radial tension joints at fold crests

Fractures of this type which are profusely illustrated in most geological textbooks are very rare in south Pembrokeshire. Some possible examples occur on the outer arch bend of a small anticline in the Stackpole Quay quarry (5040). The crestal parts of many axial buckles at West Angle Bay are shot through by irregular veins of calcite, also possibly due to the stretching of the outer parts of the folds. Occasionally associated with ripples (e.g. at 9021) are gaping tension cracks at right angles to the bedding (Fig. 3.9B).

(g) Lenses in fold crests

The parting of bedding planes in the crestal parts of folds and the subsequent infilling of the voids is also very uncommon. Lenses of this type do, however, straddle for two or three feet some of the axial regions of buckles at Greenala Point (Fig. 3.8B). Striations on the outer parts of these lenses lie perpendicular to fold axes.

(h) Thrusts

As the folds formed some, no doubt, ruptured; one part being carried over another on a thrust. Due to the difficulty of distinguishing thrusts of this type from the later ones belonging to sub-phase 3, all thrusts will be described in sub-phase 3.

(i) Distorted sedimentary structures

i) Concretionary 'race' rods

These concretionary cornstones were first named and described by Jones (in Cantrill et al.1916, p.90) and then in the present area by Dixon (1921, p.29). The term 'race' is used to describe rods of concretionary limestone 1/4 inch apart and up to 1/2 inch across set in marl. These rods are tectonically important because, as far as is known, they originally formed normal to the bedding and therefore they provide a rigorous control at right angles to the bedding which can be used to measure the distortion of a rock mass.

'Race' rods in the Orielton anticline are parallel to fracture cleavage planes, running obliquely down their dips at right angles to local fold axes. Their orientation is directly comparable to the orientation of slickensides on fracture cleavage planes (Figs. 4.1C 4.4G and Plate 4.9).

In some marls the rods dominate, so that the rock is almost a limestone. As the rods coalesce they may follow a further planar direction (Plate 4.9).

Fracture cleavage planes rarely cut the rods, so that the spacing of the planes is controlled by the width of the rods. In section the rods are roughly circular but each one individually is so irregular that any deformation to an ellipse that it may have suffered is not measurable.

ii) Limestone rods

Similar sedimentary structures to the concretionary 'race' rods of the Old Red Sandstone are limestone rods set in mudstones contained in a sequence of intercalated C_2S_1 mudstones and limestones in the coré of the Murchison syncline at Stackpole Quay. These limestone rods are oriented parallel to fracture cleavage planes (See Plate 4.10) in the centres of the mudstone bands, whilst at their margins they trail off parallel to the bedding. This trailing off is probably due to bedding drag and the 'forced' deformation of the rods.

Other distorted sedimentary structures have not been investigated in any detail.

III SUB PHASE 2. PLASTIC FLOW AND ASSOCIATED SHEARING

During sub-phase 2 the Old Red Sandstone concretionary rods of 'race' were distorted for a second time. The effect of this deformation is noticeable only in the marls of Freshwater East, especially those on the north side of the bay. There, the 'race' rods in a bed of marl may be distorted so that it appears as if the slip of adjacent bedding planes past one another was both laterally left and right handed and vertically both upwards and downwards (See Figs. 4.4B-F and Plate 4.11). The lengths of several of the chains of rods on the north side of the bay have been measured and compared with the present thickness of the band. The average ratio of present to original (i.e. prior to sub-phase 2) thickness of the bands is 0.9.

The irregular shears, also produced during this sub-phase, are not necessarily restricted to 'race' beds. They occur in many other marls and also in a few soft sandstones, especially from the lower Old Red Sandstone. In 'race' beds they are particularly common in the regions of maximum curvature of the rods. The average dip of the shears is similar to the dip of the bedding although frequently slightly lower. These irregular shears can be most closely compared to a group of small intersecting basins resting the right way up between bedding planes. It is difficult to generalise about the degree of curvature and spacing of irregular shears, the smaller shears are often 6 inches to 1 foot across and 3 to 6 inches deep, being spaced about 3 inches apart. The larger more widely spaced shears are usually more gently curved.

The walls of the shears are frequently slickensided or coarsely striated (Fig. 4.4A). These are the only fractures in the area, where the wall rocks are slickensided. The striae often radiate out sub-horizontally from the deepest parts of the basins. When the marls are red a thin film of green marl often coats the shear.

The shears cut cleanly across and sometimes unsystematically displace the earlier formed fracture cleavage planes.

IV SUB-PHASE 3 THRUSTING

The structures of this sub-phase cut and displace those of the two earlier sub-phases although relative to one another they are difficult to date.

(a) Thrusts and thrust movements on pre-existing planes

Thrusts are not as common in the Orielton anticline as Dixon (1921) or Anderson (1951) suggest. For example, no evidence has been found for the large thrust which Dixon marked as emerging on the coast near Greenala Point.

Only 26 thrusts or thrust belts have been recorded from the field zones, of these 12 are closely associated with buckling, 11 correspond to fracture cleavage planes, 4 are in part parallel to bedding planes and only 10 are typical low-angle cross cutting thrusts. Many thrusts, of course, belong to more than one of the above groups. Only five thrusts dip at less than 45°. Most thrusts trend rather more E.-W. than do the fold structures.

Low angle cross cutting thrusts are illustrated on Figs.3.3., 3.4, 3.6 and 3.10 and Plates 3,5, 4.13 and 4.14. Thrusts parallel to fracture cleavage planes on Fig. 3.7 and Plates 4.3 and 4.5, thrusts associated with bedding slip on Figs. 3.3 and 3.4 and Plate 3.8. and corresponding with strike shear joints on Fig. 3.8A.

Belts of breccia are not commonly associated with thrusts although the rocks for one or two feet on either side of a thrust may be intensely sheared, and occasionally recrystallised. The thrust plane is often coated with quartz or calcite which may be slickensided.

The thrust illustrated on Plate 4.14 is marked by 6-9 inches of coarse unlaminated breccia and clearly cross cuts both fracture cleavage planes and poorly developed irregular shears of sub-phase 2.

The thrust bringing K_2 shales over Z limestones on the north side of West Angle Bay, (Plate 4.13) is a scalloped shaped plane, the axes of the ridges running down dip parallel to slickensides. Smaller scallops break the smooth curves of the larger ones, the larger have wavelengths of 30-40 feet and amplitudes of 1-2 feet, the smaller 5 feet wavelengths and 6 inch amplitudes. Bedding drag against thrusts is uncommon, usually being restricted to a narrow zone beneath the plane (Plate 4.13). Investigated thrust displacements are small, usually being less than 20 feet.

Many thrusts probably formed during the phase of folding but others clearly cross cut structures associated with the folding (Plate 4.14). Movement may have occurred several times on some thrusts.

Thrusts are rarely accompanied by parallel joint sets and no instances of conjugate pairs are recorded. Many of the isolated miscellaneous strike joints listed in Appendix I may belong to this part of the sub-phase.

(b) Complementary strike shear joints

Although low angle thrust joints are rare, complementary pairs of strike shear joints at low angles to the bedding are more widespread (Fig. 4.5A). The intersection between a pair of joints is usually parallel to the local fold axis, the acute bisectrix being parallel to the bedding and at right angles to the local fold axis and the obtuse bisectrix being normal to the bedding. Complementary pairs of strike shear joints have been recorded from 11 of the analysed stations. However, many single isolated strike joints at less than 45° to the bedding also trace the fold axis on the bedding and these joints may also belong to this fracture class.

Some strike shear joints act as small overthrusts (less than 3 feet of movement) relative to stratification planes, but whether or not the actual displacements are of the 'thrust' or 'normal' type depends on the dip of the beds. If the strata are steeply dipping one or both sets of strike shear joints may show 'normal' displacements (Fig. 4.5B). Strike shear joints are rarely continuous across stratification planes (Plates 4.15 and 4.16). Accentuated cross bedding planes in some of the sandstones of the Old Red Sandstone suggest that they may have acted as shear planes.

If only one of the complementary shears is developed it usually dips more steeply or in the opposite direction to the bedding (70% of the 27 examples). It is impossible to generalise about the spacing of strike shear joints since they are often isolated fractures, when common they are frequently only 6 inches apart. One set of a complementary pair of strike shear joints is usually dominant. At station 7061 one set of a complementary pair corresponds to a series of joint-drags, each of which distorts the fracture cleavage in a 1/4 inch wide zone.

Quartz or calcite, according to the host rock type, vein many of the shears, any slickensides always being in the vein material and not on the rock surfaces. Such slickensides lie at right angles to local fold axes (See Table 4.8).

TABLE 4.8

Slickensides on strike shear joints

Axis calculated from slickensides	Axis calculated from bedding-rotation joint intersection
21°.096°	26°.097°
20°.116°	33°.095°
18°.102°	10°.095°
19°.098°	02°.287° (Slaty cleavage)

Appendices I and II give full details about analysed strike shear joints. Appendix II shows θ to be variable, although 37° can be regarded as a representative mean. Appendix II, Table I, also shows the close parallelism between the intersections of the complementary strike shear joints and local fold axes. Many isolated strike joints also intersect the bedding parallel to local fold axes.

Strike shear joints cross cut, distort and occasionally displace fracture cleavage planes and the irregular shears of sub-phase 2.

(c) Miscellaneous strike joints

In addition to strike shear joints subtending low-angles with the bedding many other less systematic strike joints at higher angles than 45° to the bedding occur. These miscellaneous strike joints also intersect the bedding parallel to local fold axes.

Several sets deserving fuller treatment than is possible in the Appendices are described in more detail overleaf.

i) Minor thrusts, Freshwater East

These thrust joints dipping 17°.069° occur only in the Ludlovian rocks of station 3001 (Plate 4.17). The fractures are smooth, spaced 3 inches to 1 foot apart and each plane displaces Ludlovian strata for 1/2-1 inch. These thrust-joints intersect the bedding along 16°.091°, that is, sub-parallel to the local inverse axis.

ii) Oblique low angle minor thrusts, Little Furzenip

These fractures are restricted to the Lower Old Sandstone rocks of Little Furzenip (7070 and the rocks east of that station) where they dip 29°.127°, and to the Skrinkle Sandstones north of Stackpole Quay (5000) where they dip 33°.132°. The fractures are spaced 4-5 feet apart and across each of the large planes strata are displaced northwards 1-3 inches. The thrusts cut all of the bedding and fracture cleavage planes immediately adjacent to them (Plate 4.9). The thrust-joints intersect the bedding parallel to local fold axes, subtending angles of 69° and 56° respectively with the bedding. Below some of the shear planes closely spaced (1/2 inch) minor joints splay off in a zone up to 2 inches thick. For the two investigated examples of such joint combinations the two fracture sets intersect along 08°.047° and 28°.100°.

V SUB-PHASE 4 SHEARING ON DOWN DIP DRAG ZONES

Down dip drag zones are shear zones in which cleavage and bedding planes are displaced 'normally'. They are strike fractures which could be easily confused with strike shear joints if their displacements were not detectable. Down dip drag zones are restricted to the three western coast field zones and from them only 10 have been recorded in the analysed field stations. In form the drag zones vary between joints, joint-drags and small downward facing drag folds (Fig. 4.6 and Plates 4.5, 4.16 and 4.18). Isolated broad (Y = 5-10 feet) downward facing drags characterise the Freshwater West section (Fig. 4.6A). At station 8001 some of the joint drags of this sub-phase contain infilled en-echelon tension gashes (Fig. 4.6C). At station 9024 a few intense down dip drag folds are developed between shear planes which eventually merge with the bedding (Fig. 4.6B).

The attitude of the zones is unrelated to the stratal dip although they usually intersect the bedding sub-parallel to local fold axes.

It is difficult to date the down dip drag zones relative to some of the later fold phase divisions. They clearly distort fracture cleavage planes and cross cut irregular shears of sub-phase 2 (station 8001) and at station 8013 a knick plane probably distorts a thrust developed parallel to fracture cleavage (Plate 4.5). Joint-drags at station 8001 cannot be matched on either side of a prominent minor thrust, and at station 7015 strike shear joints do not cut the drag zone (Plate 4.16), scattered evidence which suggests that this sub-phase of 'normal' or 'gravity' shear postdated the thrusting of sub-phase 3.

CHAPTER 5 STRUCTURES OF THE LATE FRACTURE PHASE AND THE SYMMETRY OF MINOR STRUCTURES

I SUB-PHASE 5 WRENCH FAULTING

(a) General geometrical considerations

The shear planes of this sub-phase are all related to fold geometries in a similar manner (Fig. 5.1A), complementary pairs of planes lying symmetrically about the axes of the folds which they cut with the obtuse bisectrix (σ_z)* parallel to the fold axis. The acute bisectrix (σ_x) is either normal to the axial plane of the host fold or near horizontal, whilst σ_y is at right angles to the other two axes. These orientations imply that the ($\sigma_y \sigma_z$) plane corresponds to the axial plane of the fold. Wrench faults similarly related to axial planes have been described from the Girvan area by Williams (1959,pp.644-645).

(b) Wrench faults

The system of complementary wrench faults in south Pembrokeshire is already well known from the work of Dixon (1921) and Anderson (1951). Figs. 3.1 and 5.1B show that the simple division of all the wrench faults of the area into either the primary sinistral or dextral classes is unrealistic. Although the two maxima correspond

* In this chapter the symbols σ_x, σ_y and σ_z will be used to describe the geometrical directions: the acute bisectrix, the line of intersection between shears and the obtuse bisectrix, without implying the stresses which these symbols represent.

to the two major classes the range of strike directions is greater, a shallow saddle separating the maxima. No doubt part of this wide spread of directions is due to the mapping of faults along hollows and wet courses which they do not necessarily follow, but it must also reflect a greater diversity of fault orientations than was suggested by Anderson.

Wrench faults show displacements from less than one inch to half a mile, although the average is only a few hundred feet. A typical small fault is illustrated on Plate 5.1. NNW. trending faults are dextral and NNE. trending faults sinistral, as Fig. 3.1. shows dextral faults outnumber sinistral faults. During this survey regions where sinistral faults are dominant have been sampled, this bias has arisen accidentally due to the particular patterns present in the field zones which were chosen for study.

Wrench faults were formed after the fold phase since they displace fold axes and thrusts, in addition they cut across or distort minor structures associated with the folding. In this part of the Armorican fold belt there is, as far as can be ascertained, complete geometrical congruity of fold structures across wrench faults (c.f. George 1940 and Gill in Coe et al 1962).

Only on either side of the largest faults (e.g. faults I and III of Fig. 3.1) are there wide belts of shattering, most faults with displacements of greater than one foot are, however, usually accompanied by zones of gouge or breccia up to one foot wide (Plate 5.2).

Slickensided fault surfaces are rare and when present the lineations are usually near horizontal, often lying normal to the line of intersection between the fault and its complement. Bedding drag against faults is also uncommon being best developed where a fault abuts incompetent strata (e.g. Fig. 5.5). Contemporaneous joints parallel to faults are rare, usually being restricted to the area immediately surrounding the fault.

(c) Systematic descriptions of wrench faults

i) Lydstep (Fig. 5.2)

On the north side of the bay all faults are dextral although displacements are rarely detectable, the movement sense being derived from bedding drag adjacent to the faults. The average fault attitude is 80°.073°, the faults therefore dip in the same sense as the fold plunge. Most fault planes are veined by calcite up to 3 inches thick and may be accompanied by breccia belts up to 2 feet wide.

The complementary set of faults on the south side of the bay is more typical of the pattern in the Orielton anticline, the acute bisectrix of the shears being normal to the axial plane of the fold and the obtuse bisectrix sub-parallel to the fold axis. The average θ value for complementary pairs is 16°. Dextral wrenches (E.g. Plate 5.3) are more common than sinistral wrenches and frequently display greater displacements, even these, however, rarely exceed 4 feet. Fault gouge is rare although most fault planes are veined with calcite up to 6 inches thick.

ii) Freshwater East (Fig. 5.3)

Both sinistral and dextral wrench faults are common although sinistral faults are dominant. Fig. 5.3 shows σ_z plunging west less steeply than the fold axis, however σ_z is parallel to the average bedding-fracture cleavage line of intersection. The $(\sigma_y\sigma_z)$ plane is not so obviously related to the axial plane of the fold as it is on the south side of Lydstep Haven, nevertheless the two planes are nearly parallel. The average ϑ value for complementary shear pairs is 16.5°.

Accompanying the larger faults are belts of breccia up to 18 inches thick, veining of the planes is, however, uncommon.

Two (3013 and 100' E. of 3003) of the faults are of special interest since in the higher parts of the cliff they curve over until their attitudes are transitional between sinistral wrench faults and north dipping thrusts (Plate 5.4). The western example, on the foreshore is a near vertical fault trending 220° although higher in the cliff its dip has become 41°.324°. The thrust components of both faults are accompanied by only half an inch of breccia.

The faults on the southern side of the bay do not form such a well defined pattern as those on the northern side. All the major faults are sinistral, or presumed to be sinistral from their attitudes, displacements being difficult to detect.

iii) Greenala (Fig. 5.4)

The fault pattern of Greenala Point is unusual since apart from the large sinistral wrench cutting the Orielton syncline axis there is no system of complementary wrench faults. Across none of the three faults shown north of Greenala Point on Fig. 5.4 can the sense of displacement be detected, although in all cases there is a lack of continuity of the near horizontal beds across the faults, evidence which suggests dip-slip movements. The attitude of the fault dipping at 54°.325° is similar to that of the thrust component of the two wrench-thrust hybrids on the north side of Freshwater East. Perhaps, therefore, these faults at Greenala are partly thrusts.

Half a mile west of Greenala Point a complementary wrench pair displaces the eastern end of the Castlemartin anticline. The stereogram accompanying Fig. 5.4 illustrates the fault attitudes and geometries relative to the fold.

iv) Stackpole (Figs. 3.3 and 3.4)

Two major dextral faults cut the field zone, they are the Stackpole Quay fault (Fig. 3.3) and the Stackpole Warren fault (Fig. 3.4). The Barafundle syncline axis is possibly displaced half a mile by the Stackpole Warren fault, which where it is exposed east of Broadhaven Bay is a vertical fault, marked by two 10 feet wide, red stained belts of gouge. Separating the two arms of the fault is a 170 feet wide zone of shattered limestone.

The Stackpole Quay fault (Fig. 3.3 and Plate 5.2) displaces the Murchison syncline axis dextrally for 230 feet. On the north side of the Quay the fault dips 75°.075° and is marked by two feet of fine gouge. West of the fault in mudstones prominent antithetic shear joints splay off in a zone two feet wide. Where the fault cuts the coast near Barafundle Bay it dips at 74°.080° and is marked by three feet of gouge. The attitude of the exposed part of the fault is unusual since it dips in the same sense as the fold axes which it cuts.

v) <u>Bullslaughter</u> (Figs. 3.1 and 3.6)

At Flimston Bay, the Flimston bay fault (Fault III of Fig. 3.1) displaces the Bullslaughter syncline axis dextrally for 2600 feet. In the bay the fault consists of three major planes all trending 145°, some dipping 80° west, others 80° east. Each plane is accompanied by 1-2 feet of fault gouge and the rocks on either side of the fault belt are shattered for 340 feet. The western plane which bounds a mass of Triassic collapse breccia bears slickensides oriented 14°.143° showing the last movement to have been nearly horizontal, probably normal to the axial plane of the Bullslaughter syncline.

vi) <u>Freshwater West</u> (Fig. 5.5)

At Great Furzenip (Fig. 5.5B) the Flimston Bay fault displaces the top of the marine Devonian shales 485 feet. East of the main fault there is a pattern of complementary minor wrench faults, intersecting at an average dihedral angle of 40°. West of the main fault the bedding drag in Lower Limestone shales contrasts with the unvarying strike of the competent Skrinkle sandstones where they abuts the fault.

At Little Furzenip (Fig. 5.5A), close to the northern end of the Flimston Bay fault the total strike slip has been reduced to 210 feet. East of the main fault there is a well developed system of splay faults intersecting the main fault at low angles. A minor dextral wrench west of the Flimston Bay fault is illustrated on Plate 5.1.

vii) Angle Cliffs (Figs. 3.7 and 5.6)

From the north side of Freshwater West to west of West Pickard Bay most wrench faults are sinistral and due to the steep plunges of local fold axes frequently deviate by more than 20° from the vertical. The system of faults at station 8003 is characteristic of the sub-zone and is illustrated on Fig. 5.6. Although the attitude of the axial plane of the host fold (the Orielton anticline) is not known the geometry of the complementary faults reflects the steep plunge of the local fold axis. The average angle of θ for these faults is 18°.

In the western part of the sub-zone complementary wrench faults displace both synclinal and anticlinal axes. Dixon (1921, p.182) having regarded the displacement of anticlinal axes by wrench faults as rare this example, together with others, is of special significance.

viii) West Angle Bay (Fig. 3.10)

A clearly defined system of wrench faults is present only on the north side of the Bay where most faults are sinistral. A small sinistral fault at station 9012 (Fig. 3.10) displaces a thrust which brings K_2 shales over Z limestones. This is the only observable example in the area of a thrust being cut and displaced by a wrench fault.

(d) Shear joints antithetic to wrench faults

Associated with a few wrench faults are complementary antithetic shear joints, usually restricted to one side of the fault, frequently the dip direction side. Their usual extent is a few feet from a fault although within this narrow zone there may be many closely spaced fractures (See Plate 5.2). Where antithetic shear joints are developed other late fractures are usually rare. These antithetic shear joints being complementary to the wrench faults are related to fold geometries in the same way as the faults are. The average value of ϑ for a wrench fault with its antithetic joint is 19°.

(e) Joint-shears

The field term joint-shear, chosen for brevity, has been used to describe the association of a prominent major shear plane with small closely spaced antithetic shear joints splaying off the major plane (See Fig. 5.7 and Plate 5.5). If the major shear is a small fault (Fig. 5.7B) the antithetic splays may be sygmoidally distorted. In most cases the major plane is not a fault and then the antithetic joints are smooth planar fractures. Rotation joints crossing the joint-shear are rarely distorted although within the shear zone they are usually more prominent than in the surrounding rocks. The major shear may extend laterally for more than six feet and several major shear planes may be developed within a few feet of each other, despite their absence in other parts of the same rock mass.

Antithetic splay joints are often spaced a half to one inch apart and they rarely extend for more than six inches from the major shear. Frequently (56% of the analysed cases) the antithetic splay joints occur only on one side of a major shear, usually the dip direction side.

Joint-shears are not evenly distributed throughout the succession nor are they common in all rock types. Out of 37 sets, 32 occur in the Lower Old Red Sandstone, 2 in the Upper Old Red Sandstone, 2 in the K zone and 1 in the S_2 zone of the Carboniferous. Within the Lower Old Red Sandstone they are most common in soft sandstones, being rare in both marls and quartzites.

Sinistral joint-shears are more common than dextral joint-shears, of the analysed examples 28 are sinistral and 9 dextral. The dominance of sinistral joint-shears may possibly be correlated with the dominance of sinistral wrench faults in the field zones which were sampled in the area.

At Greenala Point because the stratal dip is low, joint-shears lie parallel to wrench-joints (See Plate 5.6), occasional wrench-joints arising out of antithetic splays.

The geometrical relationships between joint-shears and folds are the same as between complementary wrench faults and folds. Stereogram C of Fig. 5.7 illustrates the geometries of joint-shears from the north side of Freshwater East relative to the fold structure. The direct correlation between the $(\sigma_y\sigma_z)$ plane and the axial plane of the fold is not precise, although σ_z is clearly parallel to the fold axis plunge.

Values for the angle ϑ for joint-shears have been derived and appear to be inversely related to bedding dip.

TABLE 5.1

ϑ for joint-shears compared with stratal dip

Nos. of readings	Bedding inclination	ϑ
6	84°	27.0°
10	82°	19.0°
4	69°	22.0°
2	63°	22.0°
1	55°	22.0°
5	48°	23.0°
2	22°	22.5°
4	<20°	23.0°
2	<20°	24.0°

There are, however, too few readings in each class to test the significance of this table. The average value for the angle ϑ for all joint-shears is 22°.

(f) Lens belts and joint-drags

En-echelon tension fractures indicating active shear along a fracture have been previously described by many authors including Cloos (1932, feather fractures), Shainin (1950) and Dawson-Grove (1955, h and k planes). These structures although more characteristically associated in this area with wrench-joints are occasionally parallel to wrench fault planes. Despite the existing wide nomenclature describing these structures the term lens belt will be used in this thesis since the name suggests the appearance of the structure (See Plates 5.8 - 5.10), and the individual parts of the name can be applied to the two parts of the structure. The term lens will be used to refer to the tension fractures and the term belt to refer to the shear plane. The general characters of lens belts will be treated more fully in the appropriate section of the wrench-joint sub-phase.

Plate 5.3 illustrates a lens belt parallel to a wrench fault at station 2017 on the south side of Lydstep Haven, the lenses intersect the belt parallel to the intersection between adjacent complementary wrench faults in that region. Within the belt the lenses have been rotated 27° clockwise relative to the acute bisectrix plane between the complementary faults.

The term joint-drag was first used by Flinn (1952, pp. 265-266) to describe small flexures with near vertical axes bounded by joint planes which affected cleavage planes. Later Knill (1961) expanded the term to also cover similar small flexures which were not necessarily bounded by fractures and it is this sense of the term joint-drag which will be used here. In addition, the flexure axes need not necessarily be near vertical for the structure to be termed a joint-drag. Joint-drags in South Pembrokeshire are developed in all lithologies although they most characteristically occur in well-cleaved rocks, especially soft sandstones. They will be more fully discussed in the section on wrench-joints in this chapter.

Joint-drags, like lens belts, are largely associated with wrench-joints, joint-drags and lens belts frequently occurring together.

A joint-drag associated with a sinistral wrench fault at station 8001 is equally developed above and below a minor low angle thrust, evidence which suggests that the formation of the drag post-dated the formation of the thrust (Plate 5.7).

II SUB-PHASE 6 WRENCH-JOINTING

(a) General geometries

Wrench-joints are the most numerous minor structures in the area not including fracture cleavage and rotation joints. The principal structures are primary and secondary wrench shear joints, lens belts and joint-drags. All these structures are related to fold geometries in the same manner. Their attitudes depend on the positions they occupy in a fold; there are two tectonic settings.

i. Fold limbs

ii. Fold crests

i) <u>Fold limbs</u>

On fold limbs primary wrench-joint shear planes (and lens belts and joint-drags) lie normal to the bedding and symmetrically about local fold axes (Fig. 5.8A). The acute bisectrix between shears is contained in the plane of the bedding and at right angles to local fold axes, the obtuse bisectrix also lies in the plane of the bedding although parallel to local fold axes and the line of intersection between shears is normal to the bedding.

These geometrical directions are given as $\sigma_x \sigma_z$ and σ_y in Figs. 7.2B-F which illustrate for representative examples the correspondence of the $(\sigma_x \sigma_z)$ plane with the bedding.

Secondary wrench-joints also lie normal to the bedding, usually including an acute angle around σ_z. Secondary wrench-joints are schematically illustrated on Fig. 5.8A, an example of their mutual intersections with primary wrench-joints being shown on Fig. 7.2F.

The average value for the angle ϑ calculated from all the complementary primary wrench shear joints is $23° \pm 6°$, the average angle between a secondary wrench-joint and the primary joint closest to it being $36.3° \pm 8.0°$.

As Appendix II illustrates there are exceptions to the general pattern which has been just described. The most common exception is for the sense of plunge of the local fold axis to deviate from the sense of plunge of σ_z. In many cases this departure from the standard relationship may be related to a scarcity of readings for one of the complementary sets and the consequently unprecise orientation of the stress ellipse. At Greenala Point (4003-4008), however, the local fold axis and the fold axis both plunge east whilst σ_z consistently plunges gently west. The late joint sets on the south side of Freshwater East (3029 and 3032) and from the north side of Freshwater West to West Pickard Bay (7081, 8001-8004) are also less systematic and more difficult to interpret, one possible interpretation being given in Appendix II. Both sub-zones show unusual early structure attitudes: the bedding strike on the south side of Freshwater East trending NW.-SE., and the local fold axes plunging steeply (20°-35°) from the north side of Freshwater West to West Pickard Bay. In addition the rocks on the south side of Freshwater East are largely marls and frequently late joint systems are poor in such lithologies.

Figs. 7.2B-F also illustrate that rarely is the line of intersection between shears precisely normal to the bedding. The departures from this direction are, however, unsystematic, not varying with stratal dip or the attitude of the host fold axial plane.

Joints whose attitudes vary with both bedding dip and fold plunge have not been recorded before. Knill (1959, p.538) described in uniformly dipping Dalradian rocks joint sets bearing similar overall relationships to the bedding, but because in the area he was describing there were only slight dip changes dependent variations in joint attitudes were not detectable. A similar pattern of joints oriented relative to stratification planes has also been described by Deenen (1942 in de Sitter 1956, p.133) from a coal mine. More recently Mosely (1962, pp. 301-303) has also described the same type of pattern as the present one from the Sykes anticline in the Bowland trough although the examples which he figures (Fig. 5, p.299) are diffuse.

ii) <u>Fold crests</u>

For 3-10 feet on either side of fold crests wrench-joints are oriented relative to the plunge of the fold axis, individual joints crossing the crest without deviating (See Fig. 5.8B). Complementary pairs of joints are oriented so that the obtuse bisectrix between them is parallel to the plunge of the fold axis, the acute bisectrix is near horizontal, in a plane normal to the fold axis and the line of intersection between the shears is near vertical. The departure of the later two directions from the horizontal or vertical is not systematically related to the axial plane of the fold, although there are too few examples of the structural condition to test the variations rigorously. Fig. 7.2A illustrates stress axis orientations derived from three pairs of complementary wrench-joint sets crossing different buckles in station 9010. In all three cases σ_x plunges south, this plunge may be related to the gross dip of the beds when the effects of the individual buckles are removed.

The average value of the angle ϑ for wrench-joints at fold crests is 23°.

(b) Lens belts and joint-drags

i) <u>General characters</u>

The attitudes and effects on earlier structures of lens belts and joint-drags possessing wrench-joint geometries give the most important clue to the understanding of the kinematics of these structures.

Lens belts consist of a shear plane, sometimes corresponding to a fracture, and a set of tension lenses or gashes arranged en-echelon within the shear (See Fig. 5.9 and Plates 5.8 - 5.10). If in the shear zones the tension lenses are sygmoidally distorted, the fracture cleavage planes or rotation joints are also deformed to give joint-drags (See Fig. 5.9A and Plate 5.8). Even when the fracture cleavage planes are unde-formed within the shear zones they are usually accentuated and more frequent than they are outside it. A lens belt or joint-drag may pass laterally into a wrench-joint (See Fig. 5.9B and Plate 5.9), equally the wrench-joint may continue intermittently through the lens belt or joint-drag.

Lens belts are often spaced at intervals of up to ten feet apart and they may extend on bedding surfaces for twenty feet. Commonly lenses are 3 inches to 1 foot long, 1/8th to 2 inches thick and spaced between 1/2-4 inches apart. The tension fracture is usually infilled with calcite or quartz according to whether the lenses occur in limestones or sandstones. The long axes of the crystals lie perpendicular to the fracture walls. Roberts (1961, pp.114 and 130) using micro-fabric evidence demonstrated that calcite crystals in tension gashes from the main South Wales coalfield were oriented with their c axes parallel to the blastetrix. The long axes of quartz crystals, however, he describes as lying normal to the gash walls. Individual tension lenses within a belt are frequently restricted to a single bedding unit (as suggested in Fig. 5.9A), although on the other side of a bedding surface they may be re-established. The shear usually cuts several bedding units.

ii) Occurrence

Although lens belts have been recorded from all horizons and lithologies in the area, they are commonest in Carboniferous Limestones (61%) and in the Upper Old Red Sandstone (26%), where they are restricted to the competent lithologies. In the

Carboniferous they are especially common in the thin-bedded lower zonal limestones. Geographically their distribution is patchy and best reflected by their frequency in Table 2 of Appendix I.

Joint-drags are more common in, though not restricted to, closely-cleaved lithologies, especially soft sandstones from the Skrinkle Sandstone. They are rare in limestones.

iii) Geometry and kinematics

The geometrical relationships between the shear planes of lens belts and folds have been described already.

Since lens belts indicate active shear along a plane the acute angle between a lens and a belt faces against the sense of movement, the line of intersection between a lens and a belt being normal to the sense of movement. The axes of deformed tension lenses and distorted fracture cleavage planes are also normal to the movement sense. Fig. 5.9A shows that on fold limbs the axes of deformed lenses or fracture cleavage planes, and the intersections between lenses and belts are perpendicular to the bedding. This direction together with the acute angle between a lens and a belt indicates that displacements were of a wrench type relative to the bedding regarded as horizontal.

If during this sub-phase actual or potential wrench displacements relative to the bedding occurred, only in near horizontal beds will the ideal wrench condition be developed. In vertical beds within a shallow plunging fold the apparent displacements will be of the gravity (normal) type (See Fig. 5.9C). For dips intermediate between the horizontal and vertical the movement picture will also be intermediate between the wrench and gravity classes (Fig. 5.9A and Plates 5.9 and 5.10). An additional complication arises in steeply dipping beds when the plunge of the local fold axis exceeds the angle ϑ (Average value 18°) for a complementary pair of lens belts. In these cases one shear will show a thrust type of displacement and the other gravity displacements. The lens belts shown on Plate 5.8 illustrate this condition which is also diagrammatically shown for the shear planes alone in the last two parts of Fig. 5.8C if the bedding is regarded as vertical.

It is, however, clear that all these movements can be related to either the sinistral or dextral classes of wrench shear if the bedding is considered to be the reference plane. A wrench-joint lens belt or equivalent shear plane is therefore best named by considering whether it is sinistral or dextral relative to the bedding, viewed from the stratigraphically upper side. The latter provision allows wrench-joints in inverted strata to be grouped with adjacent equivalent fractures occurring in beds not tilted beyond 90°.

The procedure for naming a wrench-joint can be summarised using a 'rule of thumb' method which is illustrated in Fig. 5.8C. The figure shows an imaginary upper surface of a bedding plane crossed by wrench shear fractures, the first pair on a limb with a horizontal local fold axis and the later two pairs on limbs with steeply plunging local fold axes. If the local fold axis is horizontal or near horizontal (<15°) on the north dipping limb the west dipping fracture will be dextral and the east dipping fracture sinistral. On a south dipping limb this situation will be reversed. If the local fold axis plunge exceeds about 15° both fractures may dip in the same direction, the class of the plane can then be told by applying the last two examples shown in the figure which are extensions of the general method for steeply east or west plunging axes. The dip direction of a joint in uninverted beds also gives an indication of whether the fracture is relatively sinistral or dextral since the sinistral set will generally strike closer to NW.-SE. and the dextral set closer to the NE.-SW. Where the beds are inverted these strike directions will be reversed.

The movement picture derived from some lens belts contradicts the displacements they would be expected to show if the attitudes of the belts are considered separately from those of the lenses. For example, at station 5040 the dominant wrench-joint set dipping 76°.268° should be equivalent to a dextral shear, a sub-parallel lens belt, however, contains lenses dipping 57°.232°, the attitude of the lenses implying sinistral shear.

In the Skrinkle Sandstones north of Stackpole Quay (5000) prominent lens belts dipping at 79°.250° contain lenses at 45°.283°, planar attitudes unrepresented elsewhere in the same rocks mass. Again the implied movement is sinistral with the shear apparently having a thrust effect.

Near Great Furzenip at station 7051 a lens belt dipping at 29°.249° contains lenses at 81°.220°, attitudes which suggest that normal displacements had occurred along the shear, however, distorted rotation joints within the shear indicate apparent thrust action.

Other less important examples of lens belt attitude inconsistencies are indicated by the relative fracture attitudes in Appendix I.

Sinistral and dextral lens belts are equally common, lenses within one belt frequently being parallel to the shear plane of a complementary belt (e.g. Fig. 5.9A and Plate 5.10). Ideally, however, the lenses being tension fractures should bisect the complementary shear planes of the lens belts. Therefore, it is possible from a complementary pair of lens belts or from a single lens belt and a complementary wrench-joint set to calculate the rotation of a lens set relative to the acute bisectrix plane. Rotation is always anticlockwise in sinistral shear belts and clockwise in dextral shear belts. The average value of anticlockwise rotation is 22° and the average value of clockwise rotation 18° (details for individual stations are given in Appendix II, Table 2). These rotation values compare closely with average ϑ values for complementary shears.

(c) Primary wrench-joints

i) Geometrical characteristics

On a fold limb there are a large number of possible joints which on a stereogram will plot as a semi-continuous girdle of poles at 90° to the bedding pole (See Fig. 5.11). It is, therefore, often difficult to differentiate between separate maxima and because of this the grouping of poles must always be somewhat arbitrary unless parallel lens belts or joint-drags especially indicate the structural function of a fracture. The two most important late joint maxima usually correspond to dextral and sinistral wrench-joints, between the maxima, however, there is frequently a scatter of less closely clustered poles, some of which possibly represent a bisecting tension joint set. No definite field evidence for regional tension joints has been recorded, however, all joints showing shear joint surface characters. Regional tension joints are, therefore, probably absent.

Because wrench-joints lie normal to bedding surfaces they superficially appear to be a system of fractures which have been involved in a later phase of folding. (Plates 5.11, 5.12 and 4.6). Only in near horizontal rocks do the attitudes of wrench-joints resemble the orientations expected of wrench fractures. For example, Plate 5.13 illustrates near vertical wrench-joints cutting the shallow dipping limestones of the Stackpole Warren cliffs.

In the immediate areas of fold crests where wrench-joints are oriented relative to fold axis plunges (See Plate 5.14) the stronger of the two possible joint sets usually crosses the axial region. This is illustrated on Plate 3.5 where a steeply plunging buckle is exposed in section on a major wrench-joint surface dipping at about 45°.

Estimates of ϑ for all analysed wrench-joints have been made, individual values of ϑ being given in Table 2 of Appendix II. There is no systematic variation of ϑ with bedding dip or with the position of the fractures in the fold, there is, however, a suggestion of a systematic variation with lithology for wrench-joints developed on fold limbs. (See Table 5.2).

TABLE 5.2.

Variation of ϑ for wrench shear joints on fold limbs

Lithology	ϑ	$\pm$ S.D
Old Red Sandstone (All rock types)	20.5°	5.20°
K shales and limestones	21.5°	2.60°
Z thin-bedded limestones	18.0°	0.50°
C_2S_1 thin-bedded limestones	21.9°	0.75°
S_2 thick-bedded limestones	26.5°	7.70°
D thick-bedded limestones	28.5°	5.60°
MEAN	23.0°	6°

In the field wrench-joints are not 'refracted' as they pass from one lithology to another, however, the gross lithology of a rock succession may affect ϑ in the manner which the Table suggests.

Over the area as a whole neither sinistral nor dextral wrench-joints are dominant although for a given fold limb one set is usually better developed. This variation has been found to be related to the stress conditions which acted during the next sub-phase and therefore will be discussed more fully later.

ii) Field characters

Wrench-joints are usually large planar fractures crossing many bedding units, individual joints often extending for more than 30 feet both laterally and vertically. Wrench-joints cross cut all other structures.

It is difficult to generalise about the spacing and surface characters of wrench-joints. In shales they are usually smooth gently curving fractures which frequently occur in swarms. In Old Red Sandstone marls they are often irregular joints which do not lie in obvious parallel sets (e.g. on the south side of Freshwater East). In competent rocks wrench-joints are usually smooth planar fractures although in thin-bedded limestones they are frequently short and irregular.

Freshly exposed wrench-joint surfaces are smooth fractures which evenly cross cut pebbles, concretions or fossils. Feather-fractures of the type described by Roberts (1961b) from the main South Wales coalfield have not been recorded. Slickensides on vein infillings are also uncommon. At station 2017 where slickensides are developed, they are oriented down the dip of the joint set showing that the actual or potential movement must have been essentially parallel to the bedding, since at that station strata are vertical.

Many wrench-joints are infilled with quartz or calcite according to whether they cut sandstones or limestones, this infilling is, however, related to the stress conditions of the next sub-phase.

Wrench-joints are spaced independently of their structural setting and of the lithologies which they cut. Major wrench-joints are usually spaced 1-10' apart and between the major planes minor parallel joints are often as closely spaced as 1/2 inch apart.

In soft sandstones of the Lower Old Red Sandstone, at stations

8001-8004, two sets of wrench-joints intersect in a manner which closely resembles joint-shears. Major sinistral joints are intersected by more closely spaced dextral 'antithetic' joints occurring beneath the major planes in narrow (one foot) zones. (See Plate 5.15).

(d) Secondary wrench-joints

In addition to primary wrench-joints other late formed fractures lie normal to the bedding and therefore share a common intersect with the primary joints. These joints also show wrench displacements relative to bedding surfaces, the geometry of an ideal pair being shown on Fig. 5.8A. Displaced primary wrench-joints and joint-drags affecting fracture cleavage show a movement picture which in steeply dipping strata corresponds to thrust action (See Plate 5.16). As Fig. 5.10C shows if the adjacent primary wrench-joint is a sinistral shear the secondary wrench-joint is a dextral shear, and vice versa.

In the field secondary wrench-joints are restricted to areas of stratal dip greater than 55°. In form they are either smooth planar fractures, sometimes displacing primary wrench-joints, or joint-drags. The secondary joint-drags are limited to the area of West Angle Bay. Of the 12 analysed examples of secondary wrench-joints 9 are relatively sinistral and 3 relatively dextral. Only at station 9007 are both sets of secondary wrench-joints developed.

The average angle a secondary shear makes with its nearest primary neighbour is $36°.3° \pm 8.0°$. This angle implies that with the bedding strike or the local fold axis a secondary wrench-joint subtends an average angle of 30.4°, a value which is close to ϑ (23.3°) calculated for primary wrench-joints.

(e) Age relationships of wrench-joints

Since wrench-joints lie normal to bedding surfaces and are symmetrical oriented about local fold axes they superficially resemble early formed joints involved in a later phase of folding. However, rotation joints are frequently distorted, displaced or accentuated in the shear zones of lens belts, whilst wrench-joints cut across rotation joints and other early formed structures associated with the folding. The structures of the wrench-joint sub-phase are, therefore, younger than those of the folding phase. If the wrench-joint structures had pre-dated the folding their surfaces would show clear evidence of the movements and possibly fold structures would have broken apart along the weakness planes which they would have afforded.

The relative ages of wrench faults and wrench-joints are, however, more difficult to determine, since in the areas immediately adjacent to faults, wrench-joints are rare. This is evidence which suggests that the faults and their associated shear planes are older than the wrench-joints since adjacent to the faults new joints would be unlikely to form, any wrench-joint stresses being dissipated on the earlier formed fractures. At Little Furzenip (7070) an infilled wrench-joint which can be traced without deviation across a small wrench-fault gives more positive support for the later formation of the wrench-joints.

Secondary wrench-joints were possibly even later formed than primary wrench-joints since they occasionally displace the primary joints. The time interval between the formation of the two systems may, however, have been short, the systems being geometrically closely related to one another.

III SUB-PHASE 7 VEINING AND ACCENTUATION OF EARLIER STRUCTURES

At most stations one wrench-joint set is dominant and frequently veined. The vein material is calcite if the joint cuts limestones and quartz if it cuts sandstones. Since they are infilled these joint sets resemble tension fractures, however, lens belts parallel to the joints show the fractures to have been initially shear planes. For example, Plate 5.17 illustrates quartz veins which infill wrench-joint planes cutting across tension lenses which had developed earlier when the wrench-joint was acting as a shear.

The type of veining is variable, some veins are only 1/8-1/2 inch thick whilst others may be up to 2 inches thick. A few of the less well defined veins may be due to percolating ground water and not to a tectonic sub-phase. Some veins are formed of massive calcite or quartz although others contain well terminated crystals and central voids. A few have gaped at least twice, two generations of vein material infilling the fracture. The long axes of macroscopic crystals are oriented normal to fracture walls. The walls of some of the coarser quartz veins in Old Red Sandstone lithologies are lined by a millimeter of striated green material, possibly chlorite.

Veins are best developed in competent bands, an inch thick vein in a sandstone may die out and be represented by only the fracture walls in an adjacent incompetent marl band (e.g. Plate 5.18).

Irrespective of stratal dip or whether the joint is relatively sinistral or dextral the dominant or veined set is usually (61% of analysed cases) the one most closely at right angles to a local fold axis (e.g. Plate 4.7). Where the plunge of the local fold axis is steep (>15°) the dominant or infilled joint is usually the shallower dipping set (e.g. Plate 5.17). At fold crests the set most closely perpendicular to the fold axis plunge is usually the best developed.

A few inverse rotation joints on the south side of West Angle Bay (stations 9023 and 9024) are infilled in the same manner as the wrench-joints of other localities. At these stations the inverse rotation joints dip steeply (>39°) and are nearly normal to local fold axis plunges, therefore, they were probably infilled during this phase of the deformation.

IV SUB-PHASE 8 FINAL ADJUSTMENTS

During a final sub-phase there must have been a number of compensatory adjustments which allowed the deformed mass of rocks to settle. The results of this sub-phase are, however, difficult to detect and limited to the minor and unsystematic displacement of earlier formed structures.

At Little Furzenip (7070) quartz veins infilling the dominant wrench-joint set are distorted, most of the movement being parallel to the bedding. As Plate 5.18 shows these displacements are unsystematic, one part of the same vein being folded about a near horizontal axis, whilst another part is down faulted in a 'normal' manner.

At station 5012, in inverted C_2S_1 mudstones and limestones, tension lenses of the wrench-joint sub-phase are thrust over one another along fracture cleavage planes, these displacements must also post-date the formation of the lenses. In addition, other small scale but not easily understood effects probably belong to this sub-phase.

V SUMMARY OF THE GEOMETRY AND SYMMETRY OF THE MINOR STRUCTURES

Fig. 5.11 illustrates, using a block diagram and a stereogram, the ideal arrangement of possible fractures on a fold limb.

Fig. 5.11A shows the large number of planes which almost "box the compass" and form a complex intersection of lines on a bedding surface. Due to each fracture set at any station usually having a 10-15° variation in inclination and declination the various sets of joints frequently merge, being distinguished only by their maxima.

Apart from inverse rotation joints the block diagram illustrates how all the fracture attitudes are dependent on both bedding dip and local fold axis plunge.

Fig. 5.11B, which illustrates more fractures than can be shown on the block diagram, also shows that the poles to most fractures lie on two great circles. One girdle corresponds to the cyclographic trace of the bedding, whilst the other girdle is normal to the local fold axis. The first girdle contains poles to both early and late formed structures although the second girdle contains only poles to early formed structures. The two girdles frequently intersect close to the pole for the rotation joints at that station. The only important structures lying off these two great circles are the fractures of the wrench-fault sub-phase. The poles to these planes usually lie on a great circle passing through, and symmetrically about the fold axis.

CHAPTER 6 AGE OF THE DEFORMATION

The purpose of this chapter is to discuss the age of the late fracture phase by examining the evidence provided by joint systems in blocks of fallen Carboniferous Limestone, making up some of the Permo-Triassic collapse-breccias.

I THE AGE, ORIGIN AND PETROLOGY OF THE BRECCIAS

Permo-Triassic rocks are represented by breccias which formed when solution caves in the Carboniferous Limestone collapsed (Dixon 1921, pp. 158-172). The breccias are, however, difficult to date precisely. Similar breccias in the Gower are overlain by a thin cover of Triassic rocks and in the Vale of Glamorgan a thicker Triassic succession rests on the Palaeozoic platform at the same level as it does in Pembrokeshire. This evidence therefore suggests that the erosion of the Palaeozoic chain to a platform was accomplished by Triassic times, and that any deposits immediately overlying the platform in Pembrokeshire will probably be of Triassic age. The matrix of red clay closely resembling typical Keuper Marl, which sometimes infills the voids between the Carboniferous Limestone blocks, also supports the idea of a Triassic age for these breccias. Dixon (p.158), however, concluded that the collapsed blocks were older than the clays and sandstones surrounding them since these sediments were frequently level bedded. In at least one instance there is evidence which suggests that mud partly infilled the caves before the collapse of their walls and roofs. In a small breccia mass on Stackpole Warren (GR: SR 98609425) red marl is crumpled in a manner which might be expected if the blocks had fallen into a pool of wet and plastic mud.

Petrologically the breccias consist of unoriented and unsorted angular fragments of Carboniferous Limestone set in a matrix of red marl or sandstone and calcite. In size the blocks vary between half an inch across to more than 100 feet across (Plates 6.1 and 6.2). The calcitic matrix is usually coarsely crystalline and usually partly lines the voids between the blocks. Between layers of calcite a thin film of red marl may be present, individual crystals may also display zones of concentric red staining. Red clays and sands are mainly associated with the larger masses. The breccias have developed only in the purer Carboniferous Limestones, most commonly in the higher Dinantian zones. The exact shape of a mass is frequently difficult to determine, it is usually exposed on the coast and therefore only seen in section. In general, collapse-breccias are usually irregular masses, rarely more than 300 feet across and sometimes occupying the whole height of a cliff. Where the floor of a mass is exposed it is generally flat whilst the walls are usually steep sided, frequently corresponding to near vertical bedding planes or joints. Breccias often grade into solid rock with tongues of breccia penetrating the 'country rocks' along bedding planes or joints. For example, many of the late wrench joints at Bullslaughter Bay have been widened and then infilled with Triassic breccia. On the north side of the same bay red staining, clearly associated with these deposits, forms concentric 'boxes' one within the other parallel to prominent late wrench joints.

II STRUCTURAL DETAILS OF THE TRIASSIC BRECCIAS

Dixon (1921, p.183) deduced that many cross faults were pre-New Red Sandstone in age although those which bounded gash-breccia deposits he considered younger than the breccias. In support of the later age of some of the faults he also cited a fault cutting the Whitesheet Rock (2022) breccia-mass, which must have post-dated the formation of the breccia (Plate 6.3). This fault, however, dies out near the base of the cliff, and although in the upper part of the cliff there is 1'6" of fault-gouge the fracture probably represents a later settling of part of the breccia-mass. The fault also dips at 45°.270° an attitude which does not accord with the observed attitudes of nearby wrench faults (See Fig. 5.2). Faults bounding a breccia-mass could possibly pre-date the deposit since it is reasonable to suppose that the limits of collapse would be controlled by such pre-existing weakness planes.

An unusual instance of an infilled wrench joint occurs at Saddle Head (Plate 6.4). There some joints of the sinistrally equivalent set have been eroded and infilled with fine grained breccia in a zone about 1 foot wide, the breccia consisting of limestone fragments set in a red marly matrix. Since the joint walls bounding the mass are smooth and because the deposit follows a joint direction it closely resembles a wrench fault with associated fault-gouge.

Some joints Dixon (p.188) thought were pre-Triassic others post-Triassic. This was because he observed that some joints were restricted to 'country rocks' whilst others passed through 'country rock' and breccia alike. In this study no evidence for joints passing uninterrupted through disoriented blocks, matrix and 'country rocks' has been found. This does not, however, necessarily indicate that the sub-phase of wrench jointing pre-dated the breccias since any joints formed after the breccias would probably not cut evenly across such hetrogenous masses, splitting apart occurring more easily on the many pre-existing fractures.

In general the joint sets within most blocks lie normal to the bedding and in some of the larger blocks of the Whitesheet Rock mass (2022), which are over 25 feet across, it has been possible to measure the attitudes of bedding planes and joints, the resulting plots for four large blocks of limestone in the Whitesheet mass are illustrated in Fig. 6.1. The joint patterns in the disoriented blocks are apparently random but by aligning the bedding planes in the collapsed blocks with those in the surrounding 'country rocks' a systematic pattern emerges. This pattern shows the joints in the blocks corresponding directly with those in the 'country rocks'. Several stereographic rotations are involved (See Fig. 6.1).

1. Bedding pole rotated to the perimeter about the horizontal axis of its measured strike; the bedding is then vertical. Joints similarly rotated on their appropriate small circles.

2. Re-oriented bedding pole rotated around the perimeter about a vertical axis until its strike coincides with the observed

regional strike of the bedding. Joints similarly rotated on concentric circles (Polar stereographic projection used for this stage).

3. Joint sets rotated about a horizontal axis normal to the bedding so as to bring either the rotation set or the inverse rotation set closest to its regional equivalent. Which fracture sets are equivalent to these joints can be deduced from field characters and the geometry of the fractures relative to the bedding. The rotation set usually shares a common strike with the bedding whatever the orientation of the bedding.

4. Bedding rotated about the horizontal axis of its strike so that its pole corresponds to the pole of the regional bedding. Joints rotated similarly on their appropriate small circles.

In the above example (Fig. 6.1) because the regional dip of the bedding is nearly vertical stage 3 can easily precede stage 4. If the dip had been shallower it would have been necessary to rotate the disoriented bedding pole so that it corresponded to the regional bedding pole at stage 3, the joint sets would then have to be aligned by rotation about an oblique axis normal to the regional bedding dip.

The central stereogram of Fig. 6.1 shows the regional fracture pattern and Figs. 6.1 A-D illustrate the disoriented joints and bedding, plus the rotations necessary to bring them into line with the bedding and joints in the 'country rocks'. Considering the scarcity and irregularity of readings in the collapsed blocks the close correspondence between them and the fractures of the 'country rocks' is good. In addition the easterly dipping wrench-joints are dominant in the 'country rocks' and after re-orientation this set is also the dominant one in the collapsed blocks. The evidence therefore indicates that the wrench-joints formed prior to the breccia and that in addition sub-phase 7 also preceded the formation of the breccia. Such a conclusion is especially interesting since Gill (in Coe et al, 1961, p.63) has suggested that the late shear phase in south-west Ireland was possibly of Tertiary age. Since sub-phases 6 and 7 can be dated as being of pre-late Triassic age it follows that all the tectonic phases must belong to the Armorican orogeny, it already having been demonstrated that the folding occurred after the deposition of the uppermost Westphalian rocks. Allowing for the time intervals required for lithification before folding and the subsequent erosion of the fold belt to a Triassic platform, the Armorican orogeny in south Pembrokeshire probably occurred during the Permian.

CHAPTER 7 INTERPRETATION

In Chapters 3, 4 and 5 structures were described geometrically and kinematically, in this Chapter a dynamic structural analysis will be attempted. The terms σ_x, σ_y and σ_z, which in previous chapters were employed as convenient shorthand descriptions of geometrical directions, will in the chapter be used to represent the three axes of the stress ellipsoid to which it is assumed the geometrical directions were equivalent. Such a procedure has been adopted in order to overcome having to use two sets of symbols for representing a single system of directions. As a consequence of doing this annotated text figures are equally applicable to descriptive or interpretative chapters.

I ANALYSIS OF THE TECTONIC SEQUENCE

(a) Folding phase

i) Sub-phase 1 Folding

Folds are generally regarded as having formed as a result of compressive stresses acting at right angles to their axial plane strikes (Williams 1959, p.633). Since the average strike of axial planes in the Orielton anticline is WNW.-ESE: (102°) it follows that the folding was caused by a compressive stress acting along a NNE.-SSW. line.

The outwardly leaning fan of axial planes relative to the centre line of the anticline Dixon (1921,p.178) regards as characteristic of compound anticlines. De Sitter (1956,p.99) also considers that a synclinal fan of axial plane cleavage on anticlines is a common occurrence. The incompetent Ordovician shales at the base of the exposed succession may have assisted in forming the outward fan of folds by allowing basal shearing above a plane of decollement to take place. Certainly, the geometry of the structures implies folds which must die out at depth, and therefore some type of basal shearing mechanism must be postulated.

The general lack of evidence for extension or stretching in the 'b' direction suggests that in this area the Armorican orogen was laterally restrained, the only direction of relief being upwards.

At the time of folding the rocks were probably at shallow crustal depths, there being no regional metamorphism.

Structure profiles show the style of folding to be intermediate between the concentric and similar classes. Bedding slickensides and fracture cleavage planes indicate that bedding-slip was universal during folding.

ii) Sub-phase 1 Minor structures associated with the folding

Fracture cleavage planes, in incompetent strata, and rotation joints in competent strata were the most important structures produced as a direct result of the folding. The formation of fracture cleavage has been commonly ascribed to shearing stresses set up as a result of bedding-slip during folding (See Wilson 1946 and 1961). Recently, however, this view has been challenged by Williams (1961) who considers that during the deformation of confined incompetent layers the usually accepted directions of bedding-slip will be reversed on some parts of a fold limb, due to rock flowage from fold limbs to fold crests (See Williams 1961, Text-Fig. 1, p.318). Therefore, fracture cleavage in such folds cannot be due to the usually accepted directions of bedding-slip. Williams (p.322) also regards fracture cleavage as grading into slaty cleavage with increasing rock reconstitution, both forms of cleavage indicating flow parallel to a direction of maximum elongation.

The development of fracture cleavage as a response to bedding-slip during folding has also been questioned by Voll (1960,p.540), who cites the work of several authors who describe fracture cleavage from unfolded strata. Some of these workers such as Heoppener (1955) consider that fracture cleavage patterns are formed during the early stages of folding, whilst others including Voll (p.550), favour its formation before folding. An early formed fracture cleavage pattern Voll (p.551) believes would rotate with the bedding during folding. In order to demonstrate this he figures fracture cleavage developed on the Sleek Stone monocline (Voll 1961, Fig. 18a, p.549) which he considers to have remained normal to the bedding during the formation of the fold.

The frequent persistence of fracture cleavage planes across fold crests, where bedding-slip would be at a minimum is thus accounted for by either Williams' or Voll's ideas. Since if fracture cleavage planes mark planar flow directions as Williams suggests such flow would be as common at fold crests as on fold limbs. Similarly a fracture pattern laid out before or just after the start of folding, as Voll suggests, would also be as well developed across crests as on limbs.

In the Orielton anticline fracture cleavage planes and rotation joints are equally well developed in competent and incompetent strata, and on fold limbs and across fold crests. Individual fractures are usually planar and terminate abruptly against bedding surfaces. Fracture cleavage planes also intersect the bedding parallel to adjacent fold axes, and the acute angles they make with the bedding always indicate the expected direction ofbedding-slip (i.e. the stratigraphically higher beds moved outwards relative to the lower beds from synclinal cores). If the lithology contains 'race' rods, or if the fracture planes bear slickensides these lineations are always oriented normal to local fold axes within the plane of the fracture (See Figs. 4.1B, C and 4.4G).

The orientation of the 'race' rods which once lay normal to the bedding indicates that within a bedding unit shearing and distortion must have occurred, the amount of distortion being indicated by the acute angle between the rods and the bedding. The sense of relative slip which must have occurred to produce this shearing is also indicated by the direction in which the same acute angle faces. Since where 'race' rods and fracture cleavage planes occur in conjunction, the rods lie between the fracture planes, it follows that in beds containing no 'race' rods the angle between the bedding and the cleavage also indicates the amount of distortion before rupture, and the relative bedding-slip directions.

The ratio of the present to the original thickness of a bed is thus given by sin γ, γ being the acute angle between the fracture cleavage and the bedding, measured in a plane normal to both. In Chapter 4, section IIb, γ variations with lithology and structural setting were discussed, the following table (Table 7.1) now converts some of these γ values in moderately dipping rocks, to sin γ values. Table 7.2 sets out similar values for different rock types from areas of stratal dip less than 10°.

The dominance of high sin γ values (usually >0.9) in Table 7.1 reflects the slight thinning of the beds which occurred during the folding, as would be expected the lowest sin γ values are associated with incompetent rocks.

TABLE 7.1

Sin γ. Different rock types from fold limbs dipping between 50-65°

Rock type	γ	sin γ
Sandstone	86°	0.996
Sandstone	73°	0.956
Marly sandstone	87°	0.999
Marl with 'race'	82°	0.990
Marl with 'race'	62°	0.883
Marl	73°	0.956
Marl	56°	0.829
Shale	29°	0.485
Shale	45°	0.707
Mudstone	63°	0.891
Thin-bedded limestone	81°	0.988
Thick-bedded limestone	87°	0.997
Thick-bedded limestone	85°	0.996

TABLE 7.2

Sin γ. Different rock types from areas of less than 10° dip.

Rock type	γ	sin γ
Marl	80°	0.985
Marl with 'race'	88°	0.999
Soft sandstone	88°	0.999
Sandstone	72°	0.956
Sandstone	77°	0.974
Thick-bedded limestone	88°	0.999
Thick-bedded limestone	84°	0.994

Table 7.2 illustrates the little stratal thinning which must have occurred in regions of low dip or at fold crests, a conclusion which again might be expected from the geometry of the fold structures.

The lower sin γ values of Table 7.1 correspond to the rock types which gave high values for the frequency of fracture cleavage planes (See Table 4.1), a further result which might be anticipated, Lovering (1928) having shown that for there to have been any considerable thinning of a bedding unit during folding,fracture cleavage planes need to be closely spaced.

The line of intersection and the acute angle between cleavage planes and bedding,in the Orielton anticline,indicates that stratal slip was normal to fold axes. The orientation of 'race' rods and slickensides on fracture cleavage planes also supports this direction of bedding-slip.

The fracture cleavage bedding relationships, which have just been described, might also have arisen if a pre-existing fracture cleavage pattern had been rotated with the bedding, provided that the fold axes developed parallel to the initial intersection of the bedding and the cleavage. However, even if this condition were fulfilled, cleavage planes and 'race' rods would most likely have been sygmoidally deformed during the folding, so that they trailed off parallel to the bedding at the margins of stratal units. In addition, each plane would have probably acted as a minute overthrust. Since sygmoidally deformed fracture cleavage planes and repeated minor thrusts parallel to fracture cleavage planes are rare in the Orielton anticline the later rotation of the fracture cleavage after it was first formed is considered to be unlikely. Thus fracture cleavage and rotation joints in the Orielton anticline are considered to have formed at a late stage in the folding process, perhaps their formation dissipating any remaining fold stresses, so that there was little further bedding-slip to distort the planar fractures. The principal objection to the above conclusion is the persistence of fracture cleavage planes across fold crests and in areas of low dip where bedding-slip would have been at a minimum. It is, however, significant that in the areas of near horizontal rocks γ is always close to 90°.

The origin of the inverse rotation joints is not understood. They are probably related to bedding-slip during folding, since they are always closely associated with rotation joints, in addition one set of bedding slickensides is related to the inverse axis, in the same way as the other set is to the fold axis. Voll (1960, Fig.18a p.549) figures a similar second set of fracture cleavage planes on the Sleek Stone monocline but gives no separate account of its origin. He describes the two fracture cleavage sets as including an acute angle around "B". In the Orielton anticline this relationship does not exist since fracture cleavage planes, sensu stricto, intersect the bedding parallel to "B".

Two separate sets of bedding slickensides at one locality are also difficult to account for, the commonly held view being that later movements obliterate pre-existing slickensides. Perhaps both slickenside directions are preserved in this area because the striations are developed in vein materials between bedding planes. Evidence which suggests that the minerals grew elongate parallel to the actual or potential directions of bedding-slip after any movements had ceased.

The restriction of slaty cleavage to the area of West Angle Bay is possibly related to both the intense buckling in the core of the Angle syncline and to the lithology of the K_2 succession, in which mineral reconstitution was easily achieved. It may also be significant that the Lower Limestone Shales in this bay are geographically closer to those of western Ireland, where such slates are common, than those of any other bay in the present region.

The absence of tension fractures in this sub-phase, except en-echelon in shear belts, suggests that although the folding was a near surface happening, it must have occurred under sufficient cover to have inhibited the formation of tensional stress fields on the outer arch bends of folds.

iii) Sub-phase 2 Plastic flow and associated shearing

The unsystematically distorted 'race' rods on the north side of Freshwater East and the more widespread curving and irregular shears are considered to be younger than the folding. Distorted rods and shears when they occur together are closely associated, and since the shears cut and displace fracture cleavage planes both the shearing and the distortion are regarded as post-dating the folding. In addition, the slip direction during folding has been shown to be essentially at right angles to fold axes, whilst the slip indicated by the deformed rods must have been approximately parallel to the strike. Two movement directions which are not compatible with one another and are therefore unlikely to have occurred simultaneously. Nevertheless the time interval between the two sub-phases was probably short.

The average ratio of present to original (i.e. prior to this sub-phase) thickness of a marl bed containing distorted 'race' rods is 0.90 . A similar ratio to that calculated for the bed thickness changes accompanying the folding.

The attitudes of the irregular shears are more difficult to account for, their curving form suggesting that they follow surfaces of pre-existing weakness, perhaps of sedimentary origin. In shape they resemble load-cast structures although the irregular shears are on a larger scale. However, they are not restricted to the under-surfaces of sandstones in the same manner as load-casts are. The near horizontal slickensides radiating out from the centres of the basins suggest essentially lateral slip, a movement sense which is supported by the distorted 'race' rods.

Although the conditions which operated during this sub-phase are difficult to assess precisely, the period probably corresponded to a tightening up of fold structures under a compressional stress field.

iv) Sub-phase 3 Thrusting

The outward fan of major thrusts relative to the centre of the Orielton anticline was noted by Dixon (1921, p.179) who regarded it as reflecting the action of outwardly directed pressures. Dixon (p. 179) also recognised that the smaller thrusts of the area did not show this systematic arrangement within the fold belt. The more truly E.-W. trend of the thrusts compared with the WNW.-ESE axial direction of the folds was also noted by Dixon. These diverging trends may indicate that during this part of the sub-phase σ_x was oriented N.-S. rather than NNE.-SSW., as it must have been during the fold phase.

Complementary low angle thrusts dipping at less than 45°, which might be expected to occur in this area are absent. This may be largely due to the thrust movement having occurred on suitably oriented pre-existing fracture cleavage planes or rotation joints. Such a possibility is supported by the work of Donath (1961), who has shown that shearing stresses may be dissipated by movement on pre-existing planes lying up to 60° from σ_x, rather than new shear planes being formed. The few low-angle thrusts which occur are rarely accompanied by parallel joint sets, complementary strike shear joints at low-angles to the bedding probably being their structural equivalents.

Strike shear joints at low-angles to the bedding were fully described in Chapter 4 (Section ivb). Complementary strike joints are oriented with the acute bisectrix (σ_x) contained in the plane of the bedding and normal to the local fold axis, the line of intersection between the shears (σ_y) also in the plane of the bedding but parallel to the local fold axis, and the obtuse bisectrix (σ_z) normal to the bedding.

Because strike shear joints cross cut, distort or displace fracture cleavage planes and are themselves unrotated fractures, the orientation of their causative stress field must have been, at any locality, controlled by the attitude of the bedding and the plunge of the local fold axis (Fig 7.1A). Fig. 7.3A illustrates the orientations of stress axes for the strike shear joint sub-phase, with the effects of bedding dip and local fold axis plunge removed (See Chapter 2, IIIc).

Fig. 7.3A shows a regional stress field in which σ_x must have been horizontal along NNE.-SSW., σ_y horizontal along WNW.-ESE. and σ_z vertical.

It has not been possible to deduce the origin of all the miscellaneous strike joints listed in Appendices I and II, undoubtedly however, most are connected with this sub-phase since they usually intersect the bedding sub-parallel to local fold axes; a further instance of fold geometries influencing the attitudes of joints.

The prominent NE.-SW. striking low-angle thrust-joints of stations 7070 and 5000 (See Chapter 4, section IVc, i) were possibly formed when locally σ_x was directed NW.-SE. Their consistent southerly dips may reflect overthrusting from the south (or underthrusting from the north), an unexpected direction since the structures always occur south of the Castlemartin Corse anticline where other evidence suggests southward overthrusting.

It is concluded that during the sub-phase of thrusting σ_x was regionally oriented horizontally along a N.-S. direction, σ_y horizontally along an E.-W. direction and σ_z vertically. The sub-phase can probably be divided into an earlier period of thrusting followed by a period of strike jointing. During the later period regional stress axis orientations (See Fig. 7.3A) must have been modified by the attitudes of fold structures. In addition, σ_x was probably regionally oriented NNE.-SSW., σ_y WNW.-ESE. with σ_z remaining vertical.

The attitudes of most of the miscellaneous strike joints also suggest that fold structures affected their orientations. The time relationships between the miscellaneous joints and the other structures of this sub-phase are obscure.

v) Sub-phase 4 Down dip drag shearing

These shear zones possibly reflect a settling of the folded mass at the close of the first compressive phase. The down dip drag zones intersect bedding planes parallel to local fold axes, once again suggesting that fold geometry can influence later formed fracture attitudes.

The type of drag zone developed is probably controlled by lithology, in closely cleaved rocks knick-zones (joint-drags) are common whilst in massive sandstone or limestones broad down dip drag flexures are characteristic forms.

(b) Late fracture phase

i) Sub-phase 5 Wrench faulting

In Chapter 5 the terms σ_x, σ_y and σ_z were used to describe the geometries of complementary wrench faults, since these directions can now be regarded as stress axes it follows that the wrench fault stress field was in general oriented as shown in Fig. 7.1C. The $(\sigma_y\sigma_z)$ plane, with σ_z parallel to the fold axis, corresponded to the axial plane of the host fold, while σ_x lay normal to that axial plane. Williams (1959, p.645), who found the same relationships to exist between folds and wrench faults in part of the Girvan area of Scotland, points out that such implied orientations of the stress field are unlikely to have arisen by the later rotation of originally horizontal or vertical stress axes, since between each fold unsystematic rotations would be required. Therefore these orientations of the stress ellipsoid must be original.

Not all wrench fault stress fields are so simply related to fold geometries. Although σ_z frequently remains parallel to fold axes the $(\sigma_y\sigma_z)$ plane may not coincide with the axial plane of the fold, nevertheless σ_x usually remains nearly horizontal. Some of the larger wrench faults cross cutting several folds bear no obvious relationships to those folds. For example, the dextral Stackpole Quay fault dips steeply east whilst cutting easterly plunging folds. In general those faults, whose attitudes are dependent on host fold geometries, are usually small in comparison with the size of the fold they cut, e.g. on the south side of Lydstep Haven.

Antithetic shear joints accompanying faults are apparently rare, perhaps because they are easily confused with the later formed wrench-joints, one set of which may lie parallel to an antithetic shear joint set. Voll (1960,p.546) frequently refers to the rotation of antithetic shear planes during a period of deformation. Since adjacent to antithetic joints in south Pembrokeshire, earlier formed fracture cleavage planes are unrotated it is concluded that the antithetic joints are also unrotated.

For a given locality both the major and the antithetic planes of joint-shears are parallel to wrench faults and therefore they were presumably formed from the action of the same stress field as produced the wrench faults. Their general restriction to the Lower Old Red Sandstone possibly reflects the ease with which they formed in those lithologies,rather than to their having formed prior to the laying down of the Carboniferous.

The occasional lens belt or joint drag parallel to a wrench fault is also regarded as belonging to this sub-phase, and as having formed during the wrench fault stress regime.

Regionally, the orientation of the wrench fault causative stress field is similar to the one described by Anderson (1951) for this sub-phase, with σ_x horizontal along NNE.-SSW., σ_y vertical and

σ_z horizontal along WNW.-ESE. However, at any locality these regional stress axis orientations are modified by the plunge of the host fold axis, and possibly by the axial plane attitude. These variables may account for the dispersion of the maxima seen on the frequency polygon of Fig. 5.1B, the strike of a fault being dependent on other factors besides the regional orientation of the stress ellipse. Although Dixon (1921,p.184) recorded wrench fault hades, Anderson (1951) when interpreting the fault pattern of the area presumably considered these hades as variations about statistically vertical faults, a view of Anderson's meaning first suggested by Williams (1959,p.644).

On the north side of Freshwater East (stations 3013 and 10' W. of 3007) there are two faults whose attitudes are transitional between the wrench and thrust classes. These two examples support Dixon's (1921,p.182) claim that elsewhere in the area the curving upwards of wrench faults into thrusts happens on a larger scale. Anderson (1951,p.63) considered three possible mechanisms whereby such transitions could arise -

1. Lateral pressures remain constant with depth so that in a lower zone the vertical pressure is in excess, and in a upper zone the lateral pressure. Under these conditions a thrust could bend very gradually down into a wrench fault.

2. Later formed thrusts deflected along earlier wrench fault fractures.

3. Later formed wrench faults deflected along earlier thrust fault fractures.

The transitions from wrench faults to thrusts mapped by Dixon were thought by Anderson to be too sudden for hypothesis 1 to be correct. The age relationships between thrusts and wrench faults suggest that hypothesis 3 is the most likely. However, since in the field the transition from one class of fault to another is sharp and occurs along a single unbroken fracture, hypothesis 1 may be partially correct, although a mechanically sound explanation is lacking.

The overall orientation of the stress ellipsoid during the wrench fault sub-phase was similar to that of the fold phase, except that σ_y and σ_z had changed positions, σ_y now being the vertical component. Perhaps this change accompanied the increase of fold overburden, causing the vertical gravitational load to be in excess of the lateral restraining pressure.

ii) Sub-phase 6 Wrench-jointing

In Chapter 5 the geometries of wrench-joints and lens belts relative to fold structures were described using the terms σ_x, σ_y and σ_z, if these terms are now regarded as stress axes the stress field which must have acted within a fold during this sub-phase is shown on Fig. 7.1B. The stress axis departures from the horizontal or vertical for this sub-phase are controlled at fold crests by the plunge of the fold axis, and on fold limbs by the plunge of the local fold axis and the bedding dip. At fold crests σ_x must have operated approximately horizontal and normal to the axial strike of the folds, σ_z parallel to the fold plunge and σ_y nearly vertical

(See Fig. 7.2A). On fold limbs σ_y was oriented normal to the bedding, whilst σ_x and σ_z were contained in the plane of the bedding with σ_z parallel to the local fold axis (See Fig. 7.2 B-F).

The orientations of the stress axes just described are the same as those which were deduced for the strike shear joint sub-phase, except that during the earlier sub-phase σ_z was the component normal to the bedding. This relative interchange of the σ_y and σ_z stress axes is directly comparable with the interchange of the same axes from the thrusting to the wrench faulting sub-phase.

Although at fold crests wrench-joint stress fields were modified by fold axis plunges, strike shear joint stress fields were modified by both fold axis plunges and bedding dips. This slight divergence of modifying factors upon the causative stress fields is illustrated at station 5020, on the southern limb of the Stackpole Quay anticline. There (See Appendices I and II), complementary strike shear joints are oriented relative to both the bedding and the fold axis plunge, whilst complementary wrench-joints are oriented relative to only the fold plunge. In the immediate vicinities of other fold crests complementary strike shear joints are rare, and therefore it has not been possible to test how widespread such divergences of control are.

Within the shear zones of lens belts,wrench-joint stress fields could be rotated, presumably due to the action of a shearing stress. If actual movement of the rocks on either side of the shear occurred fracture cleavage planes were distorted and occasionally the tension lenses themselves were buckled (See Fig. 5.9 and Plate 5.8). Even where there is little or no evidence for such distortion or buckling the tension lenses rarely bisect the acute angle between the complementary wrench shear joints, an orientation they might be expected to occupy. In most instances the lenses of one belt are parallel to the shear planes of the complementary lens belt (See Plates 5.9 and 5.10). If locally σ_z is assumed to have lain normal to a lens this implies re-orientation of the stress field within the shear belt. The average amount of rotation of the stress ellipsoid in a sinistral shear is 22° anticlockwise, and in a dextral shear 17° clockwise.

In Chapter 5 wrench-joints and associated lens belts were shown to post-date the folding and to be unrotated fractures, their causative stress fields acting relative to the bedding. Such local stress field orientations are obviously related to a regional wrench stress regime. Figs 7.3 B-F illustrate orientations of the regional wrench-joint stress field for various field zones with the modifying influences of local fold axis plunge and bedding dip resolved. The wide dispersion of inclinations and declinations for a particular stress axis in any field zone reflects the variations in bedding strike and fold axis plunge encountered in that field zone.

Exceptions to the usual relationships between wrench-joints and bedding occur in several places. Near Greenala Point σ_z consistently plunges gently west, whilst the axis of the Orielton syncline plunges east. No other structural variables occur there which might account for this unexpected relationship. Other exceptions to the usual pattern have also been described (Chapter 5) from the south side of Freshwater East, and from the area between Freshwater West and West

Pickard Bay. In those two regions either the bedding strike or the local fold axis plunge diverges widely from the expected range of orientations, and this may indicate that the standard relationships exist only where later stress fields have acted symmetrically relative to fold axis plunges and bedding dips.

The regional stress field which must have operated during this sub-phase was oriented with σ_x horizontal along NNE.-SSW. (i.e. normal to fold axes), σ_y vertical and σ_z horizontal along WNW.-ESE., a stress field orientation identical to that of the wrench faulting sub-phase.

The postulated secondary wrench-joints should intersect the primary wrench-joints parallel to σ_y, if they were formed during the action of the same stress field. Fig. 7.2F illustrates two sets of secondary wrench-joints intersecting the primary wrench-joints sub-parallel to σ_y, a condition also fulfilled at other stations (See Appendix II Table 2).

The movement picture associated with the South Pembrokeshire secondary wrench-joints does not accord with the kinematics of secondary shears as described by either McKinstry (1953) or Moody and Hill (1956) (See Figs. 5.10A and B). In their terminology the proposed secondary wrench-joints of south Pembrokeshire would not be classed as secondary shears. However, both McKinstry and Moody and Hill discuss only faults and derive their secondary patterns directly from primary faults. In South Pembrokeshire faults and joints are, however, discrete structures and therefore a secondary joint system may not necessarily resemble a secondary fault system. In addition, both McKinstry and Moody and Hill regard secondary shears as occurring only adjacent to large primary shears, in this area secondary joints occur independently of primary wrench-joints. The principal reason for regarding these South Pembrokeshire joints as secondary is that they share common intersects with the primary wrench-joints, and they show wrench displacements relative to the bedding.

The absence of a set of primary tension joints bisecting the complementary wrench shear joints is especially significant since such structural patterns have been widely illustrated from many areas (e.g. de Sitter 1951, pp. 124, 130, 132). In a survey of jointing in the main South Wales coalfield the absence of regional tension joints was also demonstrated by Roberts (1961a, p.188).

iii) <u>Sub-phase 7 Veining and accentuation of earlier structures</u>

The accentuation or infilling of earlier formed shear fractures clearly indicates the action of a later tensional stress field. The infilled or accentuated joints of south Pembrokeshire usually lie normal to fold axis plunges, they can be compared with the 'ac' joints of metamorphic terrains (See Phillips in Coe et al 1962, p.124), which are usually regarded as tension fractures. However, in the Orielton anticline the large number of fractures existing before this sub-phase makes it unlikely that any new tension joints would be formed since renewed rupturing of old fractures, lying close to fold axis normals, would be easier.

The restriction of many of the larger veins to competent bands shows that these rocks could gape more easily than incompetent lithologies under tensile stress conditions, or that incompetent beds "creep" more readily as confining pressure is reduced.

Two generations of quartz infillings indicate that in some areas at least there were two tensional phases.

Since no new structures were produced during this sub-phase it has not been possible to completely reconstruct the causative stress field, σ_z however, must have lain sub-parallel to fold axes. A characteristic this sub-phase shares with the two previous ones.

iv) Sub-phase 8   Final adjustments

The distortion of quartz veins infilling wrench-joints at Little Furzenip, together with other isolated and unsystematic distortions of one structure by another, indicates that further movements occurred after sub-phase 7. The unsystematic nature of these distortions suggests that this final sub-phase consisted of a reshuffling of beds; a process possibly accompanying the final settling of a deformed rock mass during a period of waning stress differences.

II   THE ANGLE ϑ

The angle ϑ. between σ_x and a shear plane, has been investigated by many geologists from the theoretical, experimental and observational viewpoints. An average value of 30° for ϑ is widely accepted by such geologists as Wilson (1946, p.284), Anderson (1951), Hafner (1951, p.381), Moody and Hill (1956, p.1210) and Handin and Hager (1957, p.45). Recently, Muehlberger (1961) has pointed out that the Coulomb law of the Mohr theory of failure predicts a constant dihedral angle (i.e. 2θ) between complementary shear planes for a given rock type, and that experimental studies show this angle to become smaller as confining pressure is decreased. The distinction between shear and extension (tension) fractures Muehlberger demonstrates are not great, both types of fracture being accountable for, using one theory of failure.

Small dihedral angles between complementary joints have been observed by Parker (1942), Zwart (1951), Spencer (1959) and Roberts (1961a). Muehlberger regards such low dihedral angles as indicating regions where stress redistribution was greatest before rupture (p.218), and where low stress differences prevailed (p.211). He considers these conditions could possibly occur at shallow depths in the crust. Parker (1942) however, interpreted the low dihedral angles he observed in the Appalachians as indicating a combination of compression and tension acting at right angles.

A detailed discussion of θ values calculated from different classes and ages of complementary shears in the Orielton anticline would probably be unrewarding, since many of the estimates are poor due to the semi-continuous girdles of poles between shear plane maxima tending to lower θ values.

In the field refraction of shear planes from one lithology to another has not been observed although in Chapter 5 a weak correlation between rock type and ϑ for wrench-joints was demonstrated.

Table 7.2 lists average ϑ values for different classes of shear.

TABLE 7.2

ϑ for different classes of complementary shears

Class	ϑ
Strike shear joints	37°
Wrench faults	17°
Wrench faults with antithetic shear joints	19°
Joint-shears	22°
Lens belts associated with wrench-joints	18°
Primary wrench-joints	23°
Average ϑ value for all types of shear excluding strike shear joints	20°

Anderson's (1951,p.62) estimate of ϑ for the wrench faults of South Pembrokeshire was 25°, a value higher than the one obtained during this survey.

Following Muehlberger, the llow mean value of 20° for ϑ may indicate that the south Pembrokeshire rocks fractured under low confining pressure at a shallow depth in the crust. The absence of regional tension fractures supports Muehlberger's hypothesis that complementary shear joints of low dihedral angle are intermediate between extension fractures and true shear planes intersecting at 60°, since such low dihedral angle joints would not be accompanied by bisecting tension fractures.

Feather-fractures (Roberts 1961b) on joints, Muehlberger (1961,p.215) regards as indicative of extension fractures. Their occurrence on complementary joint sets as recorded by Parker (1942), Hodgson (1961) and Roberts (1961b) is considered to reflect the intermediate character of these fractures between single extension joints, paired extension fractures of small dihedral angle and true shears. However, no plumose markings or feather-fractures on joint surfaces have been recorded from the present area and this may indicate that the joints of South Pembrokeshire are true shears. Complementary lens belts and joint-drags parallel to the main wrench-joint sets fully support this idea. In addition, the dihedral angle of 46° between the complementary wrench-joints is higher than the angles of 19° (Parker 1942) or 15-20° (Roberts 1961a) recorded for similar joint sets elsewhere. This too implies that the present wrench-joints are more closely similar to standard shear fractures.

Although the geometry of secondary wrench-joints relative to the bedding has been discussed already it is noteworthy that these fractures include an average dihedral angle of 62° around σ_z, calculated from the primary wrench-joints. This value is surprisingly close to the usually accepted dihedral angle between complementary primary shear planes. A fact which becomes additionally significant when the movement picture associated with these fractures is recalled

(See Fig. 5.10). The kinematics of these joint sets considered separately from other joints suggest a maximum principal pressure (σ_x) acting parallel to local fold axes, a direction along which σ_z acted during the formation of the primary wrench-joints. Thus σ_z may have become σ_x after the formation of the primary wrench-joints and during the formation of the secondary wrench-joints.

III STRESS SYNTHESIS

It has already been demonstrated that the various stress axis orientations for a particular sub-phase can be resolved so that a regional pattern of one vertical and two horizontal axes results. Regionally, during the fold phase σ_x was horizontal along NNE.-SSW., σ_y horizontal along WNW.-ESE. and σ_z vertical. During the wrench faulting phase σ_x retained its orientation from the fold phase, whilst σ_y and σ_z mutually changed positions so that σ_y became vertical and σ_z horizontal along WNW.-ESE. The absence of regional tension fractures associated with sub-phases 1-6 is taken as indicating that all three stress axes remained compressive throughout the period. However, σ_z in sub-phase 7 must have been a tensional stress, despite it retaining the same orientation as in sub-phase 6.

The regional stress field orientations are modified everywhere by fold geometries. Fold axis plunge universally affects fracture attitudes, whilst axial plane attitudes affect only fault orientations, and bedding dips affect only joint orientations. Because the same classes of faults and joints were formed at different times and do not necessarily lie parallel to one another they can be regarded as discrete structures. A concept which was first put forward by Price (1959) who showed that faults are formed from primary stresses and joints from residual stresses. Since residual stresses are weaker than primary stresses, displacements associated with joints according to Price should be rare, a conclusion which is upheld in South Pembrokeshire.

Price's concept of residual stresses also suggests a possible mechanism for producing stress ellipsoid orientations related to earlier structures. Hafner (1951) has shown that the orientations of regional stress axes should not deviate by more than 15° from either the horizontal or vertical, an angle frequently exceeded in South Pembrokeshire. However, if it is possible for residual stress fields to influence either later primary fields, or later residual fields, orientations of the stress ellipsoid related to earlier formed structures might possibly arise.

Therefore it is suggested, very tentatively, that in some way residual stresses related to the folding were stored in the rocks and were later able to modify subsequent stress ellipsoid orientations. The slight departure of the wrench fault stress field from its regional orientation is possibly due to the small influence a residual 'folding phase' stress field could have on a later primary wrench fault stress regime. The greater departures of the local strike and wrench-joint stress fields from their regional patterns is therefore expected, since during the formation of these structures two residual stress fields would be interacting.

CONCLUSIONS

1. A systematic fracture pattern exists in the Orielton anticline which can be related to two major phases of deformation, each divisible into four sub-phases (See Chapter 4, Section 1 and Chapter 7, Section II).

2. All eight sub-phases belong to the Armorican orogeny of post-Westphalian, pre-late Triassic age.

3. All structures were formed at shallow crustal depths probably under low confining pressures.

4. Fracture cleavage planes, rotation joints, inverse rotation joints, deformed 'race' rods and bedding slickensides, are associated with the development of the folds, and indicate bedding-slip and the shearing of beds during flexural folding.

5. Faults and joints are discrete structures, joint sets not necessarily lying parallel to the fault sets to which they are equivalent.

6. Fracture attitudes are related to fold geometries.
   a) Faults are oriented relative to fold axes and axial planes.
   b) Joints are oriented relative to fold axes and bedding planes, the commonest being wrench-joints normal to the bedding and symmetrical about the plunge of the bedding-fracture cleavage intersection. The movement picture

associated with these joints, inferred from distorted fracture cleavage planes and parallel lens belts, is of wrench displacements relative to the bedding regarded as horizontal.

7. Most fractures are shear planes, primary regional tension fractures being absent.

8. The angle ϑ (between σ_x and a shear plane) is always low, usually less than 25°. It does not appear to be affected by lithological changes.

9. The regional orientations of the stress ellipsoid deduced by Anderson for this area have been confirmed, although at any locality these orientations are modified by fold geometries.

10. The fracture pattern of the area can be understood only if small field stations showing no bedding dip or fold plunge variations are sampled. The regions immediately adjacent to fold crests are exceptions to this uniform dip rule.

List of References

ANDERSON, E.M., 1951. The Dynamics of Faulting, 2nd edition, 206 pp., Edinburgh and London.

BECKER, G.F., 1893. Finite homogeneous strain, flow and rupture of rocks. Bull. geol.Soc.Amer., 4, p.13.

BILLINGS, M.P., 1954. Structural Geology, 2nd edition, 514 pp., New York.

BUCHER, W.H., 1920-21. Mechanical interpretation of joints. J.Geol., 28, p.707, 29, p.1.

CANTRILL, T.C., E.E.L. DIXON, H.H.THOMAS and O.T.JONES, 1916. The geology of the South Wales Coalfield, Part XII, The country around Milford. Mem.geol. Surv.Engld and Wales.

CLOOS, E., 1932. Feather-joints as indicators of the direction of movements on faults, thrusts, joints and magmatic contacts. Proc.nat.Acad.Sci.,Wash., 18, p.387.

COX, A. and R.R.DOELL, 1960. Review of Palaeomagnetism. Bull. geol.Soc.Amer., 71, p.645.

DAWSON-GROVE, G.E., 1955. Analysis of Minor Structures near Ardmore, Co. Waterford, Eire. Quart.J.geol.Soc.Lond., 111, p.1.

DEENEN, J.M., 1942. Breuken in kool en gesteete. Med.geol. Stchting. Heerlen, (C.1-2), 1. p.1.

DIXON, E.E.L., 1921. The geology of the South Wales Coalfield, Part XII, The country around Pembroke and Tenby. Mem.geol.Surv.Engld and Wales.

DONATH, F.A., 1961. Experimental study of shear failure in anisotropic rocks. Bull.geol.Soc.Amer., 72, p.985.

FAIRBAIRN, H.W., 1949. Structural Petrology of deformed rocks, 344 pp. Cambridge, Mass. U.S.A.

FISHER, (SIR) R., 1953. Dispersion on a Sphere. Proc.roy.Soc. Lond. (Ser.A), 217, p.295.

FLINN, D., 1952. A tectonic analysis of the Muness Phyllite block of Unst and Uyea, Shetland, Geol.Mag., 89 p.263.

GEORGE, T.N., 1940. The Structure of Gower. Quart.J.geol.Soc. Lond., 96, p.131.

GILL, W.D., 1962. The Variscan Fold Belt in Ireland. In Coe et al, Some Aspects of the Variscan Fold Belt, 163 pp. Manchester.

GRIGGS, D.T., 1935. The Strain Ellipsoid as a Theory of Rupture. Amer.J.Sci., Ser. 5, 30, p.121.

HAFNER, W., 1951. Stress distributions and faulting. Bull.geol. Soc.Amer., 62, p.373.

HANDIN, J. and R.V. HAGER, J.R., 1957. Experimental deformation of sedimentary rocks under confining pressure. Tests at room temperature on dry samples. Bull.Amer.Ass. Petrol.Geol., 41, p.1.

HODGSON, R.A., 1961. Classification of Structures on Joint Surfaces. Amer.J.Sci., 259, p.493.

HOEPPENER, R., 1955. Das Tektonische Inventar eines Aufschlusses in den Orthocerasschiefern bei Dillenburg. Geol. Rdsch., 44, p.93.

JAEGER, J.C., 1959. The frictional properties of joints in Rock. Geofis.pur.appl., 43, p.148.

JAEGER, J.C., 1960. Shear failure of anisotropic rocks. Geol. Mag., 97, p.65.

JENKINS, T.B.H., 1962. The Sequence and Correlation of the Coal Measures of Pembrokeshire. Quart.J.geol.Soc.Lond., 118, p.65.

KNILL, J.L., 1959. The tectonic pattern in the Dalradian of the Craignish-Kilmelfort District, Argyllshire. Quart.J. geol.Soc.Lond., 115, p.339.

KNILL, J.L., 1961. Joint-drags in Mid-Argyllshire. Proc.geol. Ass., London, 72, p.13.

KNOPF, E.B. and E.INGERSON, 1938. Structural Petrology, Mem. geol.Soc.Amer., No.6, 270 pp.

LEITH, A., 1937. The Strain Ellipsoid. Amer.J.Sci., Ser.5, 33 p.360.

LOVERING, T.S.,1928. The fracturing of incompetent beds. J:Geol. 36, p.709.

McKINSTRY, H.E., 1953. Shears of the second order. Amer.J.Sci., 251, p.401.

MOODY, J.D. and M.J.HILL, 1956, Wrench-fault tectonics. Bull.geol.Soc.Amer., 67, p.1207.

MOSELEY, F., 1962. The Structure of the south-western part of the Sykes Anticline, Bowland, West Yorkshire, Proc. Yorks.geol.Soc., 33, p.287.

MUEHLBERGER, W.R., 1961. Conjugate Joint Sets of Small Dihedral Angle. J.Geol., 69, p.211.

PARKER, J.M., 1942. Regional systematic jointing in slightly deformed sedimentary rocks. Bull.geol. Soc.Amer., 53 p.381.

PHILLIPS, F.C., 1954. The Use of Stereographic Projection in Structural Geology, 86 pp., London.

PHILLIPS, F.C., The Study of Small scale Structures in the Variscan Fold Belt. In Coe et al, Some Aspects of the Variscan Fold Belt, 163, pp., Manchester.

PRICE, N.J., 1959. Mechanics of Jointing in rocks. Geol.Mag., 96, p.149.

ROBERTS, J.C., 1961a. Jointing and Minor Tectonics of the Neath Disturbance and adjacent areas. Unpub. Ph.D. thesis, University of Wales, Swansea.

ROBERTS, J.C., 1961b. Feather-fracture and the Mechanics of Rock-jointing. Amer.J.Sci., 259, p.481.

SALTER, J.W., 1863. On the Upper Old Red Sandstone and Upper Devonian Rocks. Quart.J.geol.Soc.Lond., 19, p.474.

SHAININ, V.E., 1950. Conjugate sets of en echelon tension fractures in the Athens Limestone at Riverton, Virginia. Bull.geol.Soc.Amer., 61, p.509.

SITTER, L.U.de, 1956. Structural Geology, 552 pp., New York and London.

SPENCER, E.W., 1959. Geologic evolution of the Beartooth Mountains, Montana and Wyoming, Part 2. Fracture Patterns. Bull.geol.Soc.Amer., 70, p.467.

STRAHAN, (SIR) A., T.C. CANTRILL, E.E.L. DIXON, H.H.THOMAS and O.T.JONES, 1914. The geology of the South Wales Coalfield, Part XI, The country around Haverfordwest, Mem.geol.Surv.Engld and Wales.

SULLIVAN, R., 1960. The Mid-Dinantian Stratigraphy of Pembrokeshire. Unpub. Ph.D. thesis, University of Glasgow.

SWANSON, C.O., 1927. Notes on stress, strain and joints. J.Geol., 35, p.193.

VOLL, G., 1960. New work on petrofabrics. Lpool.Manchr.geol.J., 2, p.503.

WATSON, G.S. and E.IRVING, 1957. Statistical Methods in Rock Magnetism. Mon.Not.R.astr.Soc.geophys.Suppl., 7, No.6, p.289.

WILLIAMS, A., 1959. A Structural History of the Girvan District, S.W.Ayrshire. Trans.roy.Soc.Edinb., 63, p.629.

WILLIAMS, E., 1961. The deformation of Confined Incompetent Layers in Folding. Geol.Mag., 98, p.317.

WILLIS, B., 1893. The Mechanics of Appalachian Structures. 13th Ann.Rep.U.S. geol.Surv., 2, p.211.

WILSON, G., 1946. The relationship of slaty cleavage and kindred structures to tectonics. Proc.geol.Ass., Lond., 57, p.263.

WILSON, G., 1961. The tectonic significance of small scale structures, and their importance to the geologist in the field. Ann.Soc.geol.Belg., 84, p.423.

ZWART, H.J., 1951. Breuken en diaklazen in Robin Hood's Bay. Geol.en Mijnb., 13, p.1.

APPENDICES

APPENDIX I TABLE 1a EARLY STRUCTURES

Stereogram number	Bedding	Bedding slicken-sides	Fracture cleavage and rotation joints Rock type	attitude	Inverse rotation joints	Tension joints related to bedding slip	Thrusts Attitude	mov.	Strike shears 1st set	2nd set	Miscellaneous strike shears Attitude	effect	Down dip drag zones	Figured
A	B	C	D	E	F	G	H	I	J	K	L	M	N	
2003	45.167		S_2 limestone	53.016	48.339				69.165					x
2005	42.179	30.210	"	50.017	53.354									
2006	49.164	35.130	"	59.000	51.335									
2009	65.169		"	32.023	39.317									
2011	100.000	10.270 65.090	D_1 limestone	18.054	19.289									
2012	95.000		"	25.81 (slickensides 05.000)										
2013	95.000		"	14.027										x
2015	100.355		"	30.063										
2017	100.000		"	33.046	27.296									
2018	91.359		"	20.066	14.345									
2021	97.000		C_2S_1 limestone	23.030	28.266	(2022 Triassic collapse breccia)								
2023	92.000		"	12.037	20.270									
3001	77.005		Ludlow	15.246	19.152						17.069	1" thrust		
3003	83.005		L.O.R.S. ss.	14.238	40.123	43.307								
3007	82.006		" marl ss.	17.202 15.203	20.115						43.187			
3008	83.007		Ludlow L.O.R.S. marl " conglom. " soft ss. " hard ss.	30.223 31.235 42.228 23.234 22.237	35.145						20.173 21.035	major joints		x
3009	84.007		L.O.R.S. ss.	18.208	35.140	48.345								
3013	82.004		" marl	23.204										
3015	91.007	75.010	" hard ss. marl	13.236 20.227			43.193	6"	43.193	25.350				x
3016	85.007		" hard ss. soft ss.	37.191 17.187	28.145		parallel to cleavage							
3029	66.210		L.O.R.S. ss. race marly ss.	25.010 79.034 48.021			80.212	3"						
3032	66.212		" sandy marl ss.	65.020 29.026	57.057 (Slickensides 32.065)	15.275								
4001	23.194		" soft ss.	76.027							43.025			
4003	05.107		" marl ss.	84.038 84.037										
4004	10.123		" marls	32.023										
4006	Axis 05.107					30.146					35.036 87.225	veins 1" T.P		
4007	13.107		L.O.R.S. marl ss.	87.203 85.202										x
4008	Axis 05.110		" soft ss.	80.204			46.013	6'			88.181 75.020			
4011	22.166		" soft ss.	81.010					50.200					
4012	Axes 10.100 26.155 32.028 35.180	Bp.29.042 " 36.030 33.170	" ss. " marl " marl " ss. " ss. " ss.	75.190 78.198 86.190 70.012 73.188 67.007			13.017	9"	55.022 44.135 43.350 60.200	 60.010				x
5000	76.179		U.O.R.S. ss " qtzte " marl	37.059 38.054 76.008	26.300						33.132	13" T.P		x
5005	113.200 (63.036 87.185	 53.015	" ss. K oolite K shale	40.161 57.175 52.357	 rotation joints may be bedding)		50.170	3'						
5006	112.193		K shale	35.028	(Slickensides 15.340)		60.012	1-6'	31.009		64.167			
5007	130.216		C_2S_1 limestone	57.161					78.005					
5012	110.203		C_2S_1 mudstone	36.065			parallelto cleavage							x

APPENDIX I TABLE 1b EARLY STRUCTURES

Reference letters as on Table 1a

A	B	C	D	E	F	G	H	I	J	K	L	M	N	Figured
5019	48.035		C_2S_1 mudstone limestone	77.002 58.179			76.181	1'6"	25.060	(Slickensides 15.000)				x
	71.177		mudstone limestone	57.012 50.049	(Slickensides 28.244)						49.016 [illegible]7.175			
5013	50.025		" limestone	58.164	45.240						06.203			
5040	46.018	39.345	" limestone	49.177							18.160 64.178			
5045	85.184		" limestone	45.091										
5020	43.012		" mudstone " limestone	72.185 54.186		45.190			81.018	32.125	67.001 88.000 57.007			
	101.184		" mudstone " limestone	51.033 48.054	(Slickensides 10.152)		75.000	200'?	26.073	58.174				
5021	98.185		" limestone	27.068										
5030	94.185 45.015		" Limestone " "	32.099 56.168	43.296		45.005	2'			73.198 65.350			
	54.176 76.184	50.200	" " " "	- 37.090										
5202	73.185		D_1 limestone	47.068					24.154		29.098			x
5211	80.008		"	22.107	31.272				30.059	78.187				
5212	73.011		"	34.050	39.240				34.0900					
5213	10.341		"	82.164										
5221	05.133		"	83.183										x
5071	14.167		S_2 limestone	89.339					34.148	40.025				
5230	55.170		"	-	56.343									
5240	56.008		"	29.127	40.217				76.178		80.002			x
5241	59.005		"	43.138	35.215									
5250	61.183		"	40.051	33.314						19.097			
5091	48.358		D_1 limestone	48.197	59.169									x
6001	46.002	45.029 45.354	"	30.165	47.224									x
6002	77.178		D_2 limestone	25.017					80.005					
6003	17.057		S_2 limestone	79.197	70.340									
7015	65.186		Z limestone mudstone	36.009 68.007					35.174	86.005			25.145	x
7016	63.187		Z limestone	37.001					32.160	79.171	70.003		20.148	
7020	54.168		K flggy lst. " shale " limestone	45.040 25.039 36.045	48.320									
7051	67.171		U.O.R.S.ss. " marly ss. " conglom.	35.037 34.029 22.039	19.300									
7030	71.181		" soft ss. " marl " qtzite	23.042 24.027 35.060					75.015	41.169	(Slickensides 35.205)			x
7040	66.175		" soft ss. " conglom.	30.032 26.030									15.135	
7061	64.175		" qtzite	38.037					43.175					x
7062	80.175		" ss.	44.057							38.155 35.113			
7063	78.177		L.O.R.S. marl " conglom	39.011 48.039			40.35	8"-2'	75.032	40.154	(Slickensides 64.337 on 75.032)			
7070	34.183		" marl ss.	73.004 32.051							45.002 29.127	major thrusts assoc. tension 16.338		x
7081	60.030		" marl " ss.5 " soft ss. " conglom.	67.232 51.226 69.227 24.235	51.188				90.045	25.005	11.225			
8001	53.006		" marl " ss. " marly ss. " hard ss. " marl " mar,ly ss. " marl " qtzite.	52.221 67.215 60.217 61.217 71.215 65.225 74.220 25.227	(race rods oriented 59.178)		39.192	9'					11.018	

APPENDIX I   TABLE 1c   EARLY STRUCTURES

Reference letters as on Table 1a

A	B	C	D	E	F	G	H	I	J	K	L	M	N	Figured
8002	49.000		L.O.R.S. ss.	67.219										
			" marl	66.218										
			" marly ss.	65.221										
			" ss.	65.217										
8003	48.350		" marl	79.209	(race rods oriented		70.195	3"-2'6"						
			" ss.	71.228	72.169)									
8004	41.344		" marly ss.	55.225			87.034	5'						x
			" marly ss.	68.219										
			" hard ss.	71.204										
			" ss.	68.216										
			" ss.	70.206	(65.159 slickensides)									
8012	11.315		" ss.	83.007							80.007			
			" marl	87.012										
	19.247		" ss.	69.020										
8013	28.255		" ss.	68.046			77.025	10'			76.015		28.353	x
			" ss.	72.033			75.018	8'						
			" soft ss.	80.013			76.024	20'						
8018	28.213	23.218	" ss.	58.017									35.004	
			" ss.	65.004										
	13.229		" marl	75.018										
	18.207	15.204	" ss.	77.015	77.033									
8019	23.002		-	-									25.353	
8020	67.217	62.251	L.O.R.S. ss.	36.019	39.044		80.025	3'					27.029	
			" fine ss.	57.012										
			" race	60.035										
9002	64.182	55.180	" marly ss.	46.013	34.297				85.190					
			" ss.	30.017										
			" ss.	36.355										
			" race	52.355										
			" soft ss.	37.343										
9003	62.198	61.200	U.O.R.S. ss.	33.033	14.356						25.120			
			" marl	83.020										
			" soft ss.	33.048										
			" ss.	28.047										
			" race ss.	33.027										
			" race	38.041										
9004	64.192	64.192	K_m limestone	30.037	34.293									
			" oolite	27.050										
			" ss.	31.031										
			" limestone	31.052										
			" ss.	28.067										
			K_1 limestone	32.044										
			" shale	86.010										
			" nodular lst.	37.020										
9007	74.195		K_2 slaty clvg.	70.012					73.028				32.026	x
9008	Fold axes 01.280		-	-			66.198	?						x
9010	Many buckles						54.185	?						
	50.170		K_2 mudstone	79.357										
	51.325		" "	70.190							77.006			
	32.205		" "	75.190										
	36.196		" "	71.199										
	46.213		Z limestone	77.352										
	60.349		K "	30.195										
			" mudstone	61.188										
	90.350		Z limestone	37.185										
9011	Fold axes 00.280													
9012	75.194	74.169	Z limestone	23.328	28.064		54.193	?						
	71.007		-	-										
9013	63.030		Z limestone	55.198										
	44.192		" "	51.043							58.013			
9020	54.014	50.325	K_2 slaty clvg.	71.195					70.016 (slickensides 55.340)					
	45.015	30.337	" "	74.196										
9021	43.019		" "	76.015			33.017	?	69.165		77.197			
			" "	72.016							36.209			
			" "	62.200										
			" "	87.013										
			" mudstone	75.196										
9023	52.020		L.O.R.S. ss.	34.197	42.165		80.210	?			73.189			
			" marl	85.200							56.179			
	54.015		" race	39.233	25.164						87.347			
			" race ss.	39.223										
			" ss.	33.245										
			" ss.	49.267										
			" ss.	42.256										
9024	52.022		" ss.	32.235	39.148 (slickensides		82.355	1'	82.355	30.068			48.038	x
			" ss.	37.218		37.170)								
			" race ss.	44.198										

APPENDIX I TABLE 2a LATE STRUCTURES

Stereogram number	FAULTS No.	Dextral Sinistral	Strke slip	Attitude	Antithetic shears	JOINT SHEARS Major shear	Antithetic shear	LENS BELTS Belt	Lenses	PRIMARY WRENCH JOINTS Sinistral equivalent	Dextral equivalent	SECONDARY WRENCH JOINTS Attitude	Relative sense of movement	MISCELLANEOUS JOINTS
A	B	C	D	E	F	G	H	I	J	K	L	M	N	O
2003	F2	D	-	85.080				05.181	05.150	68.280	68.068			87.259
	F3	D	-	74.069										
	F4	D	-	83.075										
2005	F5	D	-	85.075				80.067	90.105	83.284	77.067			70.320
2006	F6	D	-	75.068				s.195	s.150	70.286	83.060			85.263
	F7	D	-	90.050										
2009	F8	D	-	80.075						69.258	71.070			57.335 70.020
	F9	D	-	75.065										
2011	F1	S	14"	80.281	85.228					60.090	78.267			
2012	F2	D	7"	73.257						73.087	60.275			
2013	F3	S	2'	73.293	65.246					71.094	54.273	40.066	[illegible]	65.240 (parallel to dextral faults)
	F3	D	2'5"	50.245										
	F4	D	1'	51.245										
2015	F5	D	3'	60.236				65.230	65.260	59.069	57.273			90.065
	F6	S	2'	75.273										
2017	F7	D	14"	63.256				75.257	85.291	52.099	76.257			
2018	F1	S	14"	80.281	67.242					47.092	56.267			
2021										74.080	57.268			
	(2022 Triassic collapse breccia)													
2023										73.087	58.267			
3001	F1	D	-	90.050						81.095	72.275	39.290	S	
3003	F2	D	12'	75.075	82.101					65.091	81.277			
	F3	D	1'	62.075										
3007	F6	S	55'	90.130		70.110	87.64			79.093	81.277	47.264	S	
		T.P		50.325										
	JF	D	4"	90.031										
3008	F7	S	50'	80.105						75.096	81.277	46.269	S	
	F8	D	3'	75.065										
3009	F9	S	5'	85.104		73.065	75.103			80.099	70.280	44.254	S	
	F10	D	-	85.070		77.100	75.072							
	JF	S	6"	90.090	75.055	85.089	90.066							
	JF	S	3"	90.100	80.060									
	JF	D	1'6"	70.060										
	JF	D	1'	80.070	69.106									
	F11	S	40'	62.095										
3013	F12	S	130'	80.100						71.092	71.279			
	F13	T.P	-	41.234										
	F14	S	12'	75.100										
3015	F15	D	20'	84.065		72.105	87.240			69.093	72.278			
						90.068	80.090							
3016	F16	S	60'	80.103						73.071	75.281			14.314
3029	F8	D	-	83.096		60.120	80.075			48.328	76.118			
	F9	S	-	73.140										
3032	F11	S	-	s.220	80.098	75.126	76.085			66.325	73.124			82.263 72.086
	JF	S	1½"	80.130										
4001						84.308	81.079			87.303	82.094			85.056
4003	F2	?	-	90.150		76.113	78.068			73.106	73.070			88.327
	F3	?	-	54.325										
4004	F4	?	-	83.347						90.119	85.078			53.220
4006	F5	S	130'	90.120		87.120	81.072			89.127	86.078			75.006
4007						85.122	83.080			88.296	77.079			90.355
4008	F8	D	-	85.085						86.119	79.073			
4011						90.110	88.253			86.110	84.073			
						71.265	85.130							
4012	F1	D	275'	70.260						85.296	84.067			59.262
	F2	S	25'	80.290										
5000	F6	S	-	78.100		65.093	70.055	79.250	45.283	69.290	74.085			
	JF	S	20"	70.100		80.062	88.133							
5005	JF	D	-	90.085						51.255	89.112			36.279
5006										58.261	90.102			
5007										42.283	86.302			
5012								36.262	75.270		59.287	(Sinistral displacement on 36.262 belt)		
								66.272	30.276			(Dextral displacement on 66.272 belt)		
5019										83.136 80.282	76.279			

APPENDIX I TABLE 2e LATE STRUCTURES

Reference letters as on Table 2a

A	B	C	D	E	F	G	H	I	J	K	L	M	N	O
9003	F3 JF	S D	60' 3"	60.105 60.300						45.332	77.298	66.115	S	41.000
9004	JF	D	3-14"	60.064		75.125	80.079			77.289	65.096			56.251
9007										76.290	64.100	34.106 34.299	S D	
9008								s.210	s.158	84.304	84.088			
9010										80.113 86.307 75.113	57.070 71.070 42.074	(Fold axis 32.260) (" " 07.273) (" " 45.250)		
9011										83.299	78.078	(" " 00.280)		
9012	JF Cuts thrust	S S	9" 13'	56.130 s.203						82.291 64.105	63.095 81.289	(north limb) (south limb)		
9013								s.225	50.000	71.306		(Fold axis 11.114)		
9020										81.292				
9021	JF JF	D D	- -	90.160 75.105						86.287	55.259			90.22[illegible]
9023						70.120	70.075			50.127	81.292	46.121	S	52.262
9024										73.122	55.263			64.293

Notes for Appendix I

1. Only fully analysed stations shown.
2. Stereogram numbers equivalent to field station numbers.
3. Attitudes quoted as inclination followed by declination about a 360 degree compass. Inclinations and declinations are mean values for a group of related readings.

   s. in place of an inclination indicates the strike direction of a plane whose dip was not measurable.
4. Some faults lie outside but close to the station with which they are grouped. Abbreviation JF - small fault (joint fault)
5. Remarks in brackets are not related to Table headings but to immediately preceeding information.
6. T.P in column C of Table 2 indicates the thrust component of a wrench fault.
7. Strike slip: (-) indicates not measurable.
8. Rock type descriptions simplified, the same type occuring twice at one station indicates different bands of the same lithology.

Abbreviations :-	ss.	sandstone
	conglom.	conglomerate
	lst.	limestone
	qtzite.	quartzite
	flggy.	flaggy

slaty clvg. indicates true cleavage not fracture cleavage.

APPENDIX I

Note on illustrative stereograms

The stereograms have been chosen as representative of fracture patterns from different tectonic settings and different field zones. Most common fold dips and buckle complications are figured.

Each stereogram shows a plot of all the readings which were recorded at that station. These readings have been pa divided in order to make the pattern clearer.

Stereogram 5019 shows two dip directions corresponding the two limbs of the Murchison syncline, some joints being related to one limb some to another.

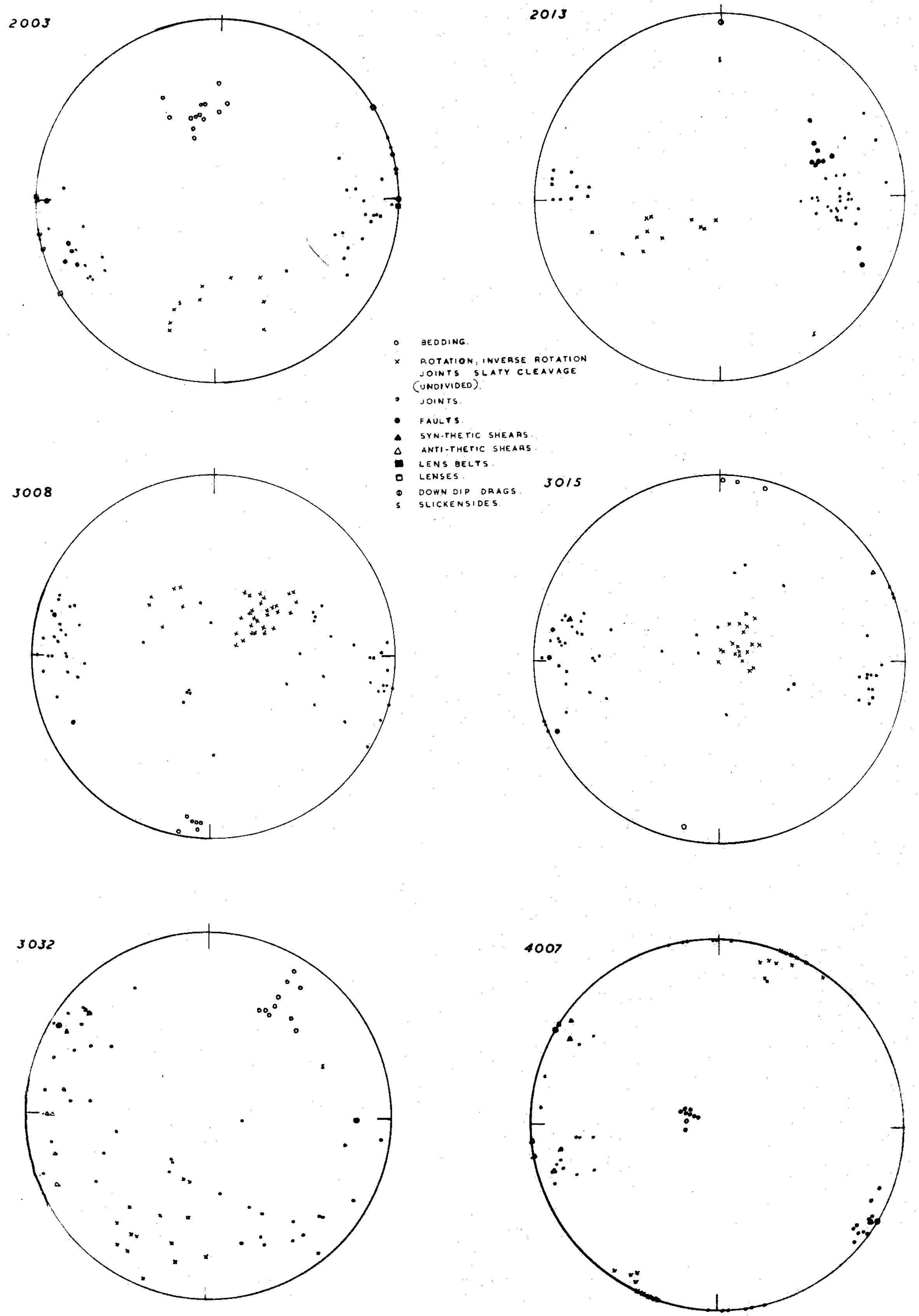

Appendix I Figs.

4012

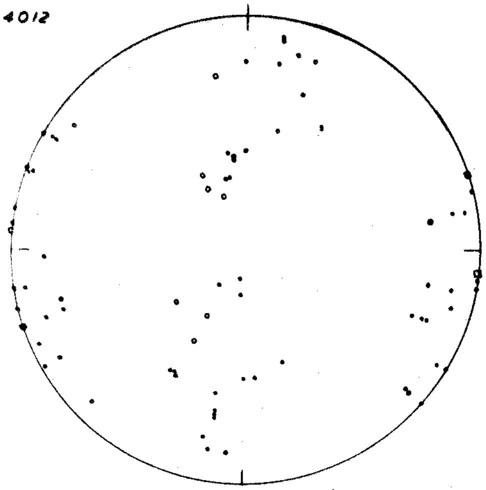

5000

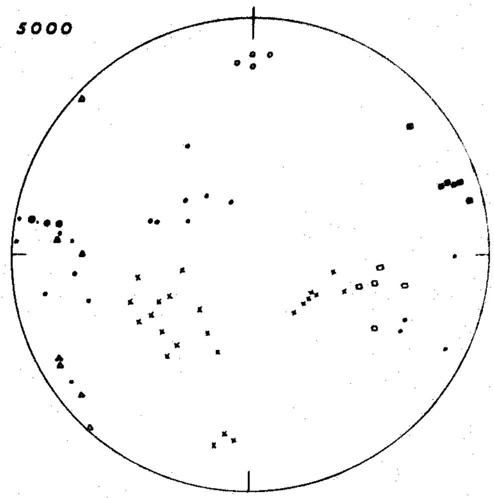

5012

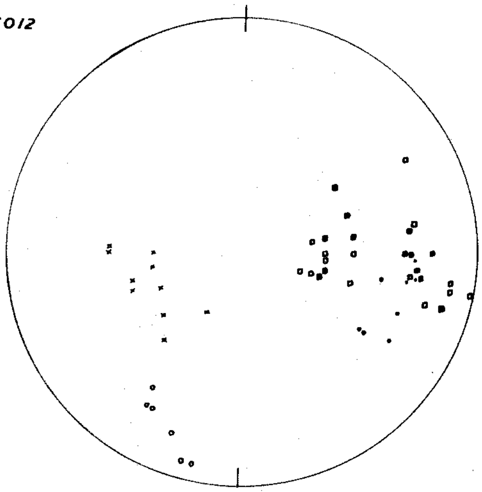

5019

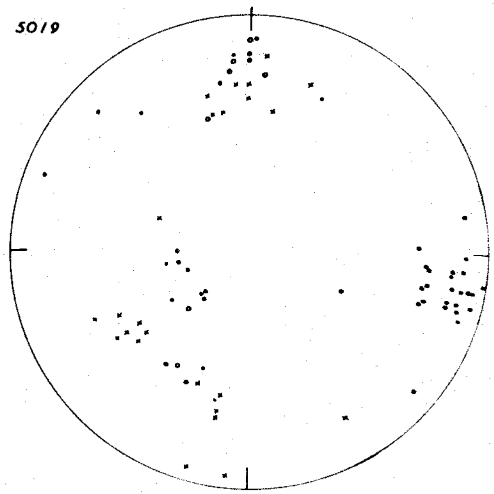

5202

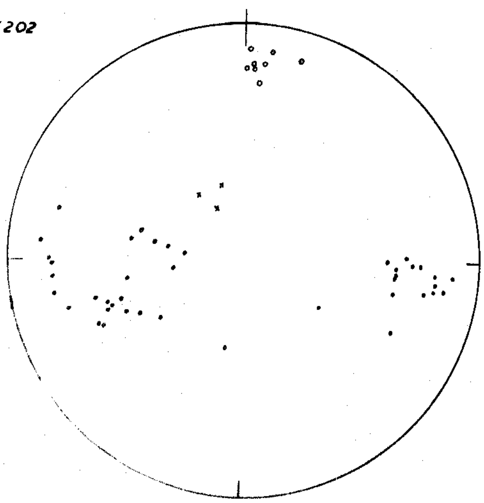

5221

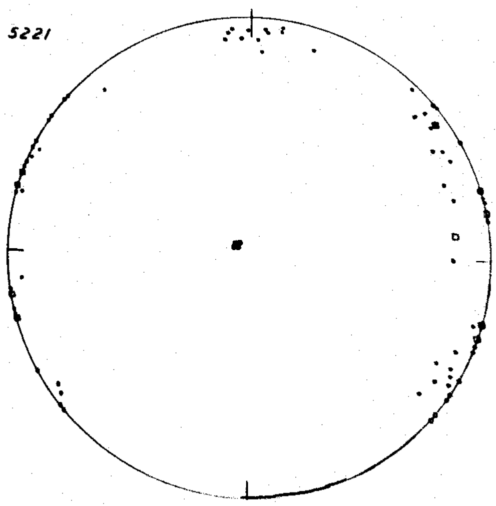

Appendix I Figs.

5240

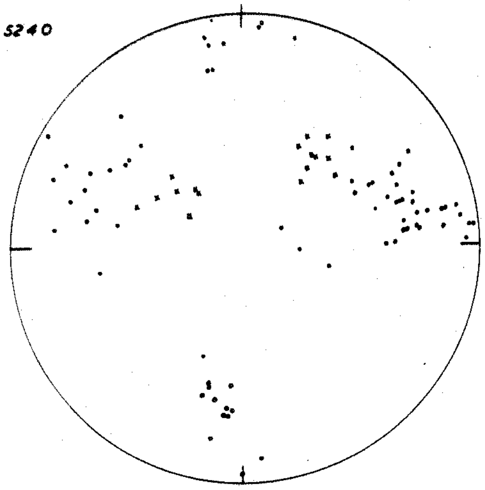

5091

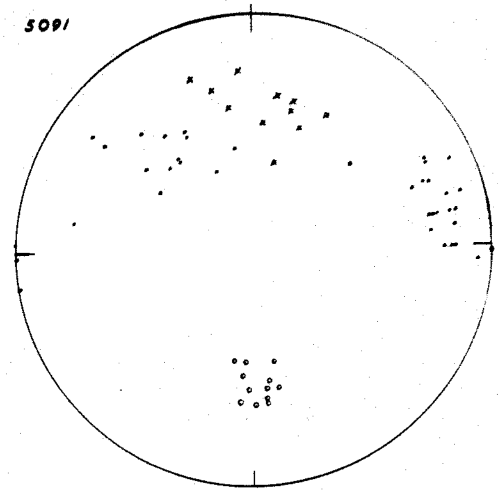

6001

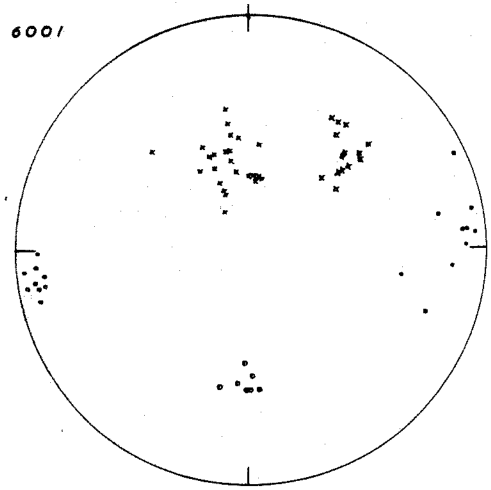

7070

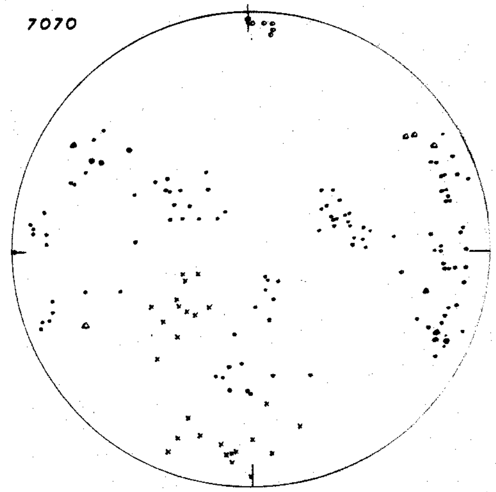

7061

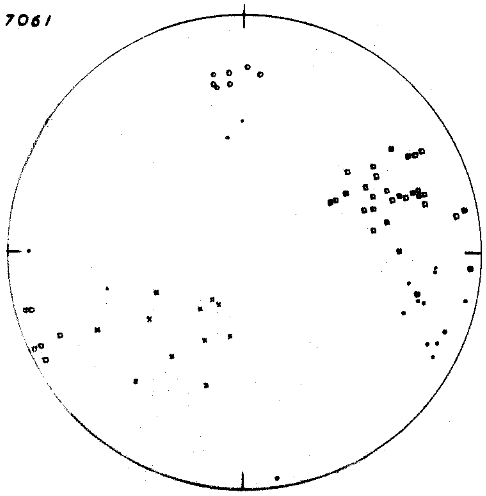

7030

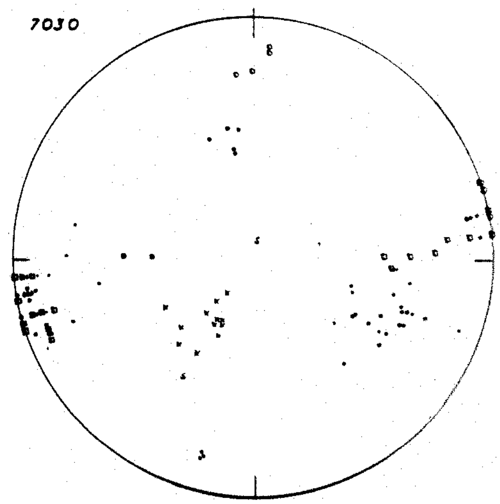

Appendix I Figs.

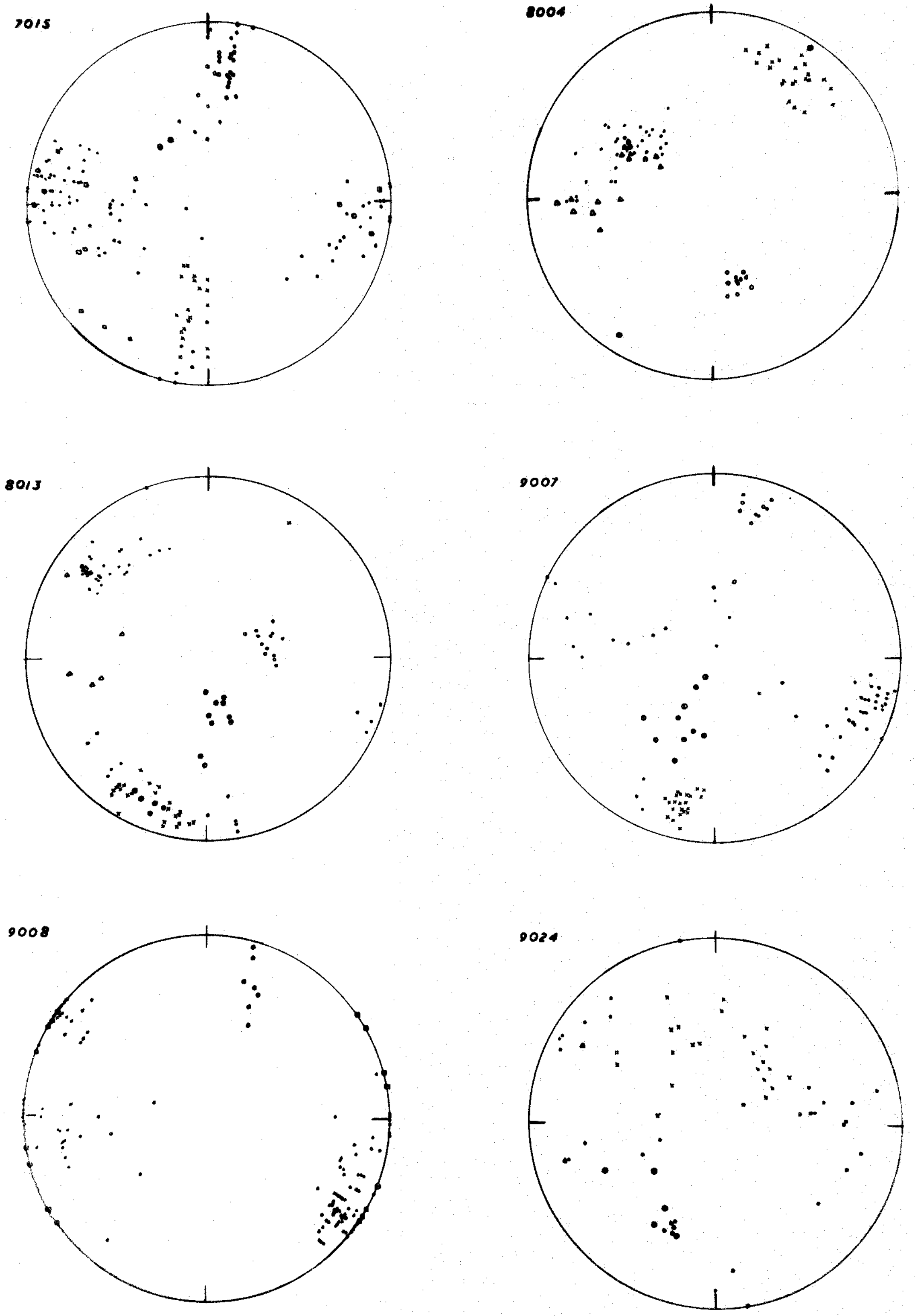

Appendix I Figs.

APPENDIX II   TABLE 1a   EARLY STRUCTURES

Primary deductions based on data in Appendix I

Stereogram number	Bedding or fold axis	Axes from bedding slickensides	Rotation joints and fracture cleavage Lithology	γ	Local fold axis	Inverse rotation joints γ	Inverse axis	Intersection bedding and tens. joints related to bedding slip	Complementary strike shear joints σ_x	σ_y	σ_z	θ	Other strike shears Type	Bedding joint inter-section	Angle bedding onto joint	Down dip drag zones bedding-fracture intersection
A	B	C	D	E	F	G	H	I	J	K	L	M	N	O	P	*
2003	45.167		S_2 limestone	86	15.093	87	04.253						J	04.253	24	
2005	42.179	16.106	" "	90	09.099	85	03.264									
2006	50.164	18.238	" "	73	10.083	80	05.249									
2009	65.169		" "	73	15.086	80	18.251									
2011	100.000	22.265 76.133	D_1 limestone	88	15.093	92	18.266									
2012	95.000		" "	90	25.092 (Axis from slickensides 25.092)											
2013	95.000		" "	83	06.091											
2015	100.355		" "	88	27.090											
2017	100.000		" "	77	24.094	83	23.265									
2018	91.359		" "	82	18.090	76	04.270									
2021	97.000		C_2S_1 limestone	73	12.091	95	28.269	(2022 Triassic collapse breccia)								
2023	92.000		" "	82.	07.091	92	20.269									
3001	77.005		Ludlow	95.	13.277	87	10.093						J.T	16.091	70	
3003	83.005		L.O.R.S. grit " marly ss.	84 89	09.270 11.276	77	36.090	40.281								
3007	82.006		" marl " ss.	82 84	05.276 04.276	89	19.093						J	02.275	56	
3008	83.007		" marl " soft ss. " hard ss. " conglom. Ludlow	78 82 84 66 73	22.280 16.279 16.279 28.281 17.279	72	25.093						J J	05.097 10.095	79 64	(20.173 set) (21.035 set)
3009	84.007		L.O.R.S.	80	07.277	73	24.093	25.279								
3013	82.004		" marl	77	09.274											
3015	91.007	16.276	" ss. " marl	82 75	10.276 14.276				78.043	07.275	08.184	57				
3016	85.007		" hard ss. " marl	58 78	03.277 00.278	74	19.095									
3029	66.210		" ss. " marly ss. " race	90 66 37	08.297 08.297 14.126								T	05.123	14	
3032	66.212	01.121	" ss.marl " ss. " marl	51 85 32	12.296 03.301 21.292	62	22.132	14.303								
4001	23.194		" soft ss.	90	05.115								J	04.112	65	
4003	05.107		" marl	81	05.127											
4004	10.123		" soft ss.	96	10.112											
4006	Axis 07.107		" -	-	07.107			06.224								
4007	13.107		" marl " ss.	89 86	13.114 13.114											
4008	axis 05.110		" marl	90	04.115								T in J fold			
4011	22.166		" ss.	79	08.098								J	15.123	35	
4012	Axis 10.100	05.262	-	-	-								J T J J J J	16.100 outs fold 11.086 32.039 25.133 20.122	29 79 25 29 29	
5000	76.179		U.O.R.S. ss. " conglom. " marl	84 81 37	31.097 29.097 12.092	89	22.263						T	27.096	56	
5005	113.200	12.120	" ss. K_1 shale " oolite	80 45 72	22.100 08.273 32.108											
5006	112.193		K_2 shale	35	14.097 (slickensides axis 23.081)	92	02.284						T J	02.284 27.091	08 54	
5007	130.216		C_2S_1 limestone	91	32.094								J	38.086	39	
5012	110.203		C_2S_1 mudstone	48	32.099											

APPENDIX II TABLE 1b EARLY STRUCTURES

Reference letters as on Table 1a

A	B	C	D	E	F	G	H	I	J	K	L	M	N	O	P	Q
5019	Axis 26.097		C_2S_1 mudstone	53	15.092	(Axis from slickensides 43.088)							T	25.097	31	
	48.035 (S.limb)		" "	41	36.083								J	17.108	26	
			" limestone	81	22.113								J	16.093	62	
5013	50.025		C_2S_1 limestone	81	26.091	90	19.310						J	01.115	56	
5040	46.018	18.090	" "	87	11.097								J	09.099	61	
													J	12.097	82	
5045	85.185		" "	87	45.099											
5020	43.012		" mudstone	65	04.098				24.350	30.103	46.230	45	J	16.085	26	
			" limestone	85	04.098								J	00.103	43	
	102.184		" mudstone	38	36.086	(Axis from slickensides 27.083)			19.199	24.099	58.323	34	T	45.295	04	
			" limestone	53	44.083								J	12.089	16 (for dip of 43.012)	
5021	98.185		" mudstone	71	25.091											
5030	Axis 09.095		" limestone	95	32.098	72	43.296						J	22.070	43	
		12.095	" "	84	16.089								J	02.287	63	
			" "	98	36.104											
5202	73.185		D_1 limestone	83	39.110								J	15.100	52	
5211	80.008		" "	85	21.094	85	31.284		54.336	24.102	25.204	41				
5212	73.011		" "	94	27.092	80	29.290						J	27.092	48	
5213	10.341		" "	88	00.253											
5221	05.133		" "	101	04.093											
5071	14.167		S_2 limestone	78	03.249				04.358	19.090	70.258	32				
5230	55.170		" "	-	-	70	06.255									
5240	56.008		" "	74	22.082	93	16.287						J	10.091	49	
													J	13.089	24	
5241	59.005		" "	89	25.079	90	14.283									
5250	61.183		" "	95	22.260	90	26.108						J	19.103	60	
5091	48.358		D_1 limestone	83	11.277	73	06.081									
6001	47.002	04.088	" "	76	06.086	86	21.293									
		14.285														
6002	77.178		D_2 limestone	80	08.090								J	15.091	24	
6003	17.056		S_2 limestone	88	11.109	113	16.063									
7015	65.185		Z limestone	79	02.096				65.201	08.094	24.001	32				30.110
			" shale	47	02.096											
7016	63.187		" limestone	80	03.275				54.185	08.083	35.347	24	J	05.274	47	15.104
7020	54.169		K shale	109	16.091	82	17.245									
			" limestone	102	24.097											
			" flggy lst.	93	27.100											
7051	67.171		U.O.R.S. ss.	89	20.090	100	14.255									
			" marl	84	19.090											
			" conglom.	97	15.088											
7030	71.181		" marl	87	10.095				66.232	17.101	17.006	34				11.096
			" qtzite.	90	27.103											
			" ss.	93	14.096											
7040	66.175		" ss.	89	16.092											11.090
			" conglom.	92	13.091											
7061	64.175		" qtzite.	86	22.095								J	00.085	20	
7062	80.175		" ss.	79	38.093								J	17.088	46	
													J	47.095	14	
													J	34.091	66	
7063	78.177		L.O.R.S. marl	64	09.089				50.252	32.112	20.009	41				
			" conglom.	66	33.095											
7070	84.183		" ss.	75	24.095								J	00.093	51	
			" marl	23	03.093								T	26.095	69	
7081	60.030		L.O.R.S. ss.	54	18.310	73	16.110		51.067	17.315	34.213	36				
			" marl	56	20.312											
			" ss.	70	12.306											
			" conglom.	97	09.305											
8001	53.006		" marl	73	24.294	(Axis from race rod orientation 21.304)							T	04.277	37	03.093
			" qtzite.	107	14.286											
			" marl	82	24.294											
			" ss.	68	28.298											
			" marl	62	30.300											
			" marl	62	22.292											
			" ss.	66	24.294											
			" marly ss.	72	29.299											

Reference letters as on Table 1a

A	B	C	D	E	F	G	H	I	J	K	L	M	N	O	P	Q
8002	49.000		L.O.R.S. ss.	73	27.296											
			" marly ss.	76	27.296											
			" ss.	73	25.293											
			" marl	73	26.295											
8003	48.350		" marl	74	31.293	(Axis from race rod orientation 11.296)										
			" ss.	82	37.303											
8004	41.344		" ss.	86	28.293	17.287										
			" hard ss.	77	24.285											
			" marly ss.	87	29.296											
			" fine ss.	100	23.293											
8012	Axis 13.290		" marl	80	-											
			" ss.	77	-											
			" ss.	81	-											
8013	28.255		" ss.	87	17.308											19.301
			" ss.	87	12.321											
			" ss.	86	23.286											
8018	22.216	03.127	" marl	94	06.290	94	02.122									05.251
			" ss.	94	06.290	86	02.126									
			" ss.	88	04.286											
			" ss.	90	12.280											
8019	23.002		" -	-	09.292											21.027
8020	67.217		" fine ss.	61	20.296	75	04.128						J	18.297	35	03.305
			" ss.	78	10.301											
9002	64.181		" soft ss.	80	09.267	98	27.256									
			" ss.	88	02.269											
			" marly ss.	70	08.095											
			" marl	36	03.109											
			" ss.	86	07.094											
9003	62.198		U.O.R.S. race	83	12.115	105	04.285						J	25.122	60	
			" soft ss.	89	14.116											
			" ss.	93	12.115											
			" marl	36	03.109											
			" ss.	86	07.112											
			" race ss.	86	04.110											
9004	64.192	00.102	K_m limestone	89	11.107	105	31.265									
			" oolite	94	15.109											
			" ss.	87	09.106											
			K_1 limestone	90	18.110											
			" ss.	98	12.113											
			" nodular lst.	78	04.104											
			" limestone	88	15.109											
			" shale	29	01.231											
9007	74.195		K_2 slaty clvg.	-	04.283								J	21.111	36	06.106
9008	Axes 01.288															
9010	Axes												T	14.092	55	
	19.261		K_2 mudstone	51	07.086											
	15.270		" "	73	33.266											
	18.263		" "	45	11.276											
	18.263		" "	37	03.110											
	32.260		Z limestone	68	30.270											
	19.261		K limestone	92	11.265											
	19.261		K mudstone	61	16.269											
	32.260		Z limestone	55	11.260											
9011	Axes 00.280															
9012	75.194	06.281	Z limestone	87	16.278	89	20.109						T	06.278	55	
9013	63.030		" "	63	09.115								J	00.103	70	
	44.192		" "	88	15.119											
9020	36.015	20.077	K_2 slaty clvg.	-	02.287								J	02.288	54	
	54.014	23.086	" "	-	00.284											
9021	43.019		" "	-	06.103								J	04.105	25	
			" "	-	06.103								J	04.104	36	
			" "	-	02.289								J	03.291	80	
			" "	-	04.105											
			" mudstone	63	02.107											
9023	62.020		L.O.R.S. marl	35	01.290	82	20.099						J	13.103	47	
			" ss.	92	01.109								J	13.098	69	
	54.015		" soft ss.	50	06.288	106	11.097						T	17.296	48	
			" ss.	103	09.290											
			" race ss.	90	14.294											
			" race	95	18.298											
			" ss.	102	20.300											
			" ss.	100	29.307											
9024	52.022		" ss.	100	14.302	100	24.091		36.325	30.079	40.197	37				44.063
			" ss.	92	08.298											
			" race ss.	84	02.110											

APPENDIX II TABLE 2b LATE STRUCTURES

Reference letters as on Table 2a

A	B	C	D	E	F	G	H	I	J	K	L	M	N	O	P	Q	R	S	T	U
5202															77.196	12.359	04.090	24		
5211															87.036	04.190	01.281	29		
5212															54.322	27.187	22.095	34		
5213															02.012	75.108	15.281	27		
5221										05.354	84.197	03.086	21	6 C 10 A	00.359	87.257	04.090	28		
5071											67.215			?	28.159	62.229	04.067	26		
5230						10.346	77.205	08.078	13						45.178	46.006	02.073	19		
5240															58.008	32.185	00.275	32		
5241															51.001	38.199	08.103	39		
5250															45.205	45.018	03.111	35		
5091															50.034	36.181	16.283	41		
6001															NO COMPLEMENTARY SHEARS					
6002															80.310	08.172	08.082	22		
6003															14.171	70.279	18.080	38		
7015											69.346 54.020 06.002			? ? ?	87.181	02.010	00.099	17	30	18.004 30.018
7016											30.010			?	85.226	04.006	03.096	18	29	30.014 18.000
7020											37.356			?	64.180	24.339	08.073	23		
7051											16.307			?	46.185	44.354	06.090	23		
7030										53.203	34.355	14.095	25	23 C 30 A	53.203	34.355	14.095	25		
7040											35.337			10 A	81.201	10.013	01.103	13		
7061										69.275	07.171	22.079	17	18 C 31 A	NO COMPLEMENTARY SHEARS					
7062											12.337			20 A	54.311	18.185	31.094	23		
7063															75.144	10.351	10.276	21		
7070						08.177	80.288	09.085	28						53.293	15.185	33.089	25		
7081											33.209			6 C	11.196	71.071	15.290	27		
8001						13.006	67.131	18.272	24						33.028 28.027	32.141 30.135	41.263 47.263	20 14 (low angle 'joint shear')		
8002						20.048 18.045	69.201 69.195	09.314 11.313	21 16						20.059 17.047	32.162 65.179	51.302 18.311	18 16		
8003	F3 F4 F3 A	16.017 32.019	72.168 55.174	06.284 12.282	18 19	14.177	72.033	10.269	32						NO OBVIOUS COMPLEMENTARY SHEARS					
8004															30.042 28.042	38.137 33.151	38.285 45.279	16 16 (low angle 'joint shear')		
8012															02.178	72.080	18.280	33		
8013						20.182	55.060	27.283	21						NO OBVIOUS COMPLEMENTARY SHEARS					
8018															27.189	60.037	12.285	2[illegible]		
8019						16.195	71.053	13.288	12						NO OBVIOUS COMPLEMENTARY SHEARS					
8020															65.049	23.212	07.304	25		
9002	F2bA F2aF2b	01.359 02.189	82.353 87.043	06.088 02.279	21 28	18.354 09.187	72.173 82.305	01.083 06.095	20 24						73.254	08.021	11.111	25	56	35.356 51.035
9003															40.252	25.019	30.132	23	41	02.027 23.038
9004	F3 JF	02.173	59.081	31.264	18	07.013	75.130	13.281	23						71.175	18.015	06.283	20		
9007															76.171	14.017	07.285	21	30 43	03.020 06.157 07.019 10.015
9008											90.000			38 A	18.196	72.016	01.106	19		
9010															28.170 45.166 15.188	52.073 34.034 76.019	23.274 33.277 03.279	23 (Axis 32.260) 23 (" 45.250) 29 (" 07.273)		
9011															26.186	64.014	02.278	23		
9012															65.171 11.186	23.017 03.018	10.283 09.286	19 18		

APPENDIX II TABLE 2c LATE STRUCTURES

Reference letters as on Table 2a

A	B	C	D	E	F	G	H	I	J	K	L	M	N	O	P	Q	R	S	T	U
9013											63.016			?	NO COMPLEMENTARY SHEARS					
9020															NO COMPLEMENTARY SHEARS					
9021															47.341	36.201	21.095	20		
9023															69.074	14.205	16.298	26	06	33.070 09.203
9024						01.009	68.101	21.277	22						55.359	34.300	10.103	31		

<u>Notes for Appendix II</u>

1. Notes 1,2,3,5,8, of Appendix I apply.
2. Not all the structures tabulated in Appendix I have been submitted to a stress analysis,mainly due to insufficient field data.
3. Meaning of column headings fully explained in text.
4. TABLE 1

    Column N Abbreviations J joint

    T thrust

5. TABLE 2

    Column B Indicates what pairs of faults used. Fault nos. equivalent to those of Table 2,Appendix I.

    Abbreviations A antithetic shear joints to the fault.

    JF small fault (joint fault).

    Column L Full stress analyses of lens belts only given if complementary pair of belts present,otherwise σ_y alone calculated from the intersection of the lenses with the belt.

    Column O Indicates number of degrees lenses have rotated relative to the acute bisectrix direction.

    Abbreviations A anticlockwise rotation

    C clockwise rotation

    Columns PQRS NO COMPLEMENTARY SHEARS - only single wrench joint set present

    NO OBVIOUS COMPLEMENTARY SHEARS - although single joint set present no other joint set is its obvious complement

    Column U σ_y^1 - Indicates the two intersections of the secondary joint with the two primary wrench shear joints.

APPENDIX III

Axial symmetry

Station No.	Angle- Inverse axis on to bedding dip direction	Angle-axis on to bedding dip direction	Angle-axis on to inverse axis about the bedding strike
2003	84°	68°	28°
2005	82°	76°	22°
2006	88°	70°	22°
2009	71°	73°	36°
2011	72°	75°	33°
2017	88°	66°	26°
2018	87°	77°	22°
2021	63°	77°	40°
2023	70°	83°	27°
3001	79°	77°	24°
3003	53°	79°	47°
3007	71°	85°	24°
3008	65°	74°	42°
3009	65°	84°	32°
3016	71°	88°	21°
3032	66°	78°	38°
5000	67°	58°	55°
5013	66°	55°	59°
5030	50°	58°	72°
5211	59°	68°	53°
5212	60°	61°	59°
5240	71°	64°	35°
5241	74°	61°	45°
5250	60°	66°	54°
5091	81°	70°	25°
6001	61°	84°	35°
6003	(Both axes displaced to one side of dip)		44°
7020	69°	70°	41°
7051	75°	68°	37°
7081	71°	70°	39°
8018	85°	76°	19°
8020	86°	68°	26°
9002	60°	90°	30°
9003	84°	85°	09°
9004	56°	74°	50°
9012	69°	74°	37°
9023	76°	73°	30°
9024	58°	77°	49°

APPENDIX IV

Field station grid references

Station	ref.
	SS
2003	09509857
2005	09559854
2006	09689854
2009	09889868
2011	09399773
2012	09309776
2013	09259778
2015	09129779
2017	09109780
2018	09389768
2021	08979755
2022	09109756
2023	09189751
3001	02209812
3003	02259813
3007	02309815
3008	02389813
3009	02409815
3013	02649810
3015	02759809
3016	02909811
3029	01929735
3032	02089728
4001	00809685
4003	00799670
4004	00789666
4006	00809652
4007	00769649
4008	00699654
4011	00029640
4012	00099646
	SR
5000	99579607
5005	99499608
5006	99429601
5007	99449591
5012	99409586
5019	99409579
5013	99389571
5040	99219580
5045	99309560
5020	99409561
5021	99419558
5030	99469550
5202	98889523
5211	98939490
5212	99169489
5213	99289456
5221	99519439
5071	98149398
5230	97699434
5240	97969422
5241	97699428
5250	97759380
5091	97709355
6001	94189420
6002	94149437
6003	93089444
7015	88929731
7016	88859750
7020	88809828
7051	88909848
7030	88689875
7040	88649872
7061	88759889
7062	88739898
7063	88709910
7070	88459939
	SM
7081	88000055
8001	86480088
8002	86370091
8003	86150110
8004	85940110
8012	84890168
8013	84890173
8018	84450172
8019	84430168
8020	84520187
9002	84900380
9003	84940370
9004	84960355
9007	85100346
9008	85070341
9010	85050337
9011	85150339
9012	85280330
9013	85330329
9020	85120311
9021	85000312
9023	84240286
9024	84130278

Fig. 1.1 TECTONIC DIVISIONS OF ARMORICAN PEMBROKESHIRE

For full explanation see text.
Divisions based on information in the Geological Survey Memoirs for the Geology of the South Wales Coalfield Parts XI (Haverfordwest), XII (Milford) and XIII (Pembroke and Tenby).

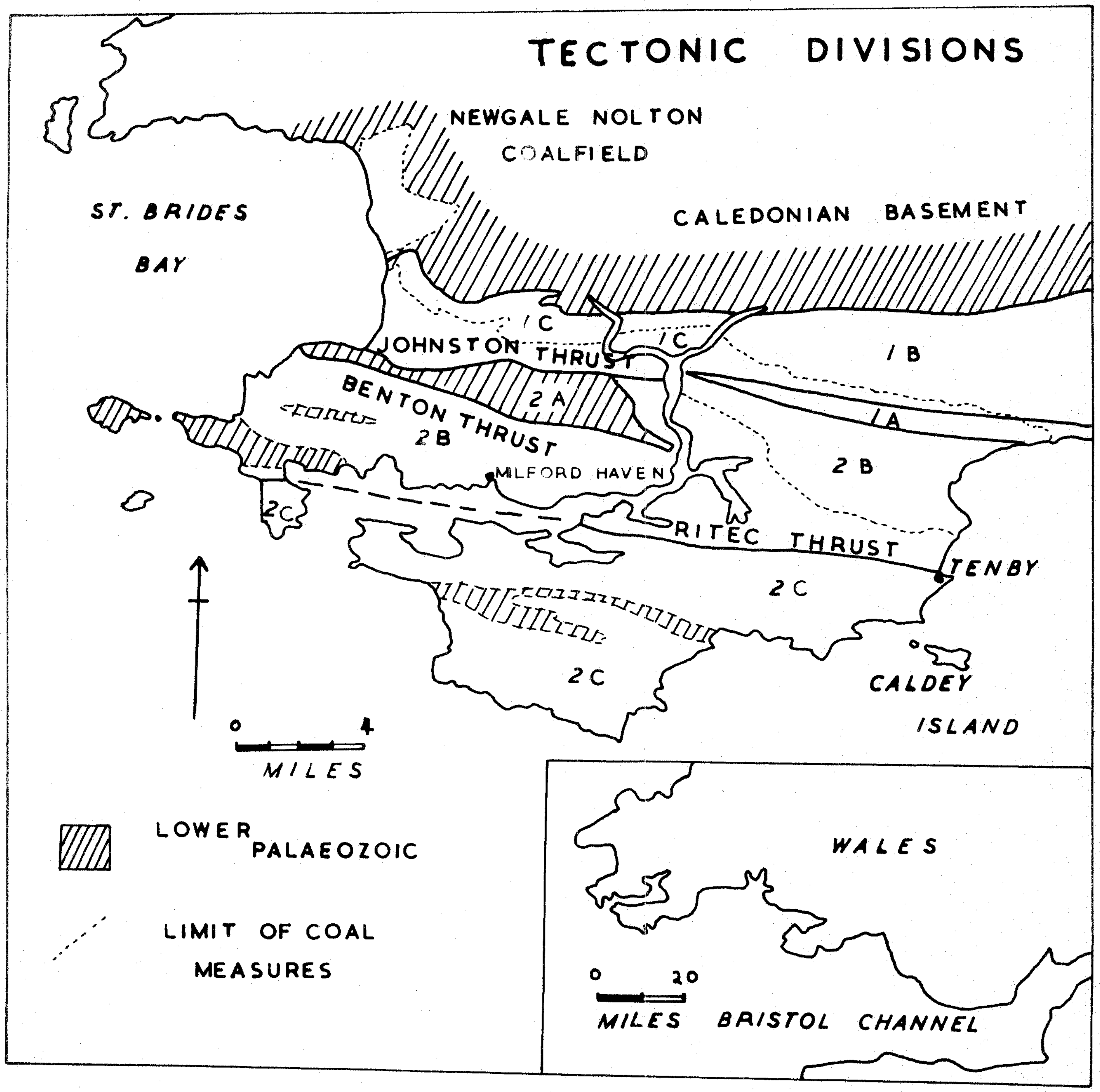
TECTONIC DIVISIONS
NEWGALE NOLTON
COALFIELD
CALEDONIAN BASEMENT
ST. BRIDES
BAY
1 C
1 C
1 B
JOHNSTON THRUST
BENTON THRUST
2 A
2 B
1 A
2 B
MILFORD HAVEN
2C
RITEC THRUST
TENBY
2 C
2 C
CALDEY
ISLAND
0
4
MILES
LOWER
PALAEOZOIC
LIMIT OF COAL
MEASURES
WALES
0
20
MILES
BRISTOL CHANNEL

Fig. 1.1

Fig. 1.2. ORIELTON ANTICLINE: OUTCROP GEOLOGY WITH FIELD ZONES AND STATIONS

Geology after the Geological Survey. The field station numbers are written closest to where they occur and are usually listed for a geographic direction around the coast.

Eight figure grid references for field stations in Appendix IV.

errata. - Field station No. 9012 should be inserted between stations 9011 and 9013.

Station No. 7018 should read 7081.

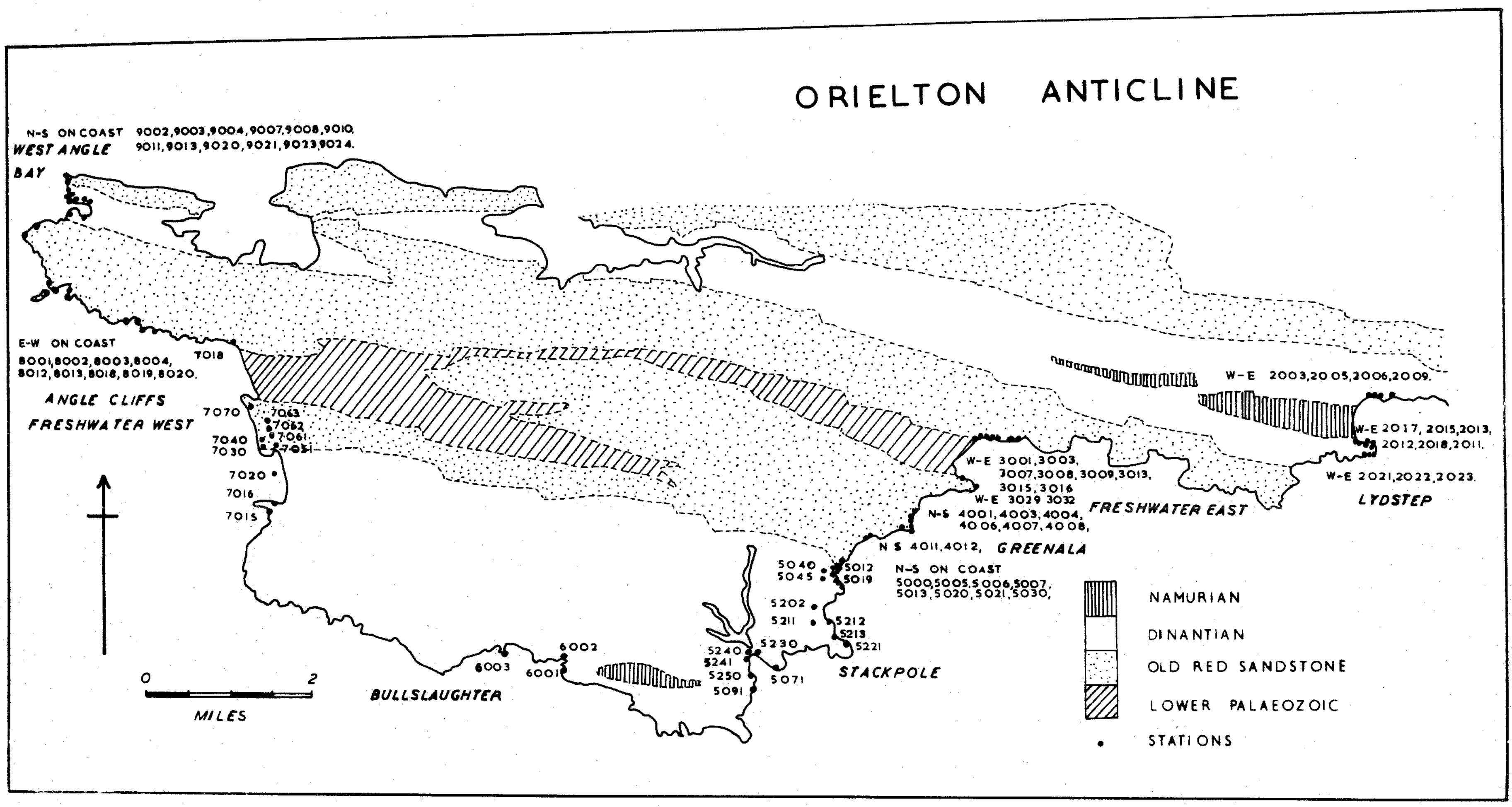
ORIELTON ANTICLINE
N-S ON COAST 9002,9003,9004,9007,9008,9010,
9011,9013,9020,9021,9023,9024.
WEST ANGLE
BAY
E-W ON COAST
8001,8002,8003,8004,
8012,8013,8018,8019,8020.
7018
ANGLE CLIFFS
FRESHWATER WEST
7070
7063
7062
7061
7051
7040
7030
7020
7016
7015
0
2
MILES
BULLSLAUGHTER
6003
6001
6002
5240
5241
5250
5091
5230
5071
5202
5211
5212
5213
5221
STACKPOLE
5040
5045
5012
5019
N-S ON COAST
5000,5005,5006,5007,
5013,5020,5021,5030,
N S 4011,4012,
GREENALA
N-S 4001,4003,4004,
4006,4007,4008,
W-E 3001,3003,
3007,3008,3009,3013,
3015,3016
W-E 3029 3032
FRESHWATER EAST
W-E 2003,2005,2006,2009.
W-E 2017, 2015,2013,
2012,2018,2011.
W-E 2021,2022,2023.
LYDSTEP
NAMURIAN
DINANTIAN
OLD RED SANDSTONE
LOWER PALAEOZOIC
STATIONS

Fig. 1.2

Fig. 2.1 METHODS

DATA REDUCTION METHODS FOR A TYPICAL STATION

A Contoured diagram Station 5211, 96 poles, 1% contour interval. Poles shown on Fig. 2.1B.

B Pole plot with angular means and 95% circles of confidence. As well as the angular mean and circle of confidence for each group of poles the limit of the poles chosen for calculating that mean have been indicated.

ANALYSIS METHODS

C Early formed structures Key

Symbol	Name	Attitude
BP	Bedding plane	60.190
BP SL 1	1st set bedding slickensides	58.213
BP SL 2	2nd set bedding slickensides	58.167
ROT	Rotation joints	41.027
SL ROT	Slickensides on rotation joints	39.007
CLV	Fracture cleavage	60.021
I ROT	Inverse rotation joints	36.347
TENS	Tension joints related to bedding slip	41.184
SJ 1	1st set strike joints	85.191
SJ 2	2nd set strike joints	36.178
SJ 2 SL	Slickensides on 2nd set of strike joints	35.199
T P	Thrust	47.034

Fig. 2.1 (Cont)

Symbol	Name	Attitude
TS	Down dip drag zone	65.344
A	Local fold axis	10.105
I A	Inverse axis	10.273
σ_x^1, σ_y^1, σ_z^1	stress axes deduced from complementary strike joints	
σ_x^2, σ_y^2, σ_z^2	stress axes deduced from a single set of strike joints and the bedding	

D <u>Late formed structures Key</u>

Symbol	Name	Attitude
DWF	Dextral wrench faults and shears	86.226
SWF	Sinistral wrench faults and shears	76.311
DJ 1	1st set dip joints and lens belts	79.097
DJ 2	2nd set dip joints and lens belts	59.304
DJ 2 SL	Slickensides on 2nd set dip joints	43.248
LENS 1	Tension lenses assoc. 1st set lens belts	68.298
LENS 2	Tension lenses assoc. 2nd set lens belts	86.102
A	Local fold axis	10.105
σ_x^1, σ_y^1, σ_z^1	stress axes deduced from the wrench faults	
σ_x^2, σ_y^2, σ_z^2	stress axes deduced from the complementary wrench shear joints (Diagonal dip joints or wrench-joints)	

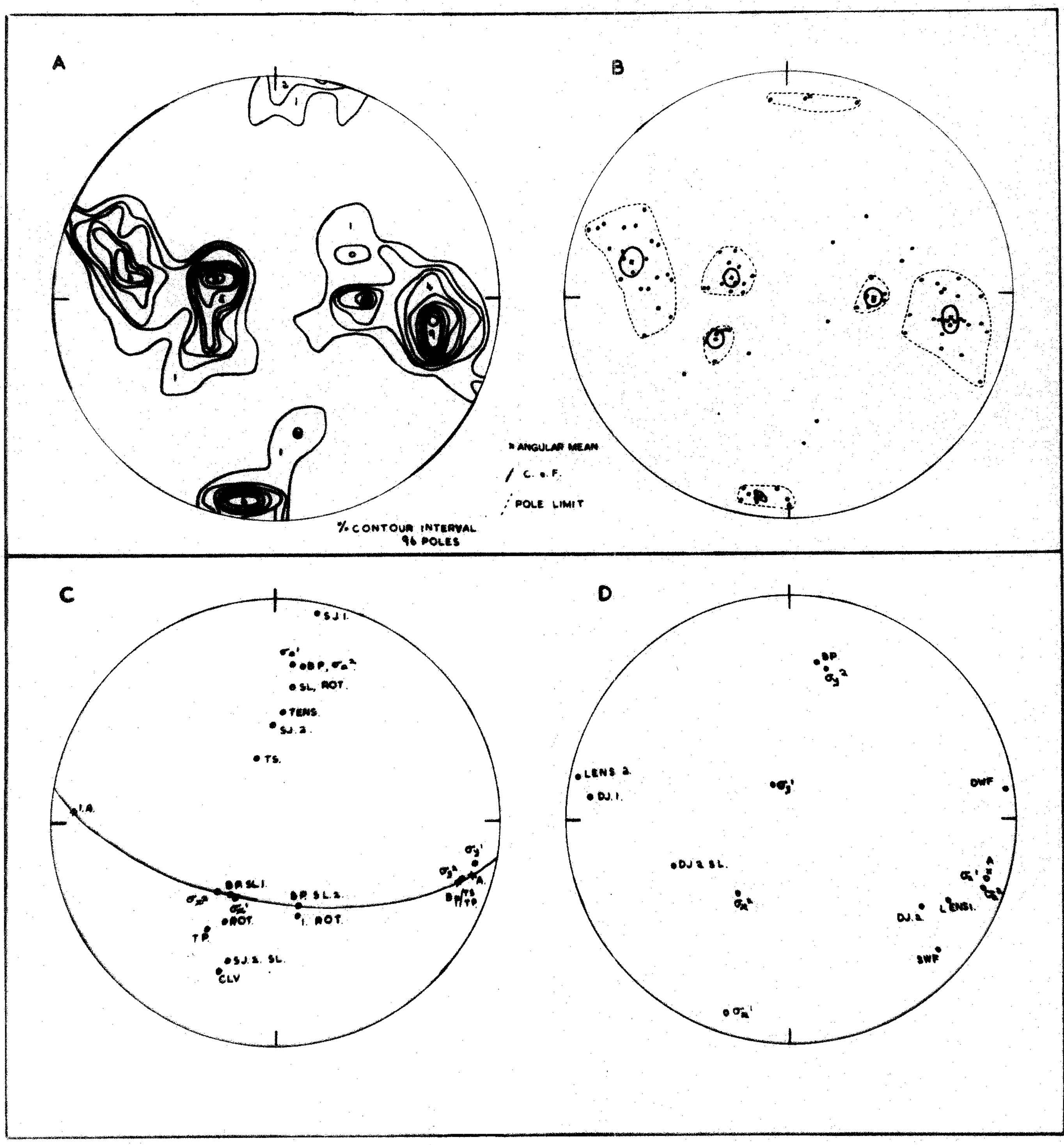
A
B
C
D
ANGULAR MEAN
C. e. F.
POLE LIMIT
% CONTOUR INTERVAL
96 POLES
SJ 1.
BP
SL, ROT.
TENS.
SJ. 2.
TS.
I.A.
BP. SL 1.
BP. SL. 2.
ROT.
1. ROT.
TP.
SJ. 2. SL.
CLV
LENS 2.
DJ. 1.
DWF
DJ 2 SL.
DJ. 2.
LENS1.
SWF

Fig. 2.1

Fig. 3.1 TECTONIC MAP OF THE ORIELTON ANTICLINE

Major folds and faults. Stratigraphic boundaries and most structural directions after the Geological Survey.

KEY	FOLDS
1.	Pembroke syncline
2.	Angle syncline
3.	Freshwater East anticline
4.	Orielton syncline
5.	Castlemartin Corse anticline
6.	Murchison syncline *
7.	Stackpole Quay anticline
8.	Barafundle syncline
9.	Stackpole Warren anticline
10.	Fish ponds syncline
11.	Lily ponds syncline
12.	Lily ponds anticline
13.	Broadhaven syncline
14.	Broadhaven anticline
15.	Bullslaughter Bay syncline
16.	New Quay anticline
17.	Warren anticline
18.	Linney anticline
19.	Linney syncline
20.	Axton Hill syncline
21.	Axton Hill anticline
22.	Corston Beacon anticline

	FAULTS
I	Stackpole Quay fault
II	Stackpole Warren fault
III	Flimston Bay fault

* so named because figured in Murchison's 'Siluria'.

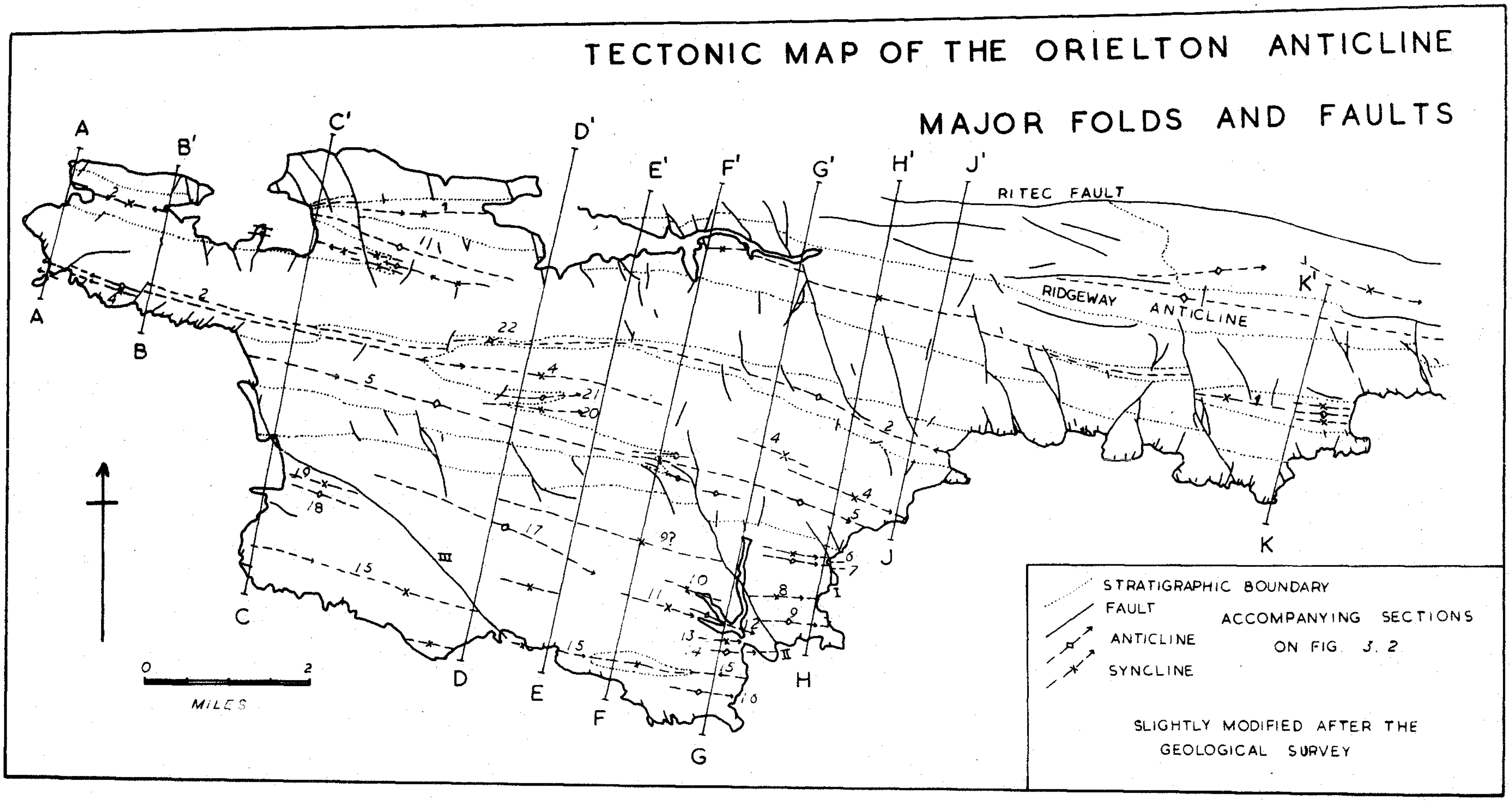
TECTONIC MAP OF THE ORIELTON ANTICLINE
MAJOR FOLDS AND FAULTS
RITEC FAULT
RIDGEWAY ANTICLINE
A A'
B B'
C C'
D D'
E E'
F F'
G G'
H H'
J J'
K K'
0 2
MILES
STRATIGRAPHIC BOUNDARY
FAULT
ANTICLINE
SYNCLINE
ACCOMPANYING SECTIONS ON FIG. 3.2
SLIGHTLY MODIFIED AFTER THE GEOLOGICAL SURVEY

Fig. 3.1

Fig. 3.2. SECTIONS ACROSS THE ORIELTON ANTICLINE

To accompany **Fig.** 3.1.

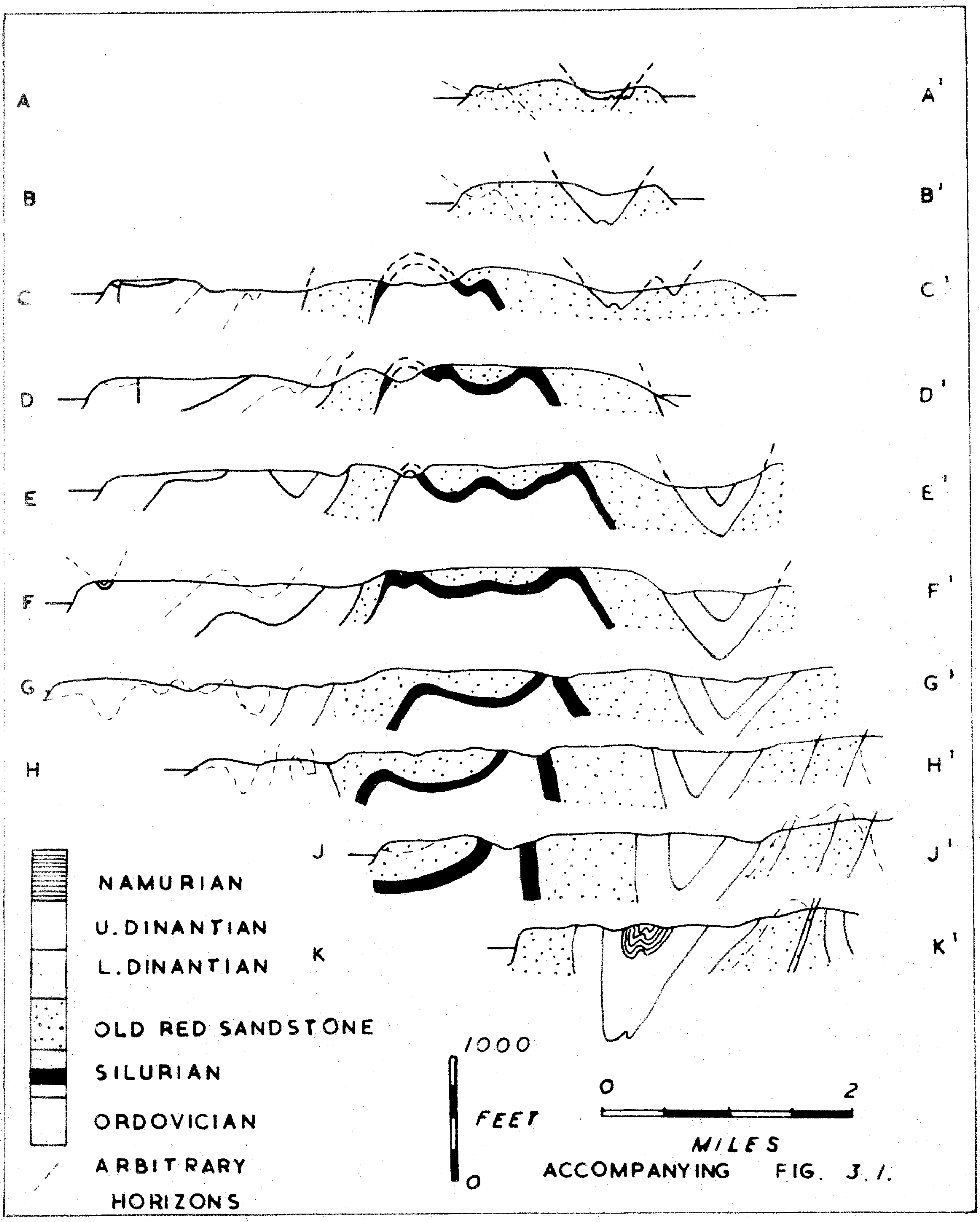
A
A'
B
B'
C
C'
D
D'
E
E'
F
F'
G
G'
H
H'
J
J'
K
K'
NAMURIAN
U. DINANTIAN
L. DINANTIAN
OLD RED SANDSTONE
SILURIAN
ORDOVICIAN
ARBITRARY HORIZONS
1000
FEET
0
0
2
MILES
ACCOMPANYING FIG. 3.1.

Fig. 3.2

Fig. 3.3 STRUCTURAL MAP AND SECTION: STACKPOLE QUAY AREA

Stratigraphical boundaries after the Geological Survey.

Structure section as seen on cliffs.

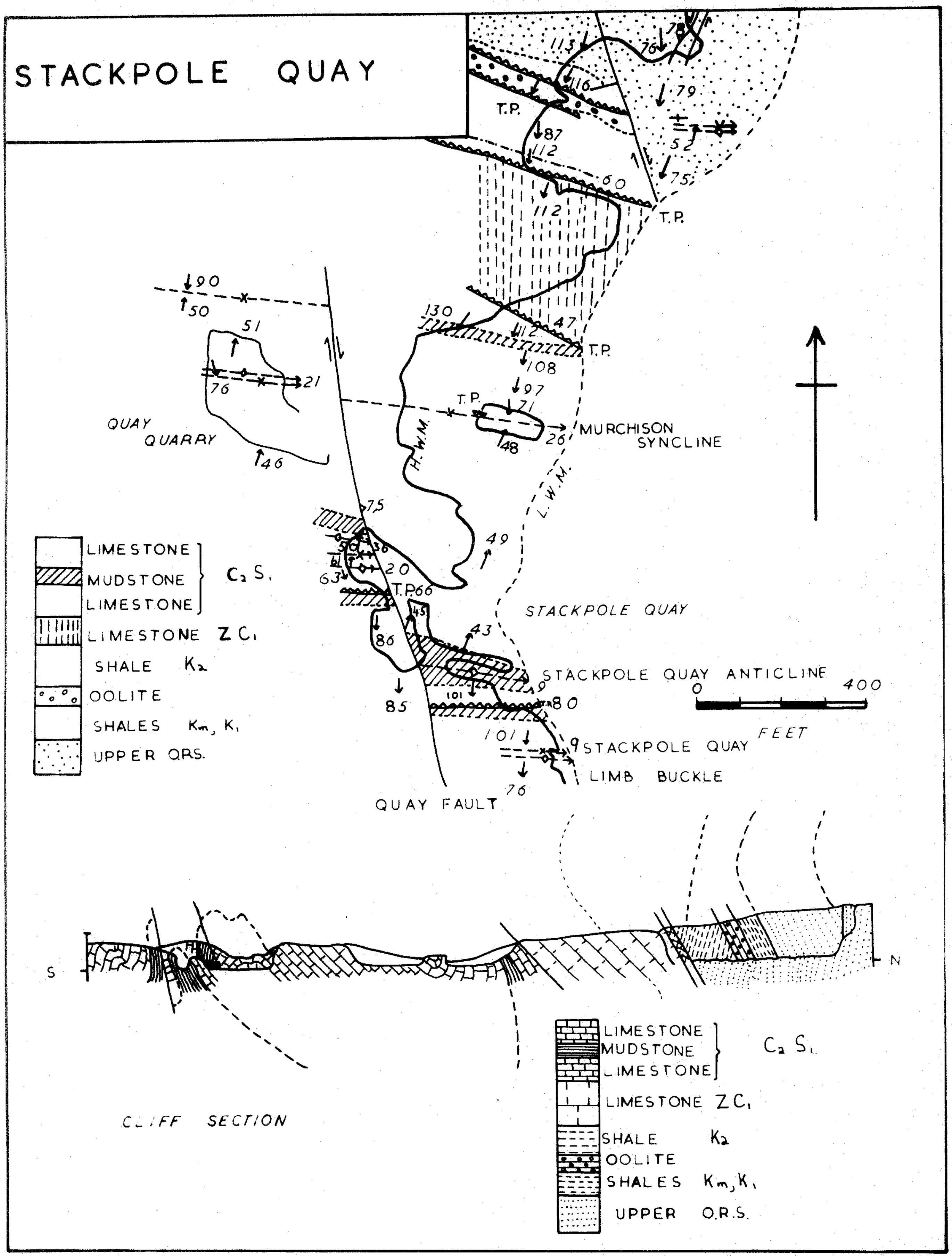
STACKPOLE QUAY
QUAY QUARRY
MURCHISON SYNCLINE
STACKPOLE QUAY
STACKPOLE QUAY ANTICLINE
STACKPOLE QUAY LIMB BUCKLE
QUAY FAULT
H.W.M.
L.W.M.
T.P.
0 400 FEET
LIMESTONE
MUDSTONE
LIMESTONE
C_2 S_1
LIMESTONE Z C_1
SHALE K_2
OOLITE
SHALES K_m, K_1
UPPER O.R.S.
CLIFF SECTION
S
N

Fig. 3.3

Fig. 3.4 STRUCTURAL MAP AND SECTIONS: STACKPOLE WARREN AREA

Stratigraphical boundaries after the Geological Survey.

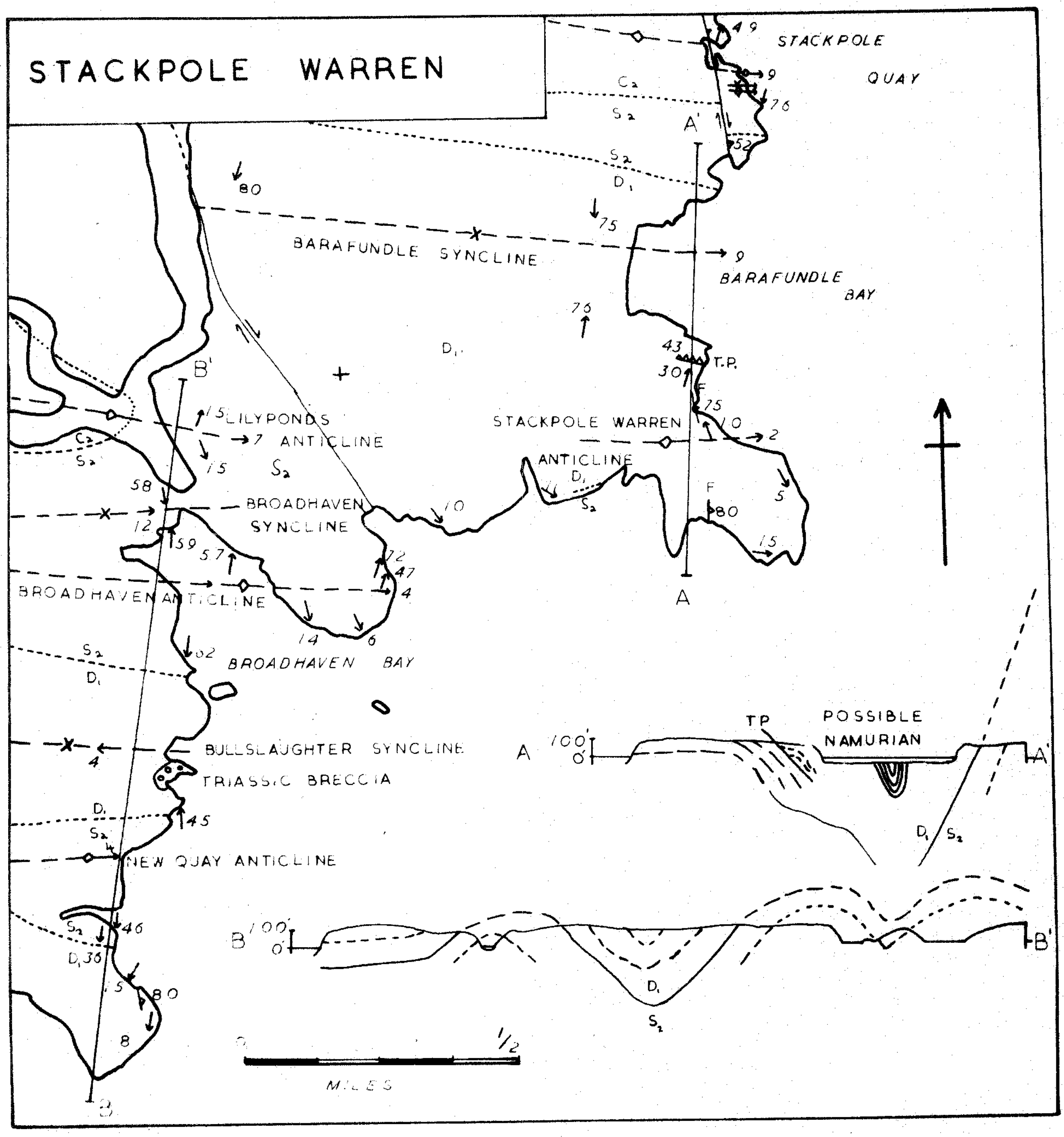
STACKPOLE WARREN
STACKPOLE
QUAY
BARAFUNDLE SYNCLINE
BARAFUNDLE
BAY
LILYPONDS
ANTICLINE
STACKPOLE WARREN
ANTICLINE
BROADHAVEN
SYNCLINE
BROADHAVEN ANTICLINE
BROADHAVEN BAY
BULLSLAUGHTER SYNCLINE
TRIASSIC BRECCIA
NEW QUAY ANTICLINE
POSSIBLE
NAMURIAN
T.P.
MILES

Fig. 3.4

Fig. 3.5 LIMB AND AXIAL BUCKLES

A <u>Stereogram of limb buckle geometry</u>

The major fold is the Bullslaughter Bay syncline at Bullslaughter Bay.

B <u>Stereogram of axes and axial planes of axial buckles</u>

Buckles on the north side of West Angle Bay compared with the symmetry of the Angle syncline.

C <u>Schematic geometry of a limb buckle</u>

D <u>Schematic geometry of axial buckles</u>

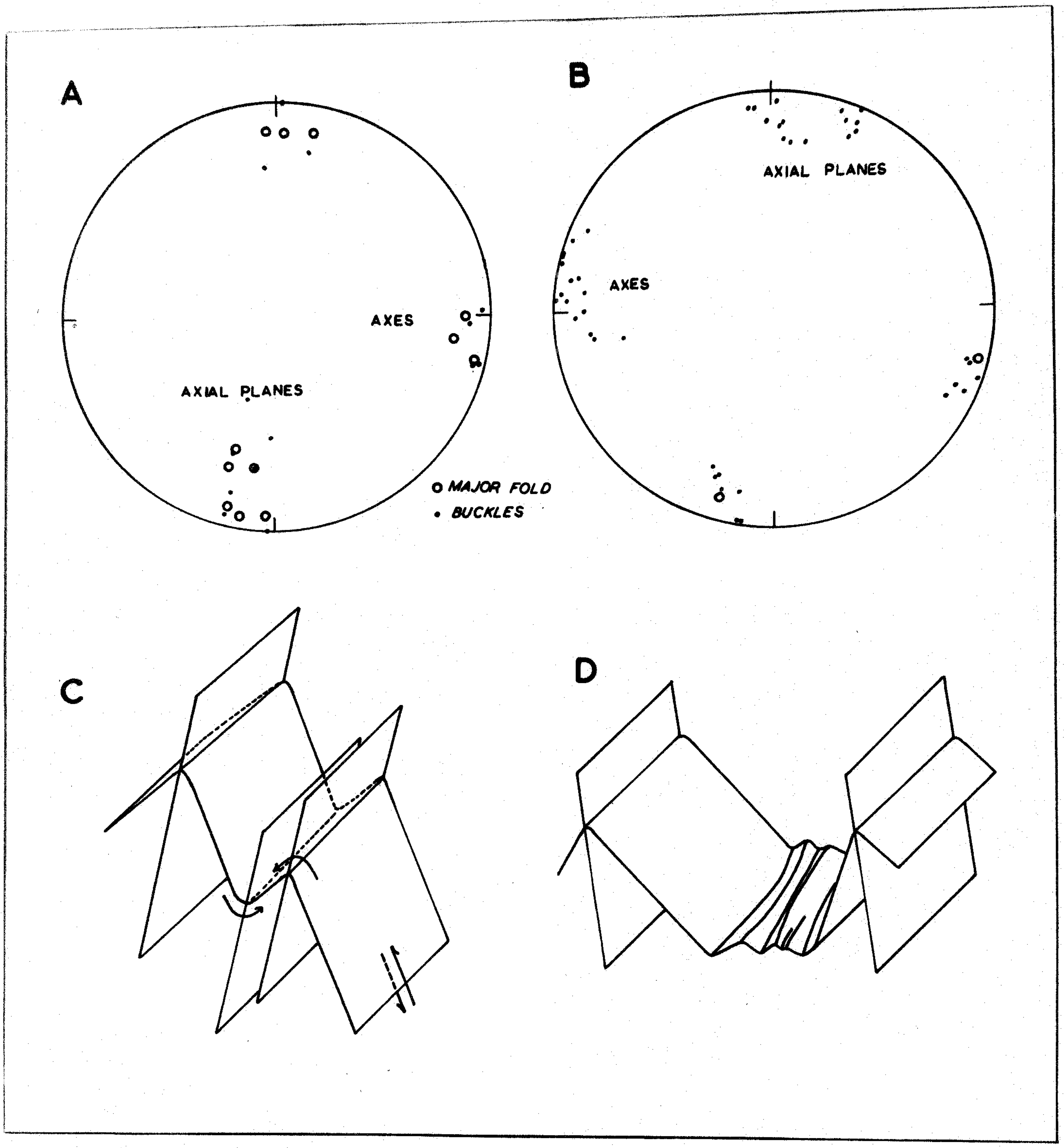
A
B
C
D
AXES
AXIAL PLANES
AXIAL PLANES
AXES
o MAJOR FOLD
• BUCKLES

Fig. 3.5

Fig. 3.6 STRUCTURAL MAP AND SECTIONS: BULLSLAUGHTER BAY

Stratigraphical boundaries after the Geological Survey.

Crocksydam anticline and Moody Nose syncline are local names for the two elements of the limb buckle south of the Bullslaughter Bay syncline.

Fig. 3.6

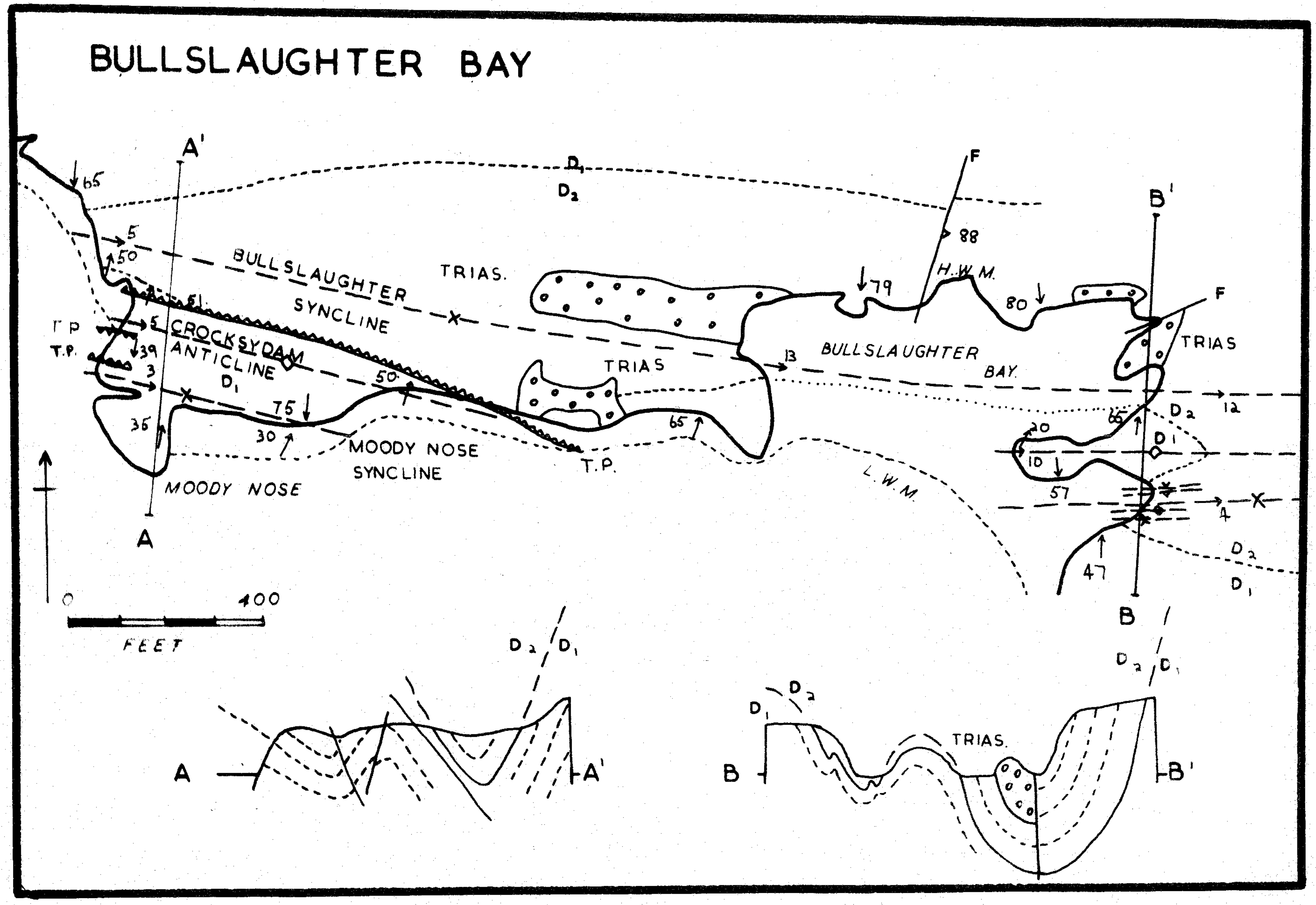
BULLSLAUGHTER BAY
A'
A
B'
B
D_1
D_2
TRIAS.
TRIAS
BULLSLAUGHTER SYNCLINE
CROCKSYDAM ANTICLINE
MOODY NOSE SYNCLINE
MOODY NOSE
BULLSLAUGHTER BAY
H.W.M.
L.W.M.
T.P.
F
0
400
FEET

Fig. 3.7 STRUCTURAL MAP AND SECTIONS: WHITEDOLE BAY AREA (ANGLE CLIFFS FIELD ZONE)

Castle's Bay anticline equivalent to Freshwater East anticline.

Sheep Island syncline equivalent to Orielton syncline.

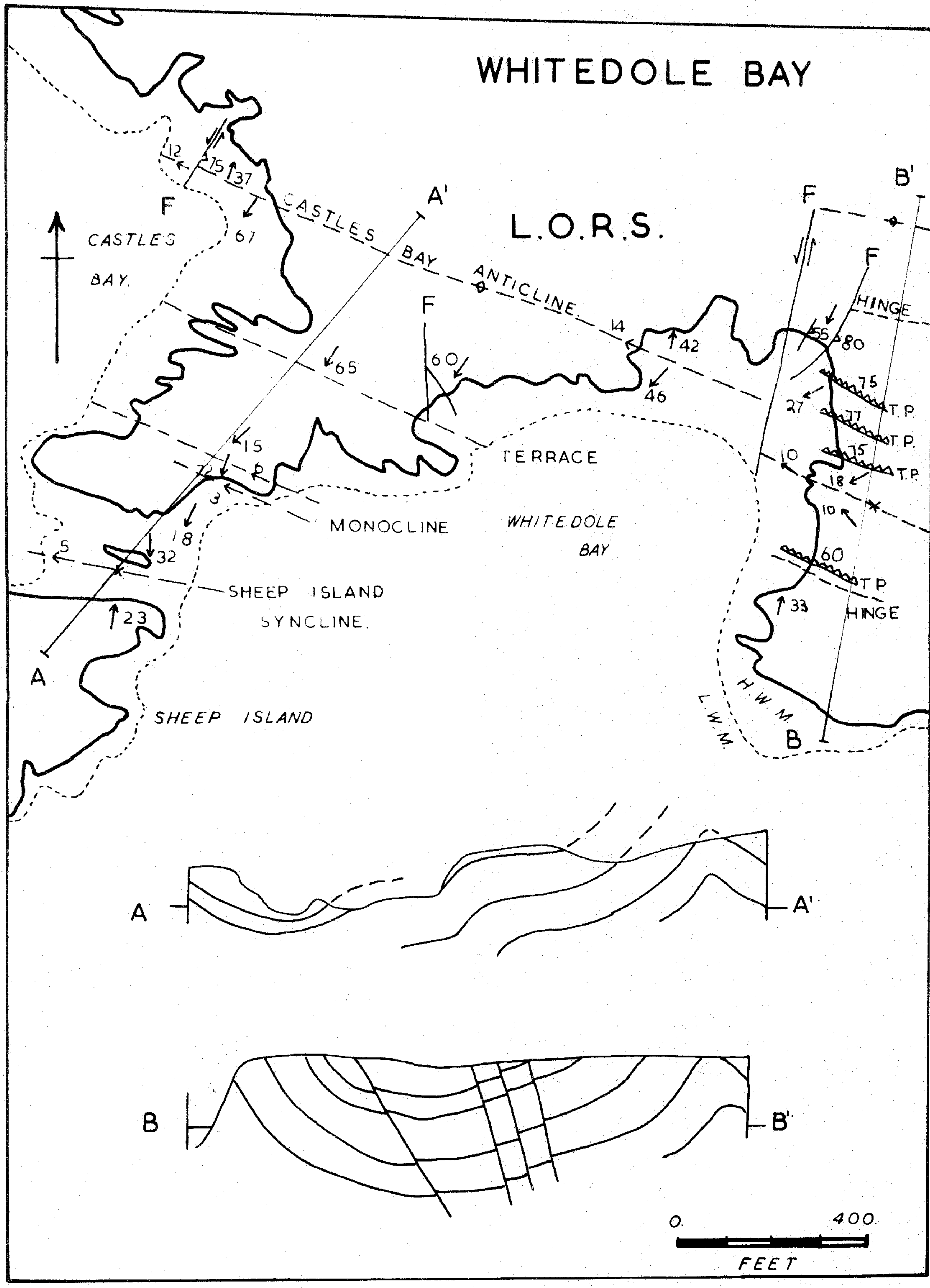
WHITEDOLE BAY
L.O.R.S.
CASTLES BAY
CASTLES BAY ANTICLINE
TERRACE
MONOCLINE
WHITEDOLE BAY
SHEEP ISLAND SYNCLINE
SHEEP ISLAND
HINGE
T.P.
H.W.M.
L.W.M.
F
A
A'
B
B'
0. 400.
FEET

Fig. 3.7

Fig. 3.8 FIELD SKETCHES OF AXIAL BUCKLES

A Eastern end of the Castlemartin Corse anticline (4012)

Sandstones (stippled), overlying marls (unstippled).
Note- fracture cleavage, strike shear joints and a small thrust arising out of a strike shear joint. (See Plate 3.4)
Lower Old Red Sandstone

B Eastern end of the Orielton syncline at Greenala Point (4006)

Lower Old Red Sandstone horizons
Note- fracture cleavage, lenses in buckle crests, tension joints related to bedding slip (far left of sketch) and irregular shears of sub-phase 2 (far left of sketch)

Fig. 3.9 FIELD SKETCHES OF RIPPLES

A Ripples in K_2 limestone bands interbedded with shales and thrust over Z limestones Station 5006, Stackpole Quay.

Shales cut by fracture cleavage dipping less steeply than the bedding (i.e. beds overturned), and small thrusts developed parallel to the fracture cleavage.

B Ripples in limestones interbedded with K_2 shales Station 9021, West Angle Bay

Note- slaty cleavage and tension cracks normal to the bedding

C Ripples on a small anticline in Z limestones Station 9013, West Angle Bay

Note- fracture cleavage persisting across fold and infilled late wrench-joints

3.8

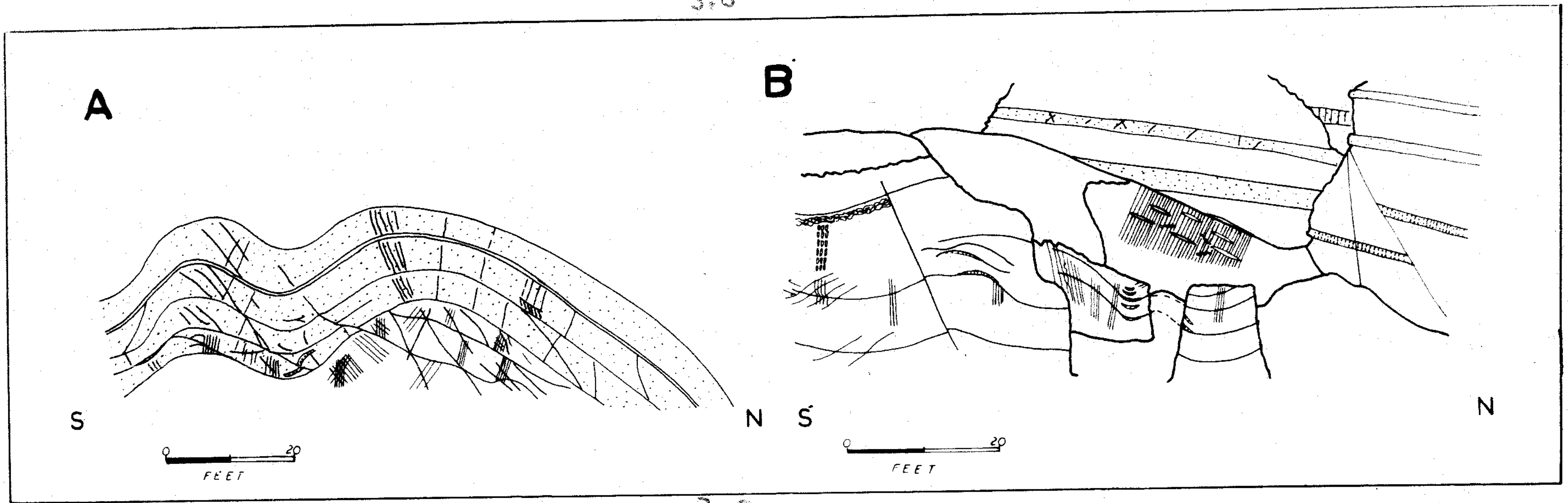
A
B
S
N
S
N
0
20
FEET
0
20
FEET

3.9

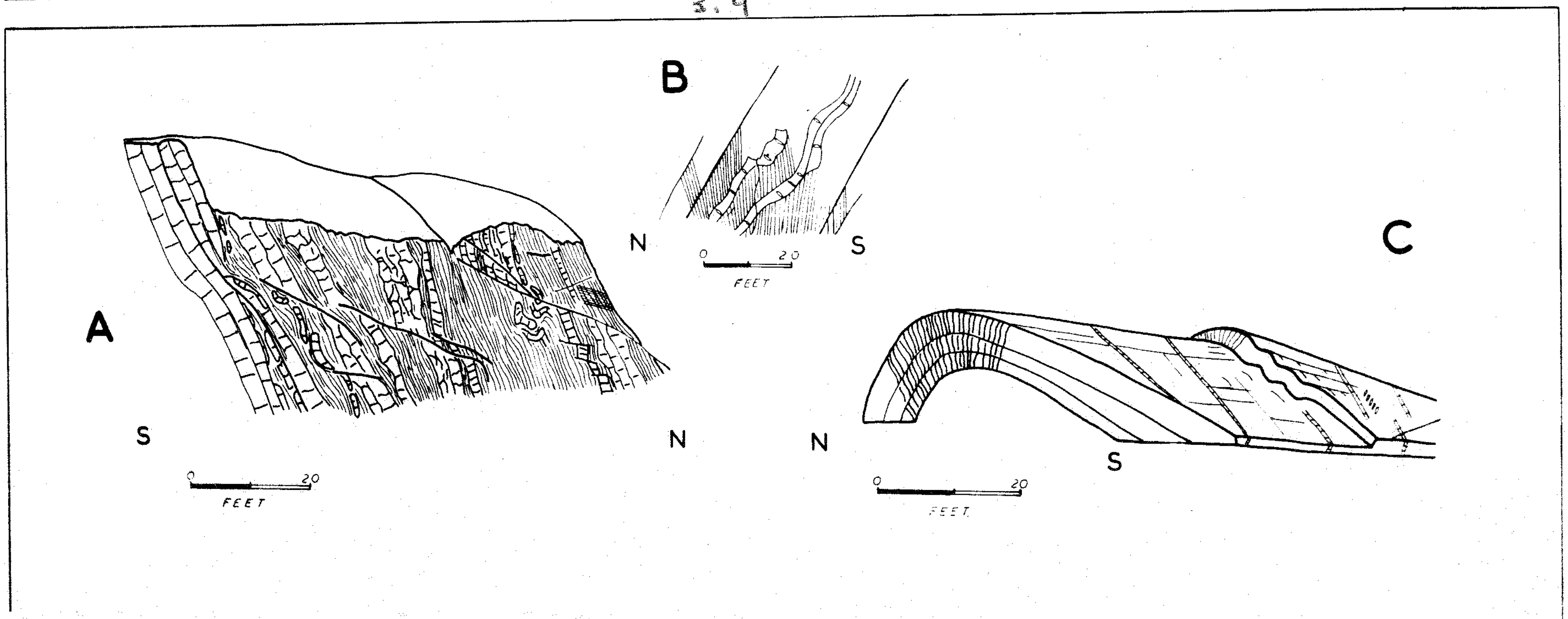
A
B
C
S
N
N
S
N
S
0
20
FEET
0
20
FEET
0
20
FEET

Fig. 3.10 STRUCTURAL SKETCH MAP AND SECTIONS: NORTH SIDE OF WEST ANGLE BAY

Zonal horizons after the Geological Survey.

Foreshore sections on same scale as map.

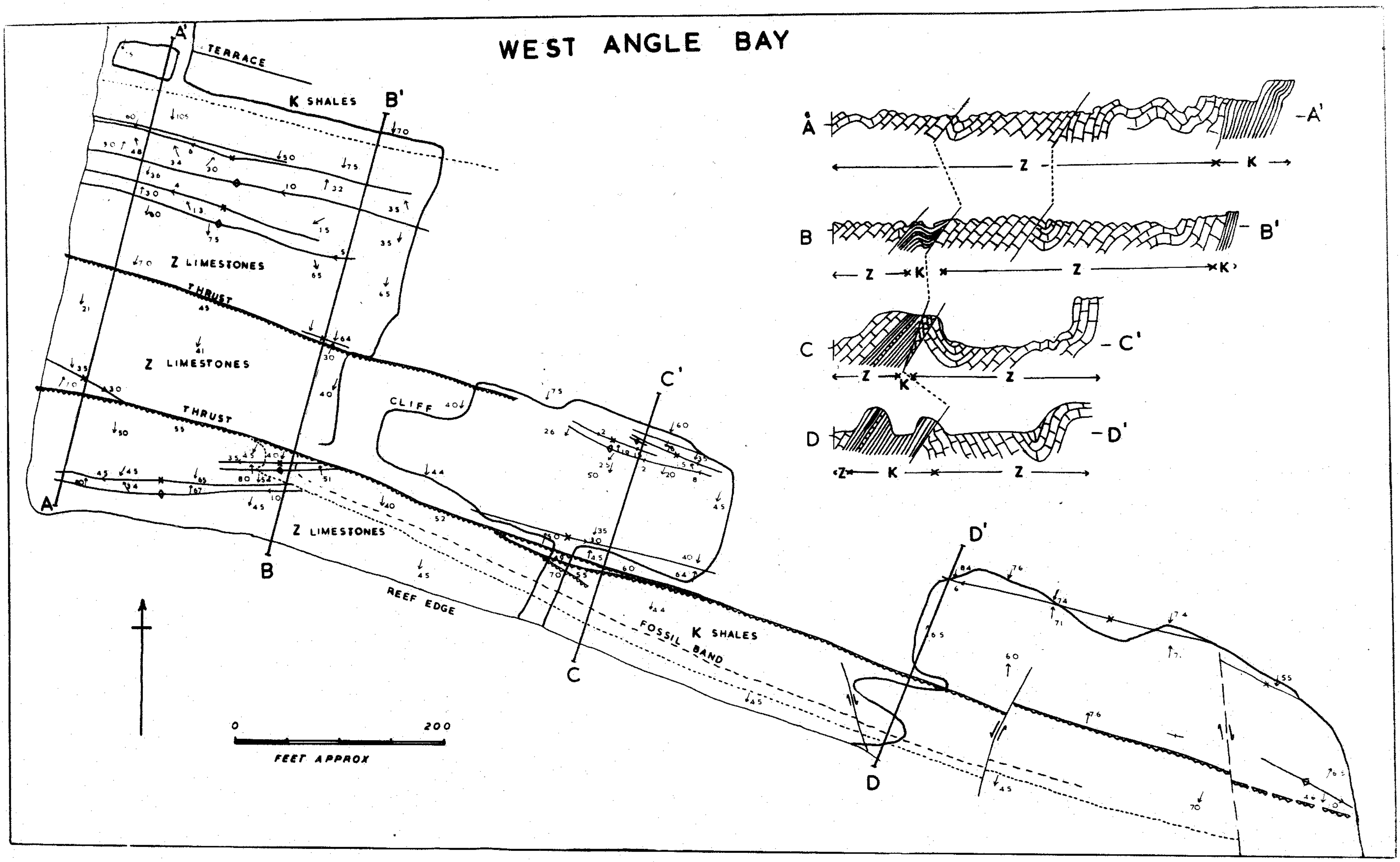
WEST ANGLE BAY
TERRACE
K SHALES
Z LIMESTONES
THRUST
Z LIMESTONES
THRUST
Z LIMESTONES
CLIFF
REEF EDGE
K SHALES
FOSSIL BAND
A
A'
B
B'
C
C'
D
D'
Z
K
0
200
FEET APPROX

Fig. 3.10

Fig. 3.11 STEREOGRAMS OF AXIAL PLANES AND FOLD AXES IN THE ORIELTON ANTICLINE

Diagrams constructed from mean dip readings for different parts of a fold, hence a single fold may have more than one axis and axial plane.

A <u>Lydstep and Freshwater East field zones</u>

B <u>Stackpole field zone</u>

C <u>Freshwater West and Angle Cliffs field zones</u>

D <u>Greenala field zone</u>

For remaining field zones see Fig. 3.5.

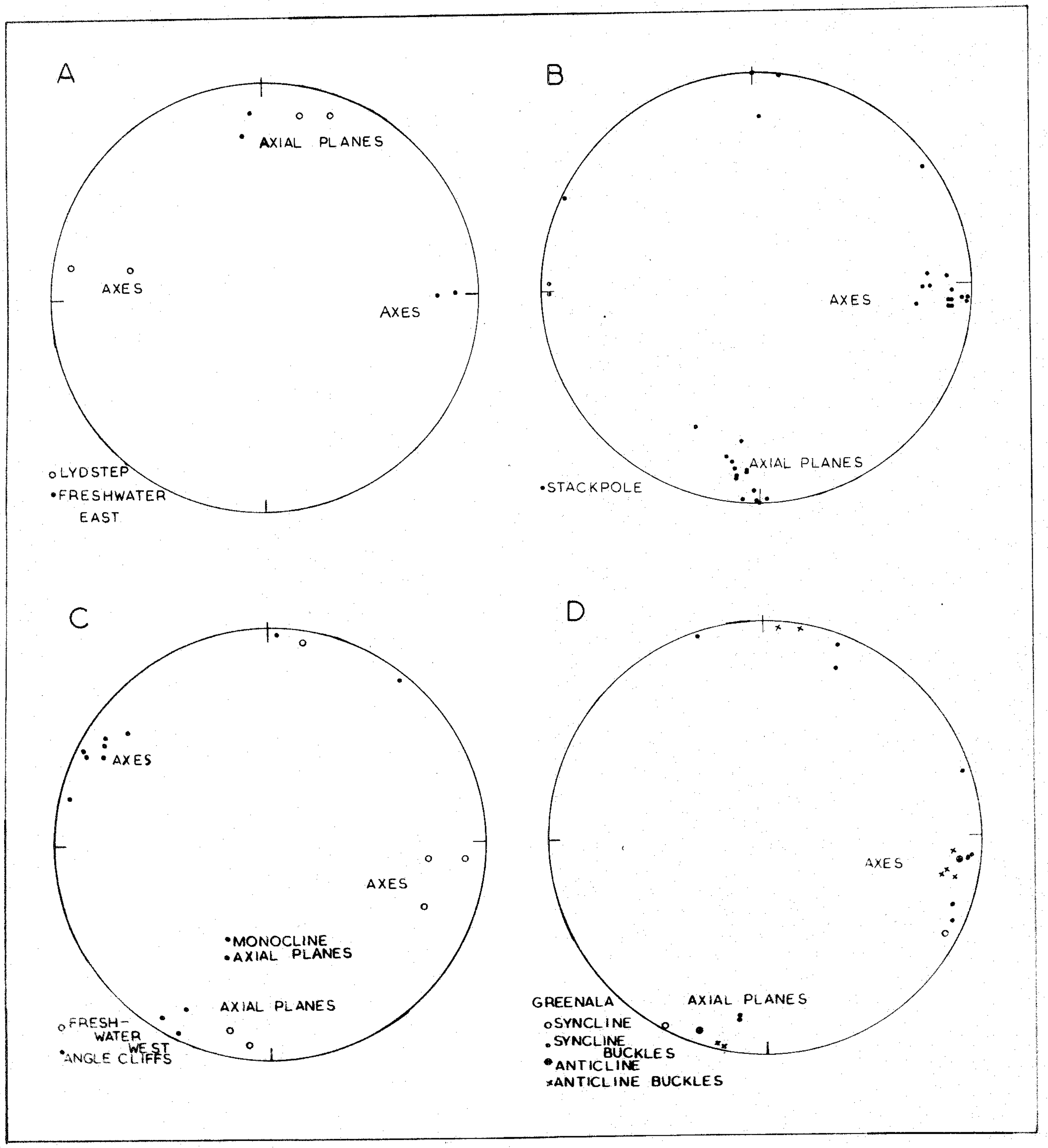
A
AXIAL PLANES
AXES
AXES
o LYDSTEP
• FRESHWATER EAST
B
AXES
AXIAL PLANES
• STACKPOLE
C
AXES
AXES
• MONOCLINE
• AXIAL PLANES
AXIAL PLANES
o FRESH-WATER WEST
• ANGLE CLIFFS
D
AXES
AXIAL PLANES
GREENALA
o SYNCLINE
• SYNCLINE BUCKLES
● ANTICLINE
x ANTICLINE BUCKLES

Fig. 3.11

Fig. 4.1 STEREOGRAMS COMPARING FOLD AXES WITH LOCAL FOLD AXES AND INVERSE AXES

A Slaty cleavage West Angle Bay. The attitudes of the axial plane and axis of the Angle syncline compared with the attitudes of the cleavage and the cleavage-bedding intersections.

B Slickensides on fracture cleavage. From station 5020. The local fold axis calculated from the slickensides compared with the localfold axis given by the cleavage-bedding intersection.

C 'Race' rod orientation and fracture cleavage From station 8001. Normal to the 'race' rods compared with the cleavage-bedding intersection.

D Inverse and local fold axes Lydstep field zone. β diagram of the intersections between bedding and rotation joints, and bedding and inverse rotation joints. Local fold axes plunge east, and inverse axes plunge west. Two limbs of the Pembroke syncline shown separated.

E Local fold axes compared with fold axes calculated from limb dips Stackpole Quay anticline. Bedding-fracture cleavage intersections separated for both limbs of the fold, and compared with the fold axis plunges of the three axes affecting the two fold limbs.

F Local fold axes compared with true fold axis Orielton syncline at Greenala. Bedding-fracture cleavage intersections compared with the plunge of the Orielton syncline.

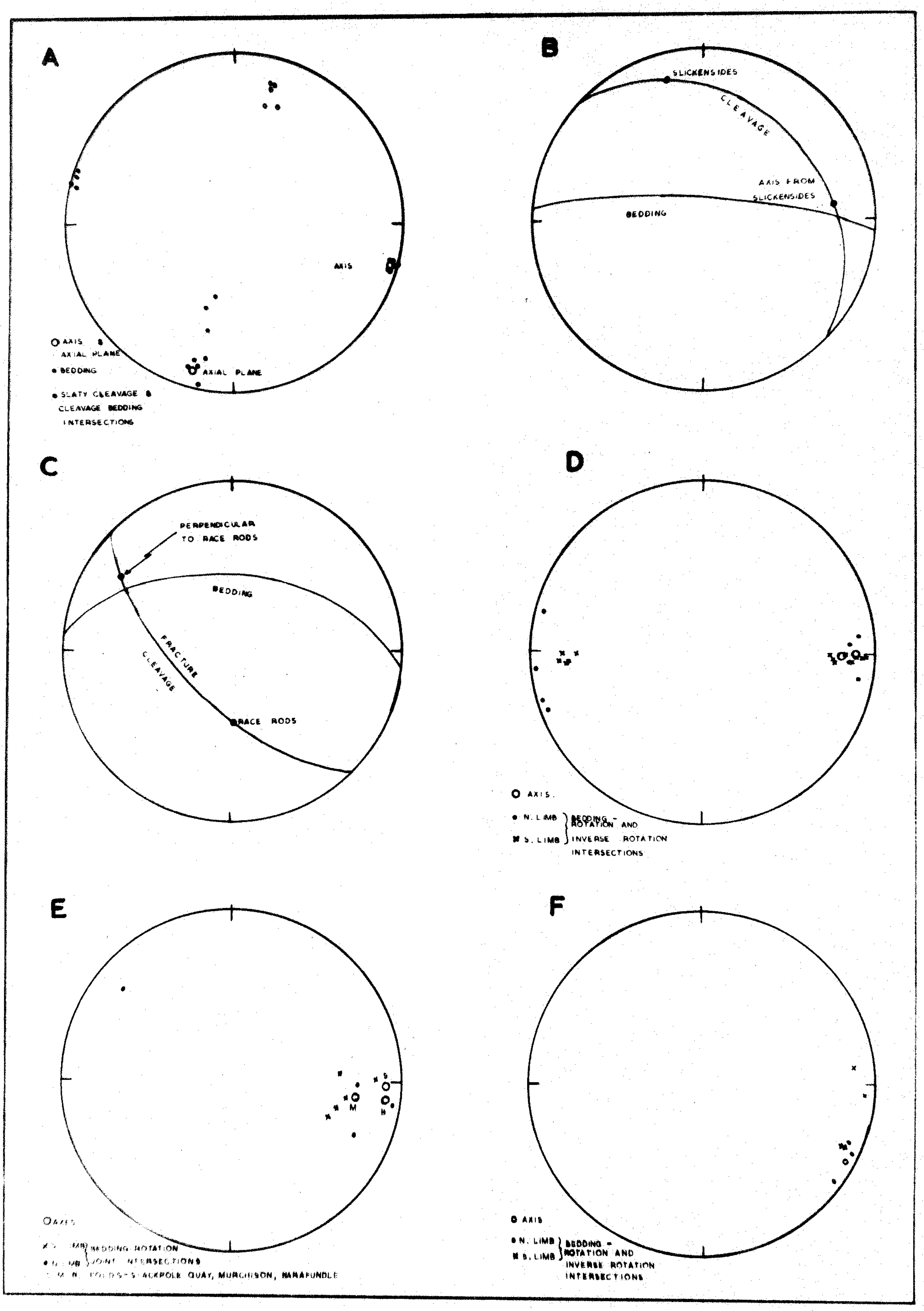
A
AXIS
AXIAL PLANE
AXIS &
AXIAL PLANE
BEDDING
SLATY CLEAVAGE &
CLEAVAGE BEDDING
INTERSECTIONS
B
SLICKENSIDES
CLEAVAGE
AXIS FROM
SLICKENSIDES
BEDDING
C
PERPENDICULAR
TO RACE RODS
BEDDING
FRACTURE
CLEAVAGE
RACE RODS
D
AXIS.
N. LIMB
S. LIMB
BEDDING -
ROTATION AND
INVERSE ROTATION
INTERSECTIONS
E
M
QUAY, MURCHISON, MANAPUNDLE
F
AXIS
N. LIMB
S. LIMB
BEDDING -
ROTATION AND
INVERSE ROTATION
INTERSECTIONS

Fig. 4.1

Fig. 4.2 FRACTURE CLEAVAGE AND ROTATION JOINTS IN INVERTED STRATA

A <u>Section across eastern limit of Stackpole Quay anticline</u>

Section as seen on cliffs.

Note - cleavage dipping in the same direction but at a lower angle than the bedding.

C_2S_1 mudstones (5020)

B <u>Rotation joints and inverted bedding</u>

Note - acute angle between joints and bedding indicating the sense of slip. South Lydstep Haven, D_1 limestones.

Fig. 4.3. LOCAL FOLD AXES AND INVERSE AXES

A <u>Stereogram of bedding plane and two sets of slickensides</u>

Axes deduced from the slickensides compared with local fold axes and the inverse axis (6001)

B <u>Schematic block diagram of a bedding unit cut by rotation and inverse rotation joints</u>

Note - consequent axes

C <u>Schematic sketch of two sets of bedding slickensides</u>

Fig. 4.2

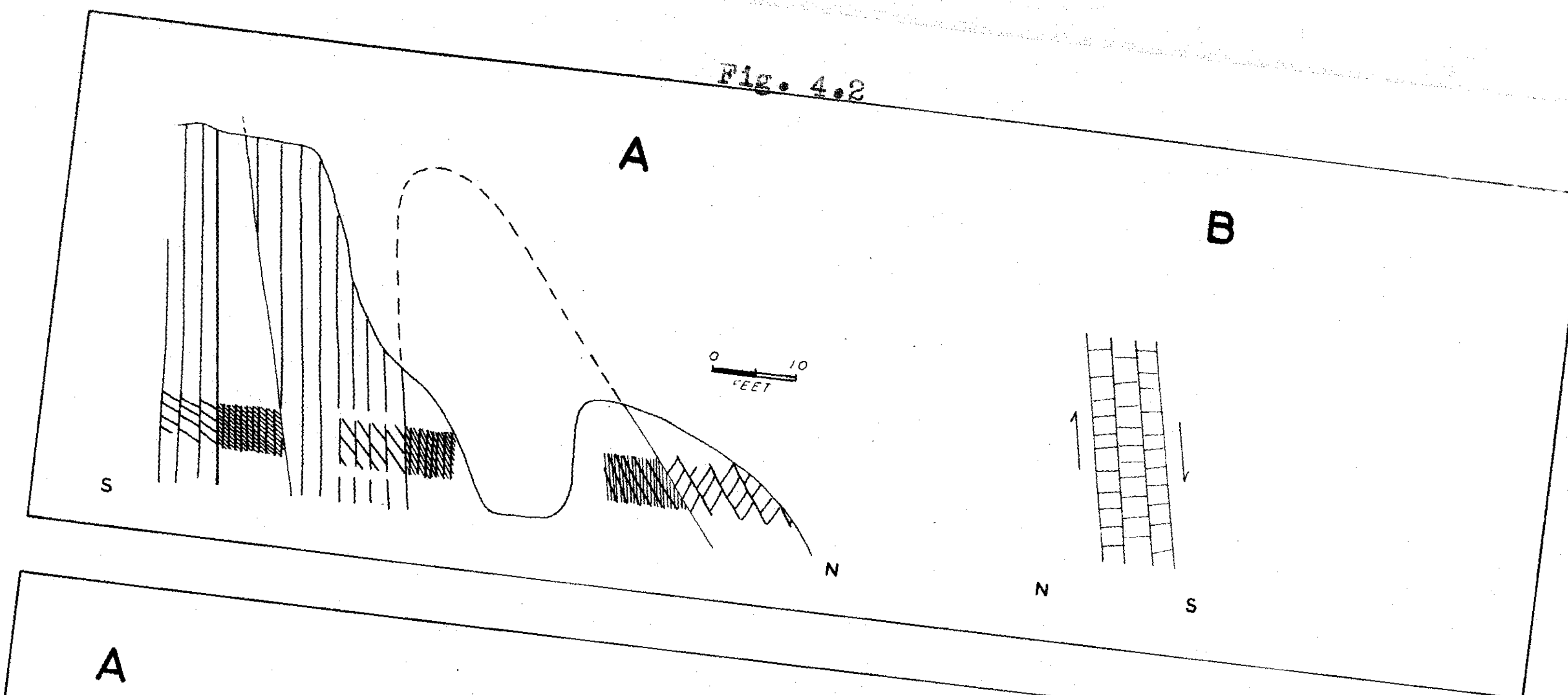
A
B
S
N
N
S
0
10
FEET

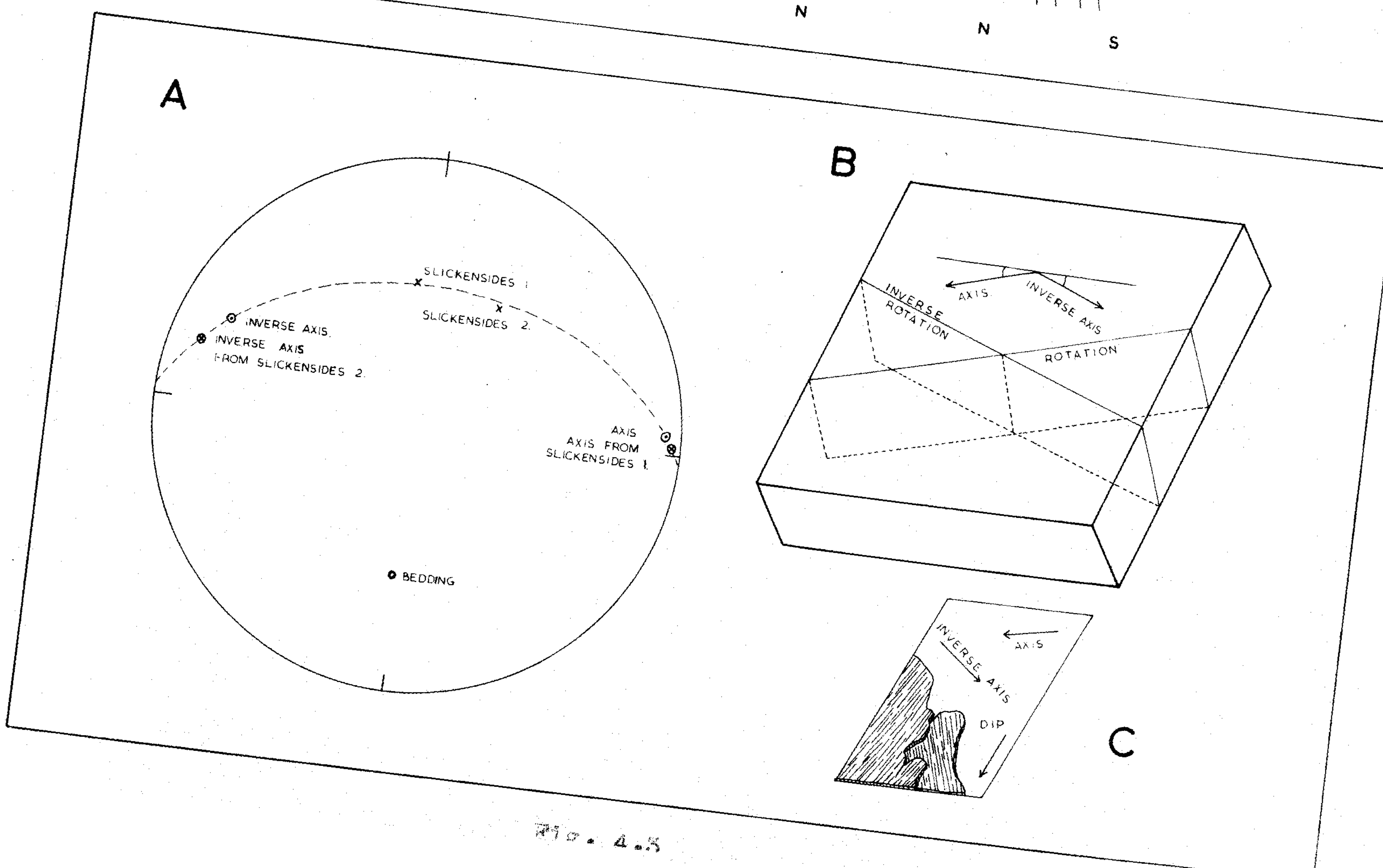
A
SLICKENSIDES 1
SLICKENSIDES 2
INVERSE AXIS
INVERSE AXIS FROM SLICKENSIDES 2
AXIS
AXIS FROM SLICKENSIDES 1
BEDDING
B
AXIS
INVERSE AXIS
INVERSE ROTATION
ROTATION
C
AXIS
INVERSE AXIS
DIP

Fig. 4.3

Fig. 4.4 IRREGULAR SHEARS AND 'RACE' ROD DISTORTION OF SUB-PHASE 2

A <u>Schematic block diagram of slickensided irregular shears</u>

Shears developed in marls below a sandstone. The shears are spaced 3" - 6" apart.

B-F <u>Field sketches of distorted 'race' rods</u>

From the north side of Freshwater East. Several rods shown close together to give the impression of their spacing, the remainder shown isolate to indicate the distortion.

G <u>Schematic block diagram to show rod orientation</u>

Rods lie between fracture cleavage planes and normal to the local fold axis (A). Bedding slip indicated by arrows.

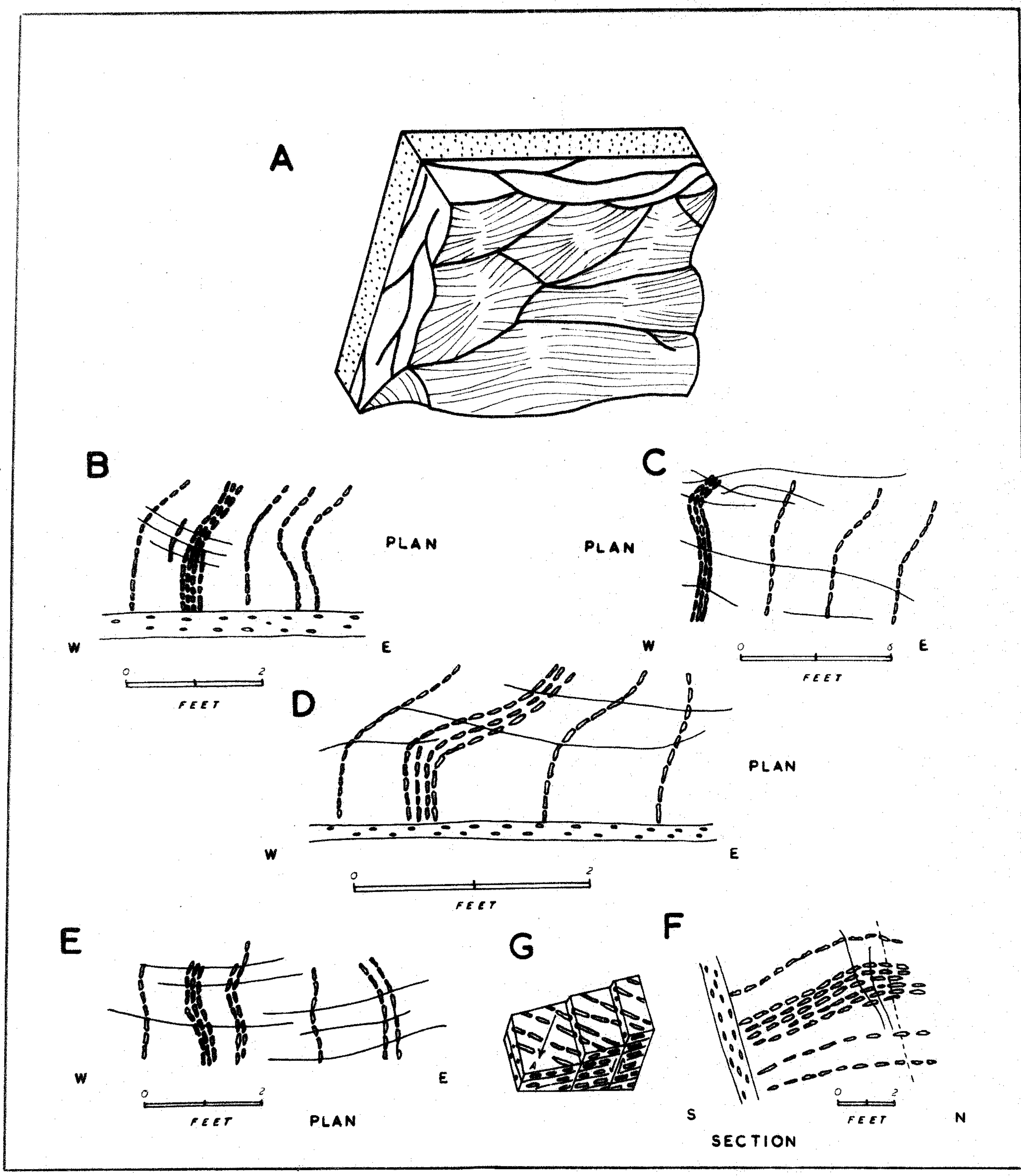
A
B
PLAN
W
E
0
2
FEET
C
PLAN
W
0
6
E
FEET
D
PLAN
W
E
0
2
FEET
E
W
E
0
2
FEET
PLAN
G
F
S
0
2
FEET
N
SECTION

Fig. 4.4

Fig. 4.5 STRIKE SHEAR JOINTS

A <u>Schematic block diagram of strike shear joints</u>

Joints oriented relative to a bedding surface, plunge of local fold axis shown (A).

B <u>Schematic section of complementary strike shear joints in steeply dipping strata</u>.

Displacements are thrusts relative to the bedding and normal faults relative to the horizontal.

Fig. 4.6 DOWN DIP DRAG SHEAR ZONES (Field sketches)

A <u>Downward facing ripple, Freshwater West</u>

South dipping Z limestones at station 7015 cut by a drag zone and later formed "wrench-joints".

B <u>Down dip drag folds, south side of West Angle Bay</u>

Drag folds developed between shear planes in sandstones of the Lower Old Red Sandstone, station 9024

C <u>Downward facing joint-drags near East Pickard Bay</u>

Lower Old Red Sandstone marls and sandstones are cut by fracture cleavage planes, a later formed thrust and downward facing joint-drags. Sandstone stippled, marls ruled. Station 8001.

Fig. 4.5

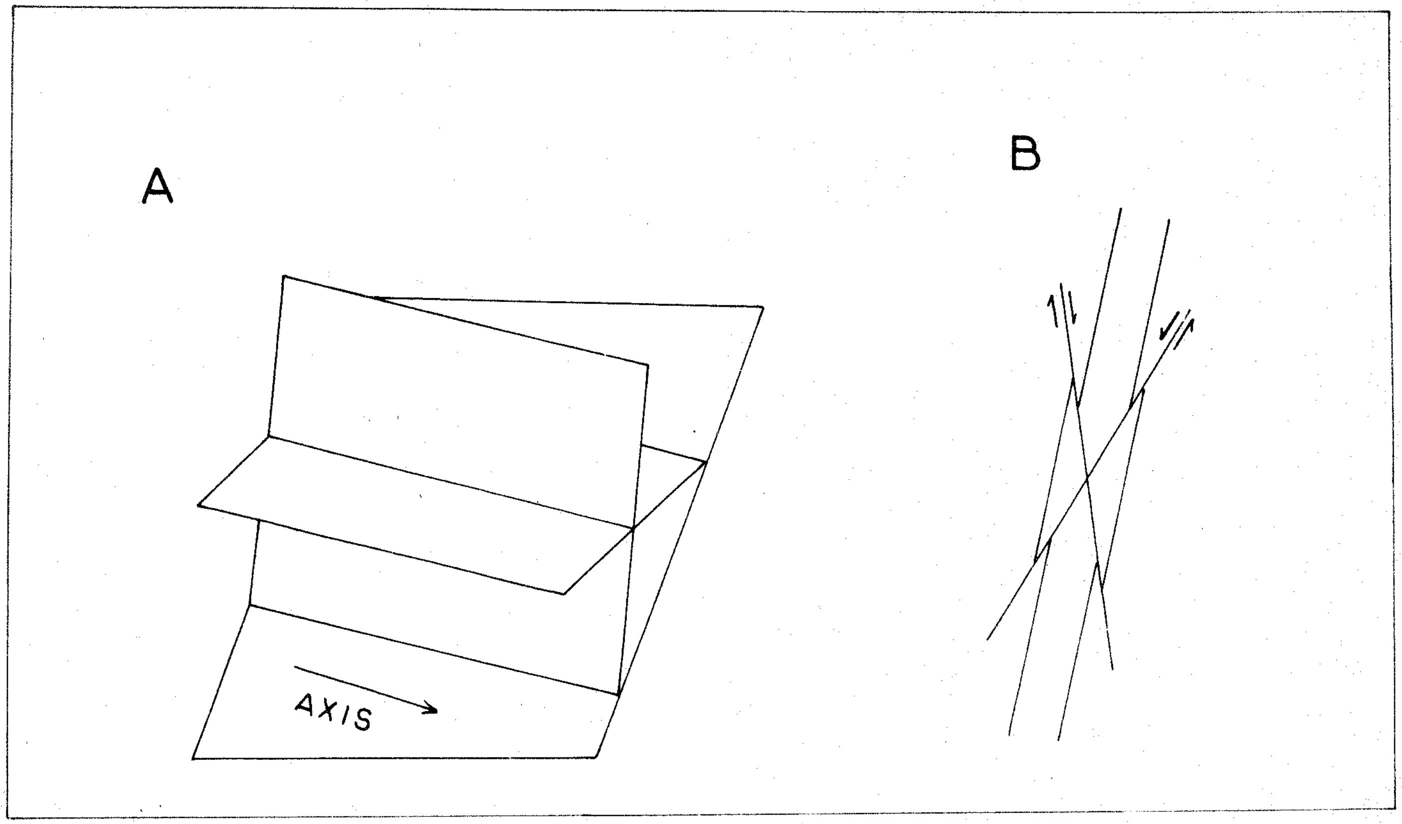

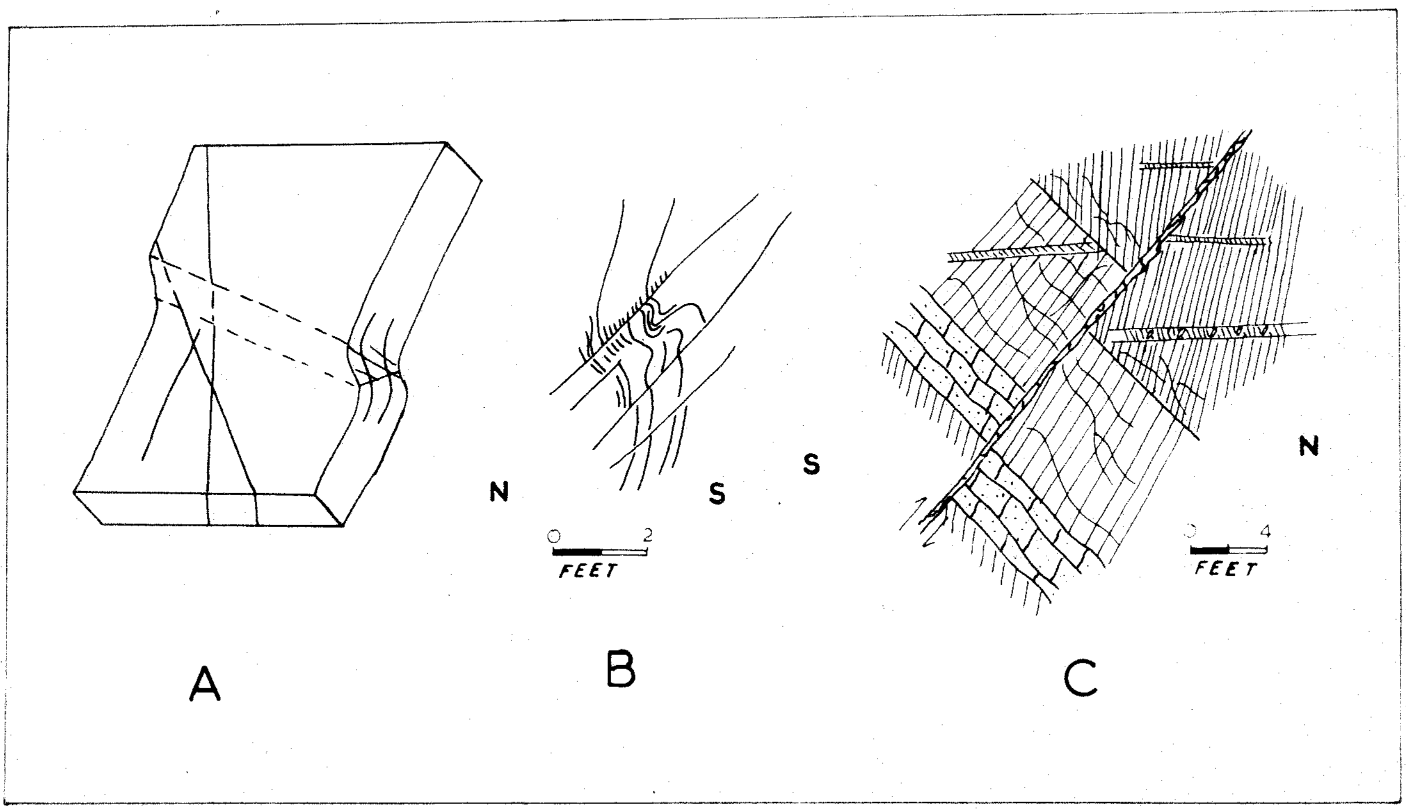

Fig. 4.6

Fig. 5.1 WRENCH FAULTS: GEOMETRIES AND FREQUENCIES

A <u>The geometry of ideal complementary wrench faults relative to a fold</u>

The shear planes are oriented relative to the plunge of the fold axis and the dip of the axial plane.

B <u>Frequency polygon of wrench fault strikes in the Orielton anticline</u>

Polygon constructed by recording average fault strike directions for every 440' of a fault's extent as depicted on the Geological Survey's 6" sheets. Results plotted at 5° intervals. F = frequency.

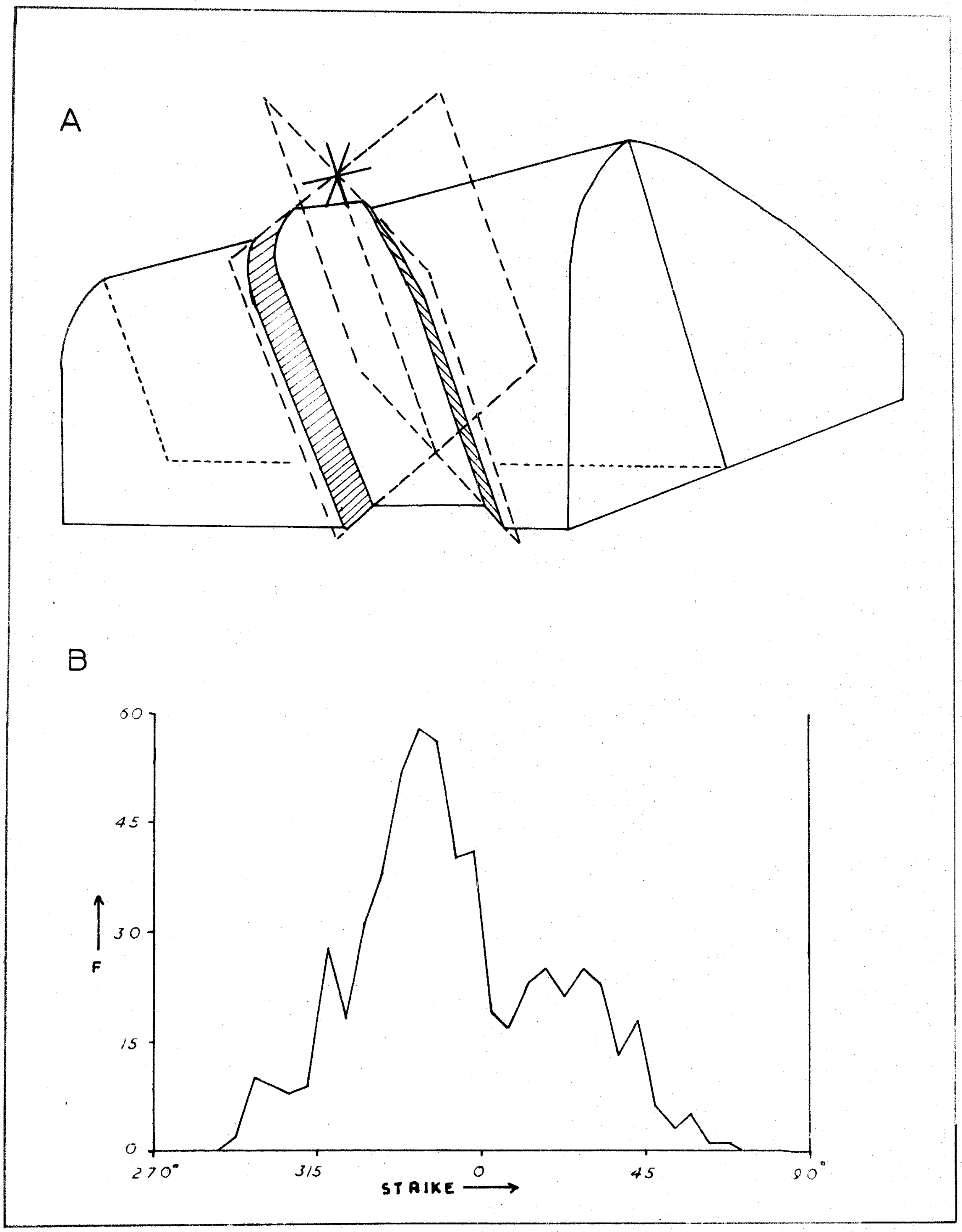

Fig. 5.1

Fig. 5.2 WRENCH FAULTS : LYDSTEP HAVEN

A <u>Map</u>

Stratigraphical boundaries after the Geological Survey

B <u>Stereogram of faults</u>

Mean attitudes for each fault shown

C <u>Stereogram of resulting geometries and consequent stress axis orientations for adjacent complementary faults</u>

Results for the south side of the Haven, there being no complementary faults on the north side. Geometries compared with the axis and axial plane of the Pembroke syncline at Lydstep Haven.

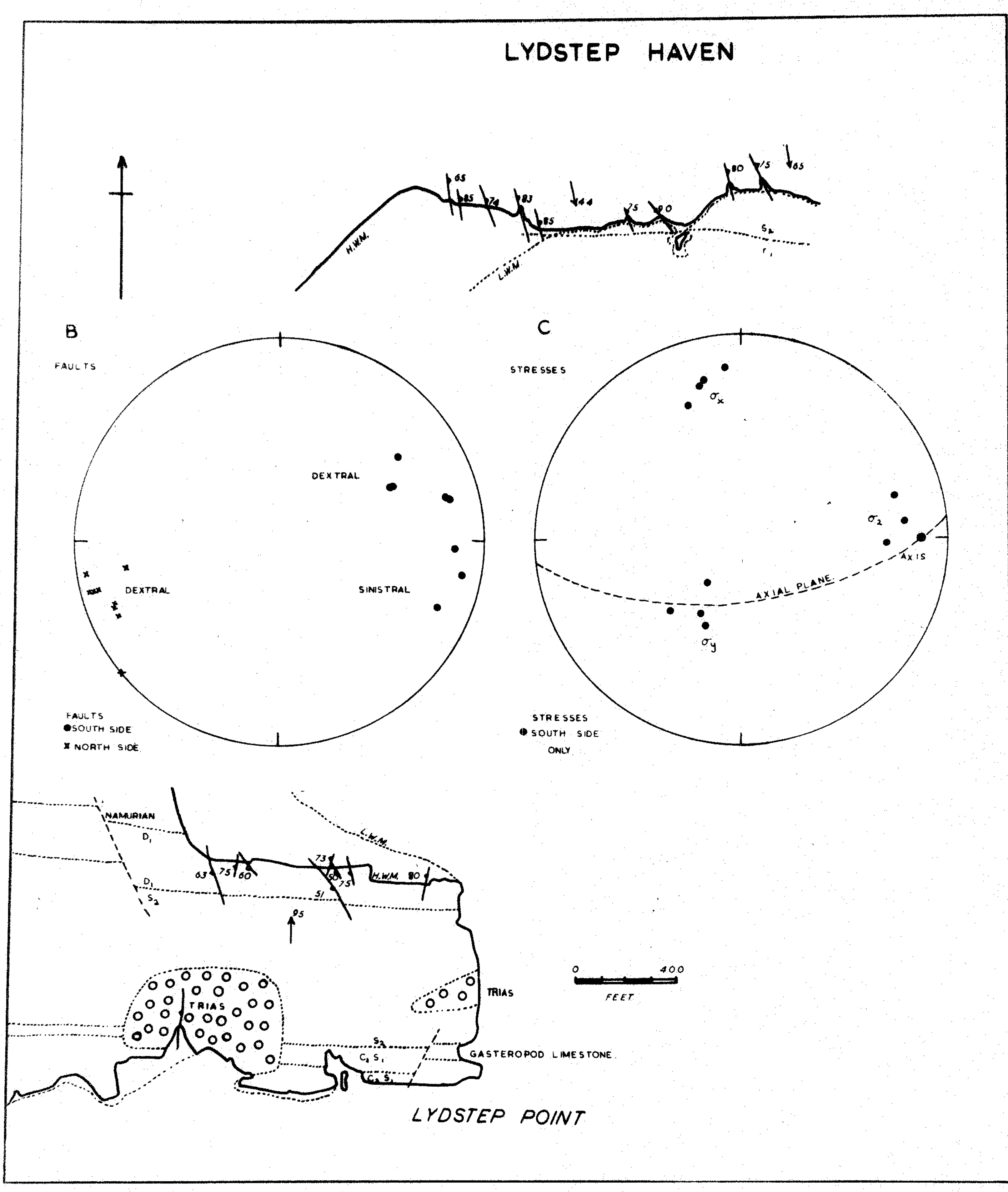
LYDSTEP HAVEN
H.W.M.
L.W.M.
B
FAULTS
DEXTRAL
DEXTRAL
SINISTRAL
FAULTS
SOUTH SIDE
NORTH SIDE
C
STRESSES
AXIAL PLANE
AXIS
STRESSES
SOUTH SIDE
ONLY
NAMURIAN
TRIAS
TRIAS
GASTEROPOD LIMESTONE
0 400
FEET
LYDSTEP POINT

Fig. 5.2

Fig. 5.3 WRENCH FAULTS: FRESHWATER EAST

A <u>Map</u>

Stratigraphical boundaries largely after the Geological Survey. Small faults with displacements of less than 2' not shown.

B <u>Stereogram of faults</u>

Mean attitudes for each fault shown. Small faults too small to be depicted on the map are plotted.

C <u>Stereogram of resulting geometries and consequent Stress axis orientations for adjacent complementary faults</u>

Geometries compared with the axis and axial plane of the Freshwater East anticline, the plunge of the axis probably being steeper than the plunges of local fold axes adjacent to faults.

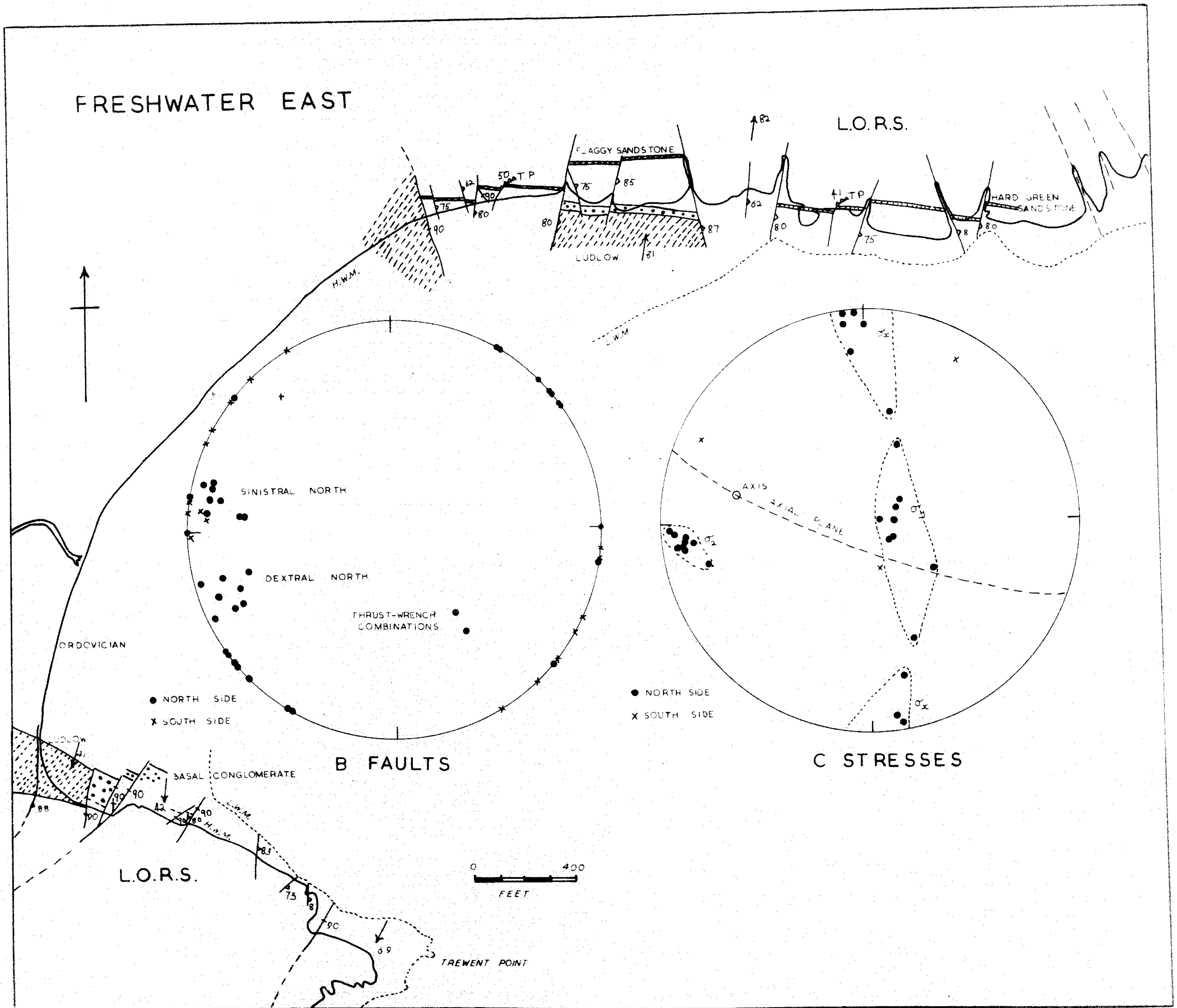
FRESHWATER EAST
L.O.R.S.
FLAGGY SANDSTONE
HARD GREEN SANDSTONE
LUDLOW
H.W.M.
L.W.M.
T P
SINISTRAL NORTH
DEXTRAL NORTH
THRUST-WRENCH COMBINATIONS
NORTH SIDE
SOUTH SIDE
B FAULTS
AXIS
AXIAL PLANE
C STRESSES
ORDOVICIAN
BASAL CONGLOMERATE
TREWENT POINT
0
400
FEET

Fig. 5.3

Fig. 5.4 WRENCH FAULTS : GREENALA

Map

Stereogram of the complementary faults which displace the Castlemartin Corse anticline axis

Fault attitudes, derived geometries (stress axes) and the axial plane and axis of the Castlemartin Corse anticline shown.

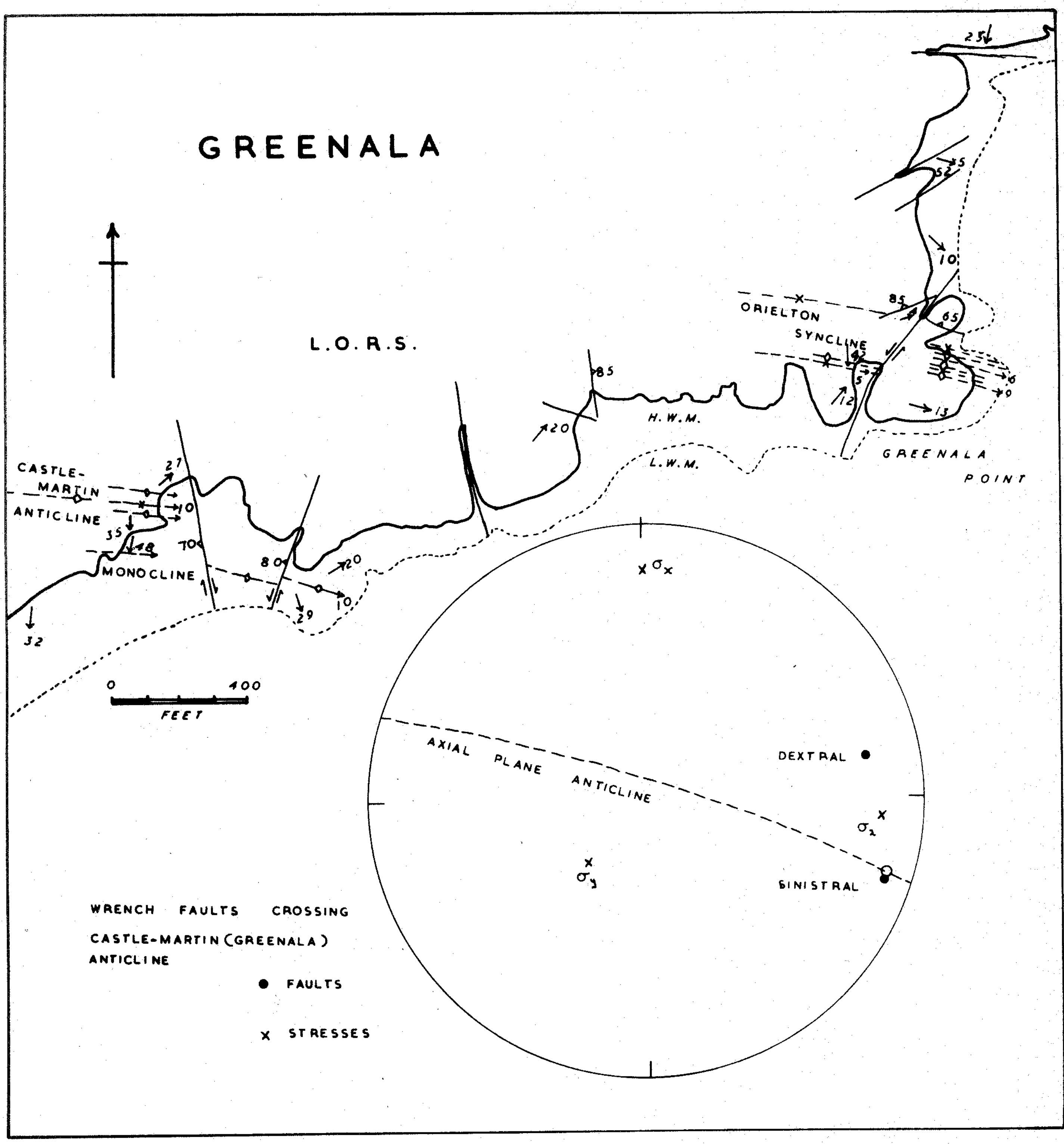
GREENALA
L.O.R.S.
CASTLE-MARTIN ANTICLINE
MONOCLINE
ORIELTON SYNCLINE
H.W.M.
L.W.M.
GREENALA POINT
0 400 FEET
AXIAL PLANE ANTICLINE
DEXTRAL
SINISTRAL
WRENCH FAULTS CROSSING CASTLE-MARTIN (GREENALA) ANTICLINE
● FAULTS
x STRESSES

Fig. 5.4

Fig. 5.5 WRENCH FAULTS : THE FLIMSTON BAY FAULT AT FRESHWATER WEST

A <u>Map of wrench fault splays, Little Furzenip</u>

B <u>Map of wrench faults at Great Furzenip</u>

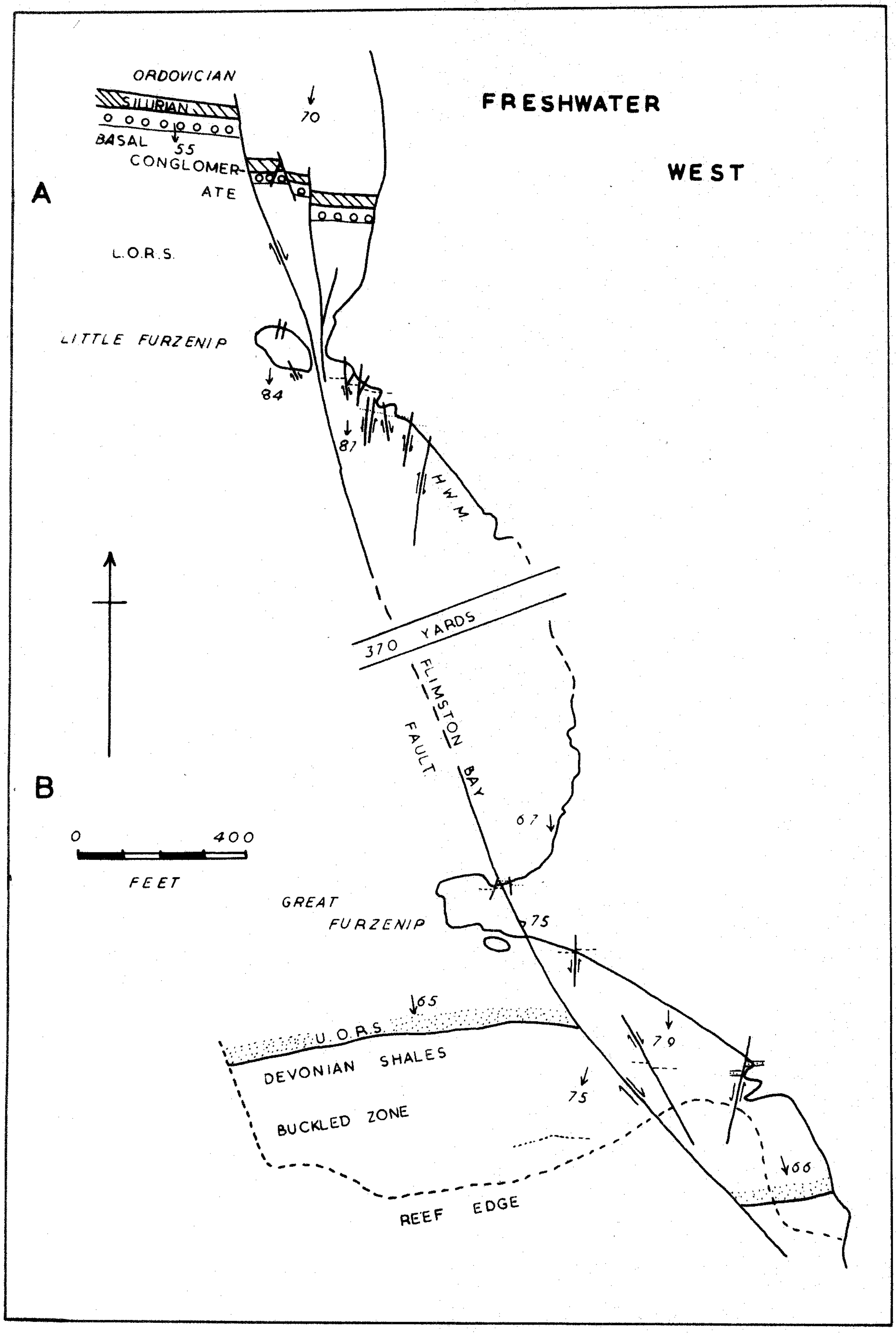
FRESHWATER
WEST
ORDOVICIAN
SILURIAN
BASAL
CONGLOMER-
ATE
70
55
A
L.O.R.S.
LITTLE FURZENIP
84
87
H.W.M.
370 YARDS
FLIMSTON BAY
FAULT
B
0
400
FEET
67
GREAT
FURZENIP
75
65
U.O.R.S.
DEVONIAN SHALES
79
75
BUCKLED ZONE
66
REEF EDGE

Fig. 5.5

Fig. 5.6 WRENCH FAULTS: EAST OF WEST PICKARD BAY

A <u>Sketch map of faults at Station 8003</u>

B <u>Stereogram of faults in Stations 8003 and 8004</u>
Mean attitudes for different branches of faults shown. Single set of derived geometries (stress axes) compared with the local fold axis plunge and the dip of the bedding.

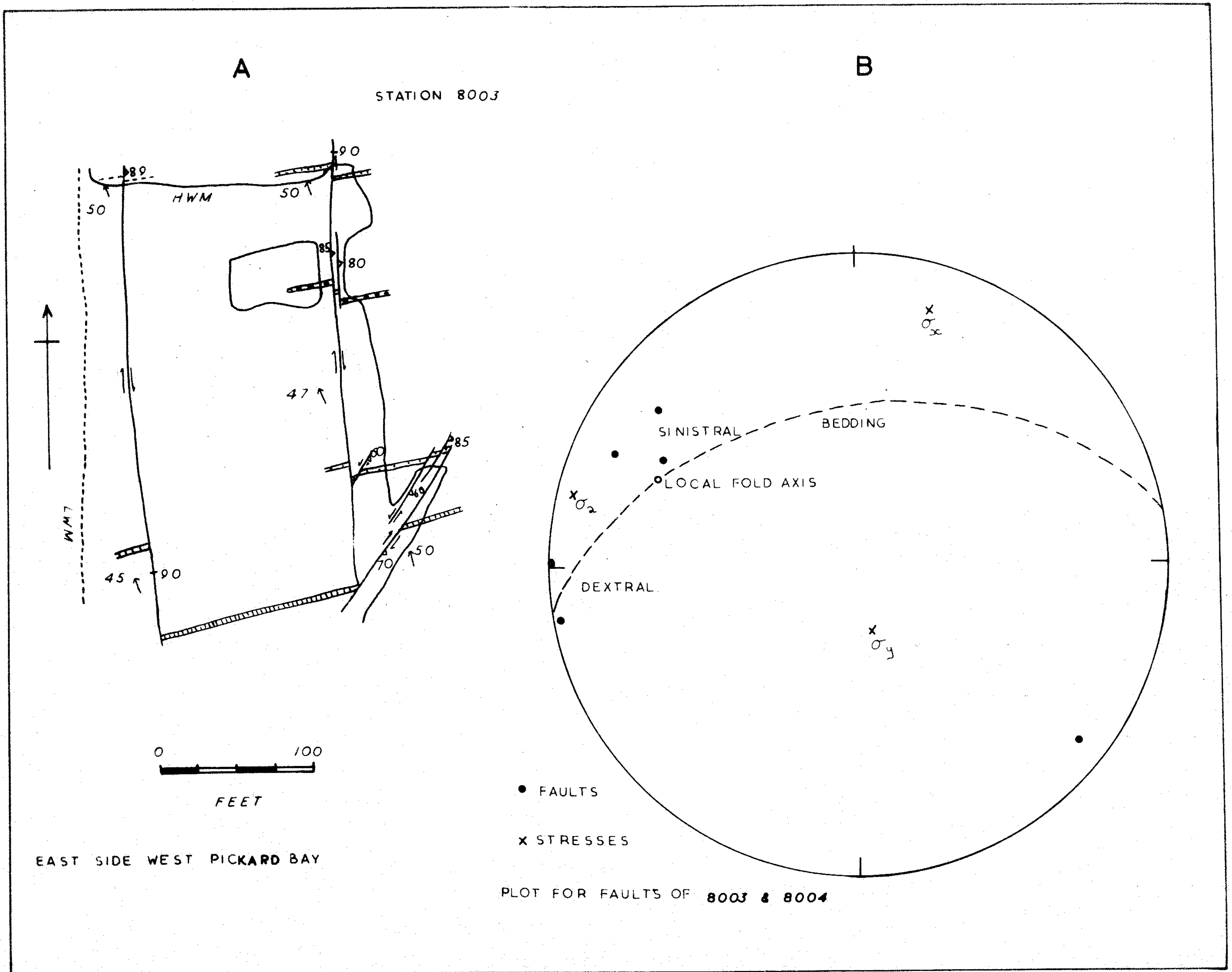
A
STATION 8003
HWM
LWM
FEET
0
100
EAST SIDE WEST PICKARD BAY
B
SINISTRAL
BEDDING
LOCAL FOLD AXIS
DEXTRAL
• FAULTS
x STRESSES
PLOT FOR FAULTS OF 8003 & 8004

Fig. 5.6

Fig. 5.7 JOINT-SHEARS

A **Schematic relationships**

The geometry of a major shear with antithetic splay joints compared with the attitude of a possible fold axis and axial plane.

Stress axes - 3 barbs σ_x

2 barbs σ_y

1 barb σ_z

B **Field sketches**

Three examples from the north side of Freshwater East, in Lower Old Red Sandstone rocks. Two of the major shears act as small wrench faults. Sandstones stippled, marls unornamented, in the lower sketch bedding is indicated by horizontal ruling.

C **Stereogram of joint-shears and resultant geometries**

Geometries (shown as stress axes) deduced from joint-shears on the north side of Freshwater East, and compared with the axis and axial plane of the Freshwater East anticline.

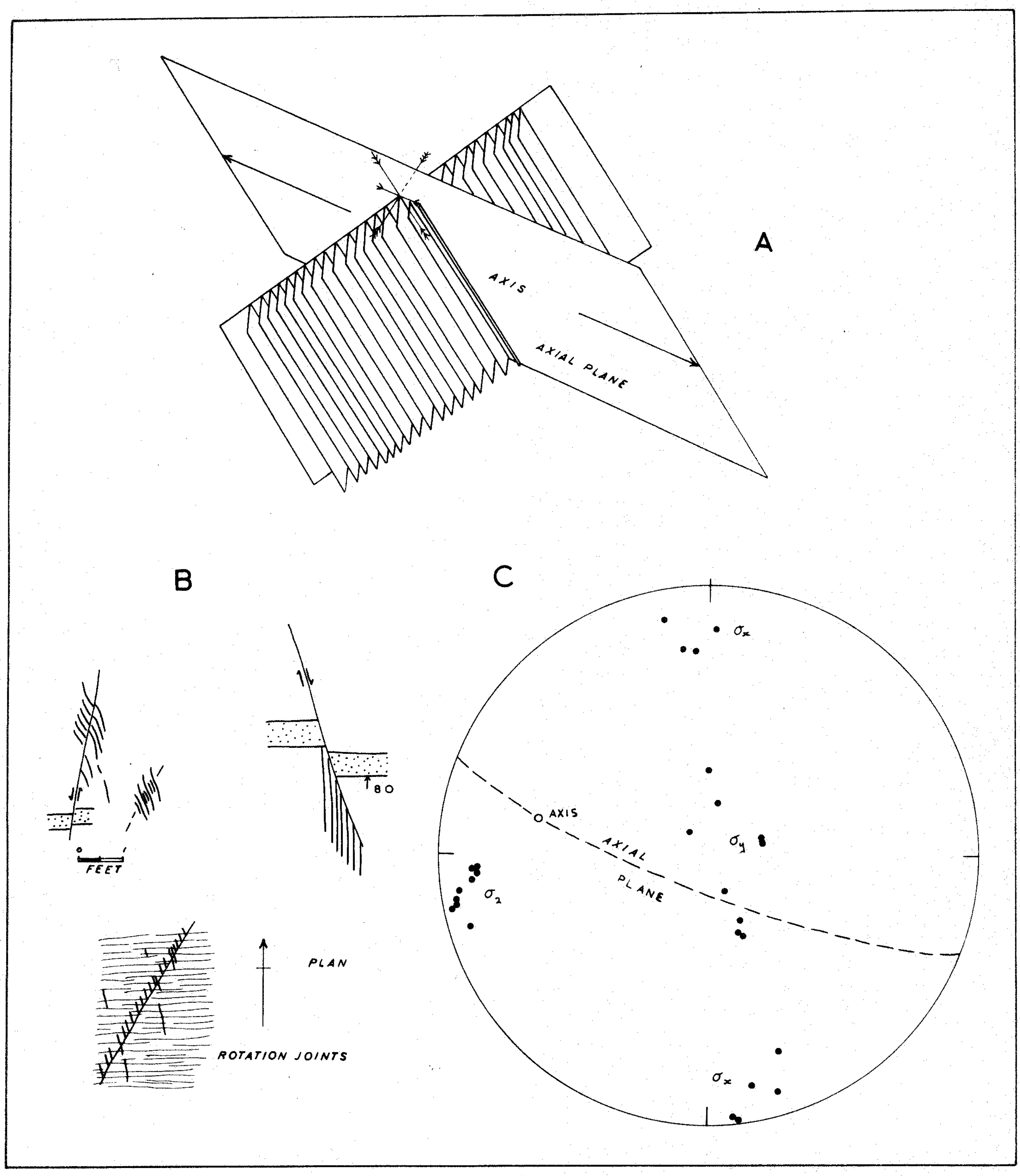
A
AXIS
AXIAL PLANE
B
FEET
80
PLAN
ROTATION JOINTS
C
AXIS
AXIAL
PLANE
σ_x
σ_y
σ_z
σ_x

Fig. 5.7

Fig. 5.8 WRENCH-JOINTS

A <u>Wrench-joints and resultant geometries relative to a bedding plane on a fold limb</u>

Explanation - (A) primary wrench-joints

(B) secondary wrench-joints

3 barbs σ_x (acute bisectrix)

2 barbs σ_y (intersection of shears)

1 barb σ_z (obtuse bisectrix)

B <u>Wrench-joints and resultant geometries at fold crests</u>

Primary wrench-joints only are shown. Geometrical legend as above.

C <u>Possible wrench-joint traces on bedding planes, and the nomenclature of the joints</u>

For full explanation see text.

Joint traces as would be seen on the upper stratigraphic surface of a bedding unit.

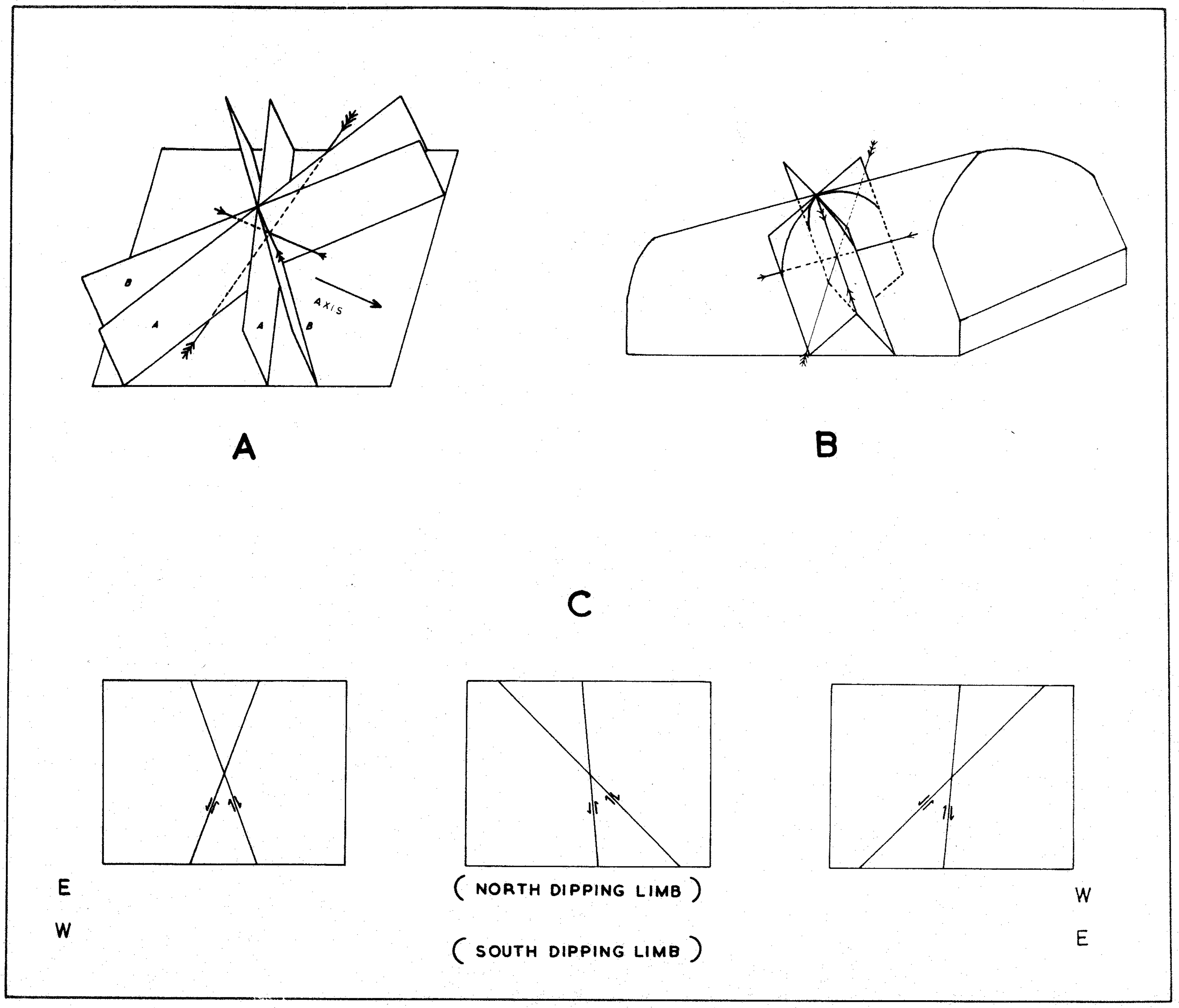

Fig. 5.8

Fig. 5.9 LENS BELTS

A <u>Schematic block diagram of complementary lens belts on a fold limb</u>

The sense of shear along the planes, shown by the arrows, is derived from the distortion of the rotation joints and the attitudes of the lenses relative to the belts.

B <u>Typical lens belt patterns on a bedding surface</u>

C <u>Complementary lens belts and wrench-joints</u> (Field sketch)

Both widened joints and lens belts exposed as traces across a vertical bedding plane. Note - large <u>Canninias</u> in the plane of the bedding.

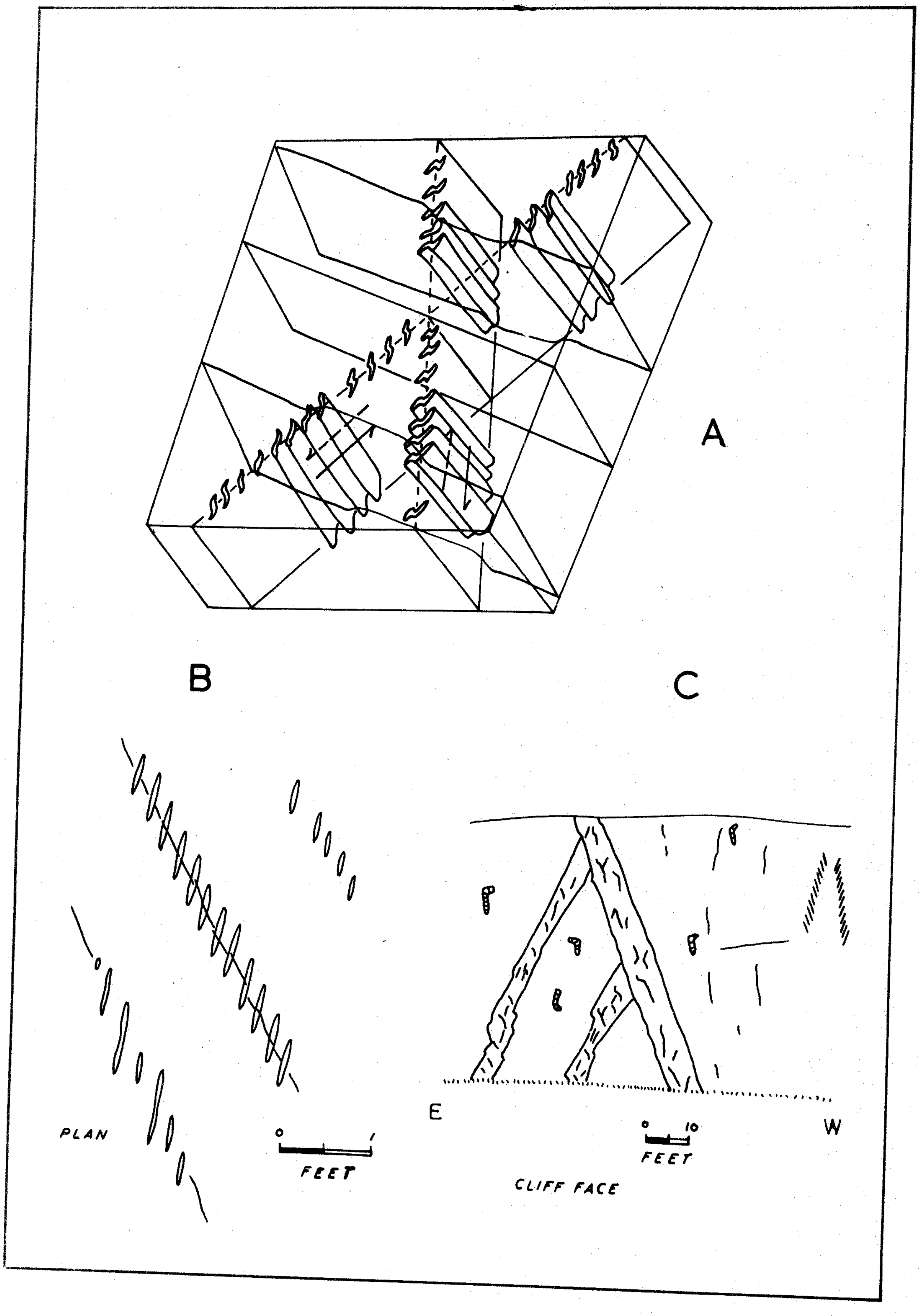

Fig. 5.9

Fig. 5.10 SECONDARY SHEAR PATTERNS

A <u>Modified after McKinstry</u> (1953, p.407)

B <u>Modified after Moody and Hill</u> (1956, p.1213)

C <u>Secondary wrench-joint pattern of the Orielton anticline</u>

In all cases σ_x is indicated by an arrow

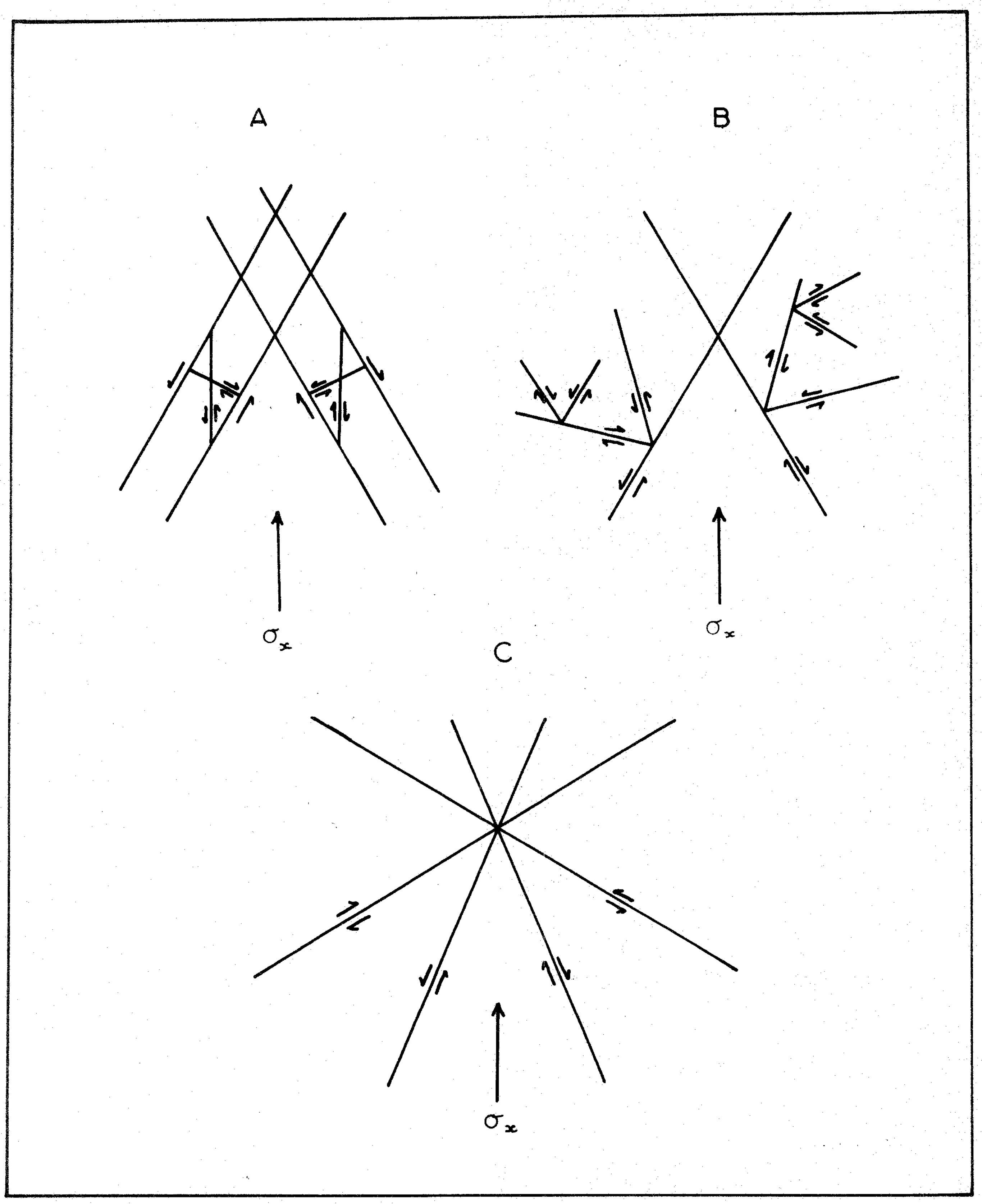

Fig. 5.10

Fig. 5.11 SYMMETRY OF MINOR STRUCTURES

A <u>Schematic block diagram of joints which commonly occur on a fold limb</u>

Joints depicted relative to a dipping bedding surface

Key -	Ruled	Rotation joints or fracture cleavage
	Stippled	Inverse rotation joints
	SS	Complementary strike shear joints
	WS	Complementary primary wrench-joints
	SWS	Secondary wrench-joints

B <u>Ideal stereogram showing the symmetry of minor structures on a fold limb</u>

Key to poles

BP	Bedding
ROT	Rotation joints
FRCTR: CLVG	Fracture cleavage
I: ROT	Inverse rotation joints
THRUST	Thrust plane
SS	Complementary strike shear joints
WS and LB	Primary wrench-joints and lens belts
SWS	Secondary wrench-joints
WF	Wrench fault
AXIS	Local fold axis
I:AXIS	Inverse axis

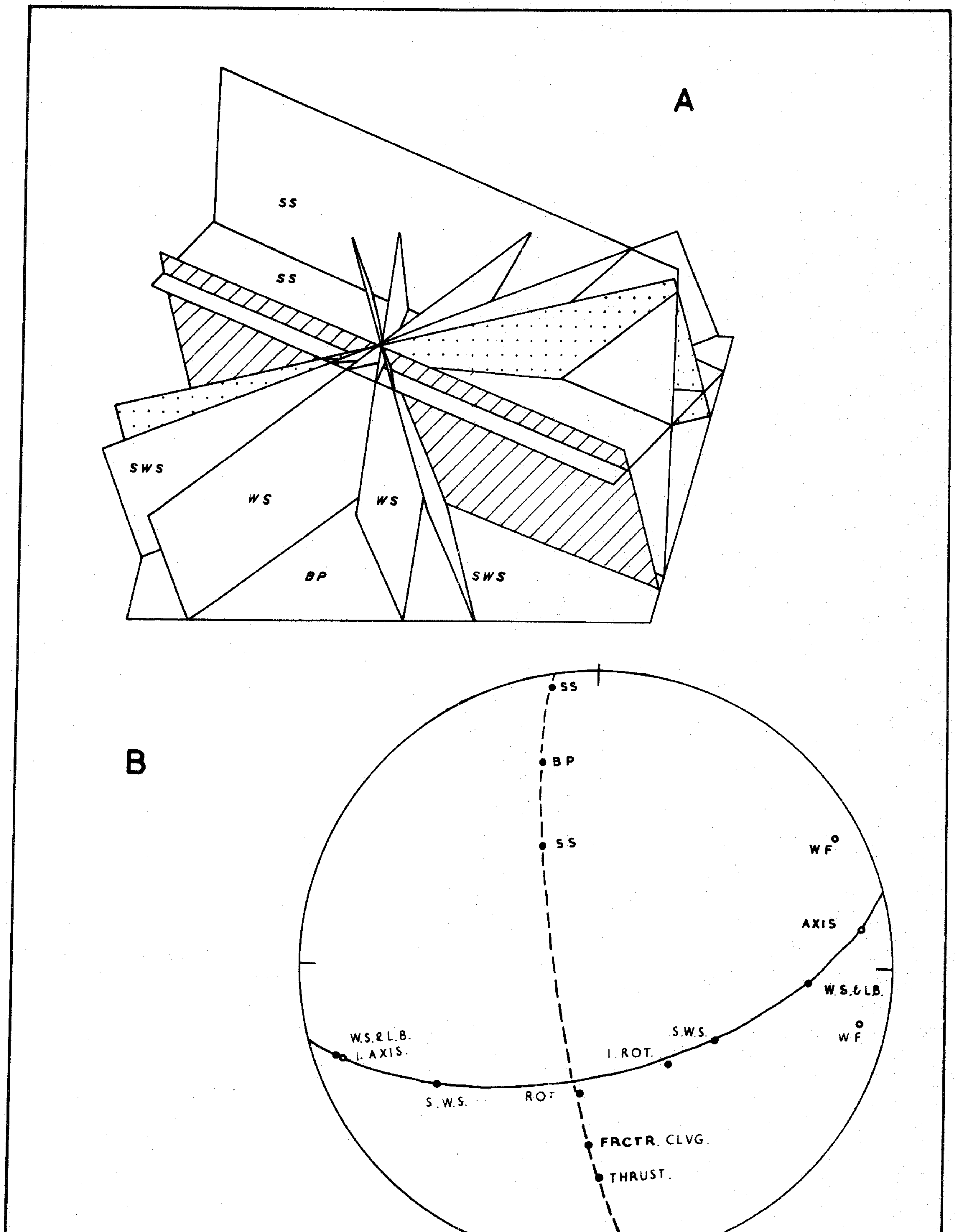
A
SS
SS
SWS
WS
WS
BP
SWS
B
SS
BP
SS
WF
AXIS
W.S.&LB.
WF
S.W.S.
I. ROT.
W.S.&L.B.
I. AXIS.
S.W.S.
ROT
FRCTR. CLVG.
THRUST.

Fig. 5.11

Fig. 6.1. THE REORIENTATION OF JOINTS IN COLLAPSED BLOCKS OF CARBONIFEROUS LIMESTONE TO THE REGIONAL PATTERN

Station 2022, Triassic collapse breccia.
The central stereogram shows mean attitudes for the regional fracture pattern.

ABCD <u>Stereograms of mean joint attitudes from the collapsed blocks</u>

In order to reorient the observed joint attitudes each pole has been rotated four times, the final rotation being only 2° is not clearly visible except where its effect has been exaggerated as in C and D.

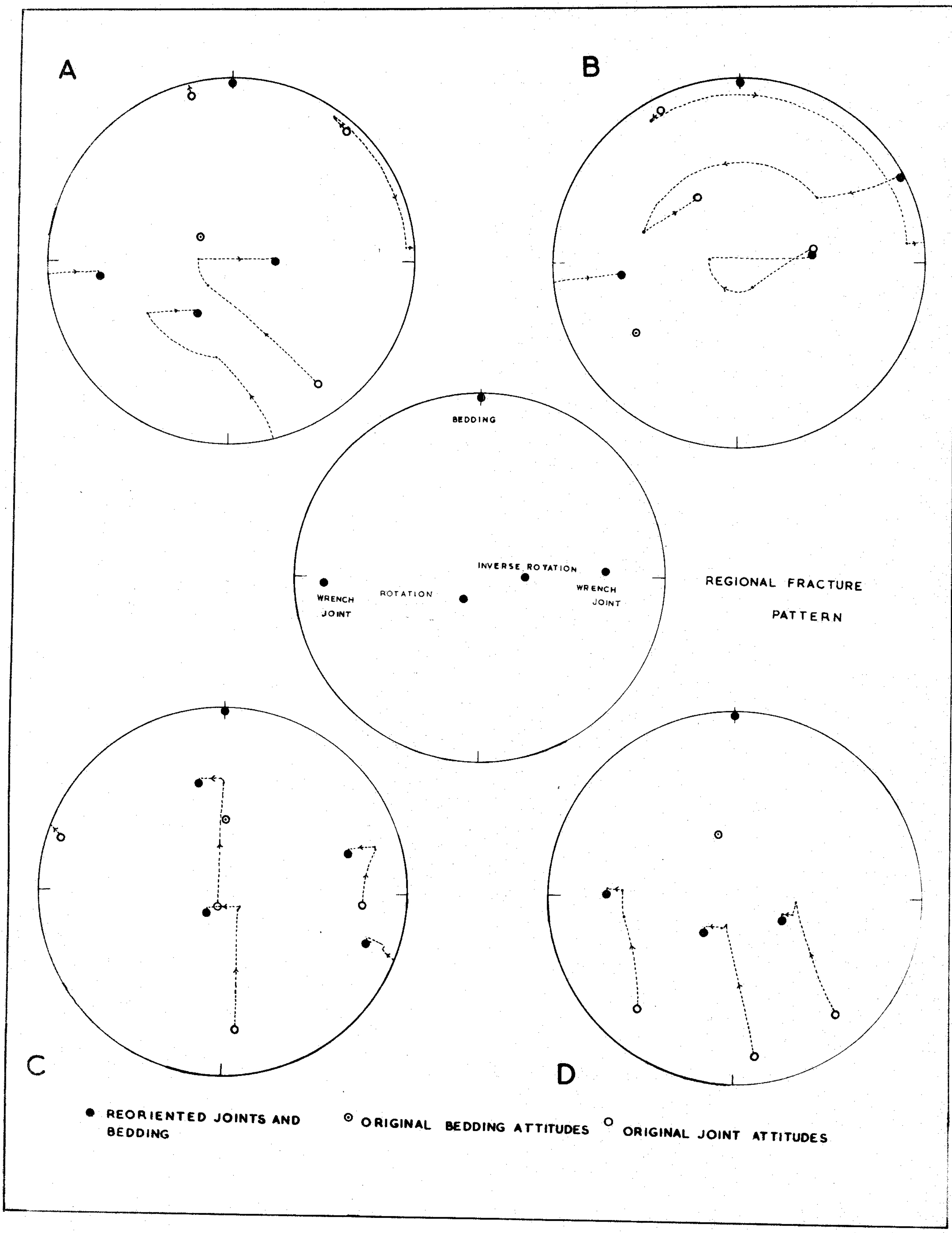
A
B
BEDDING
INVERSE ROTATION
WRENCH
JOINT
ROTATION
WRENCH
JOINT
REGIONAL FRACTURE
PATTERN
C
D
REORIENTED JOINTS AND
BEDDING
ORIGINAL BEDDING ATTITUDES
ORIGINAL JOINT ATTITUDES

Fig. 6.1

Fig. 7.1 IDEAL STRESS FIELDS ON A FOLD

A <u>During the formation of strike shear joints in sub-phase 3</u>

B <u>During the formation of wrench-joints and lens belts in sub-phase 6</u>

C <u>During the formation of wrench faults and joint-shears in sub-phase 5</u>

Within the imaginary bedding units the stress axes are shown unlabelled, the symbolism being indicated on the smaller central diagrams.

Fig. 7.1

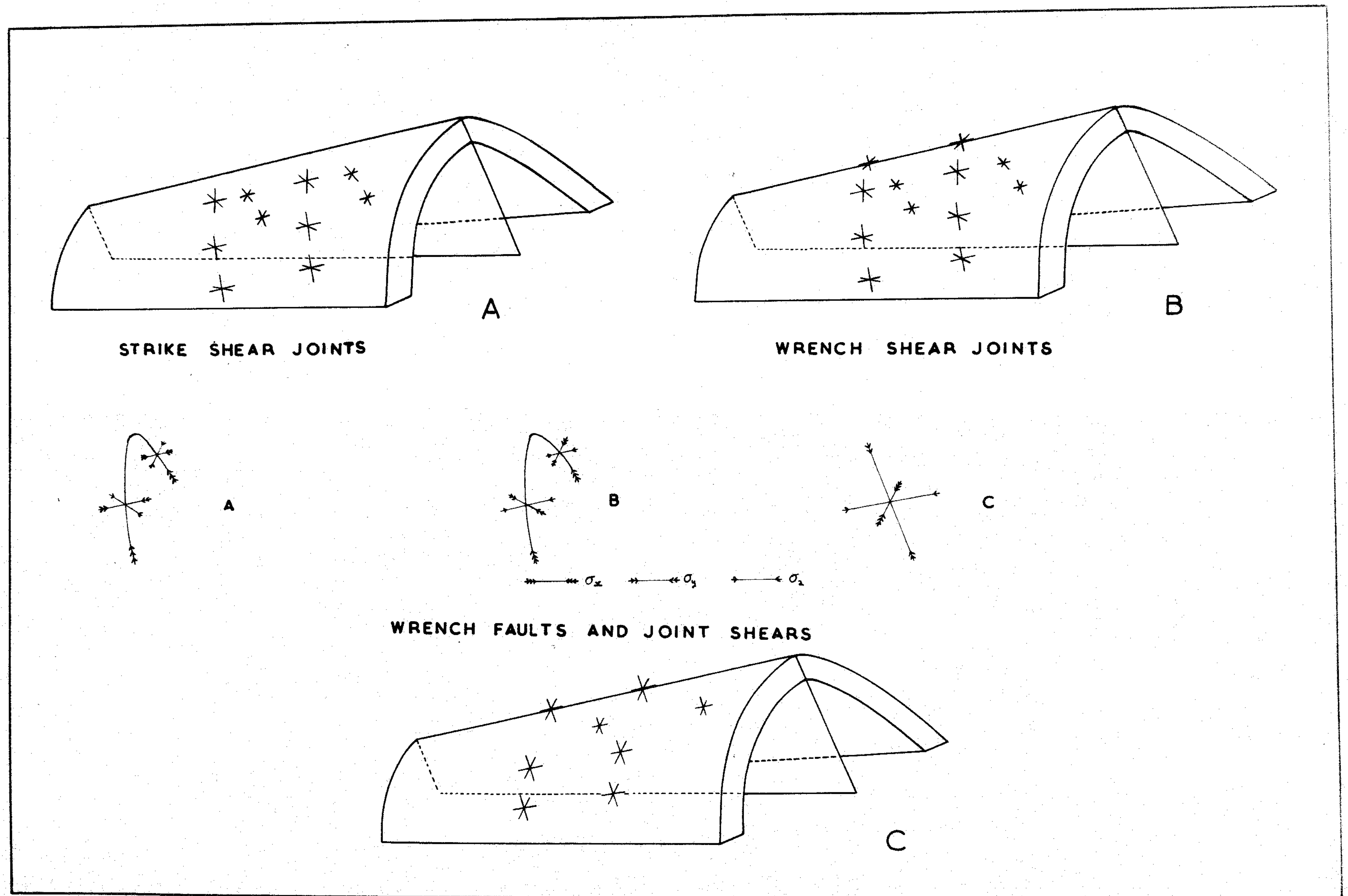
A
STRIKE SHEAR JOINTS
B
WRENCH SHEAR JOINTS
A
B
C
σ_x
σ_y
σ_z
WRENCH FAULTS AND JOINT SHEARS
C

Fig. 7.2 THE OBSERVED ORIENTATIONS OF CERTAIN WRENCH-JOINTS AND STRESS AXES DEDUCED FROM THEM

Mean attitudes of wrench-joints

A Station 9010

Stress axes for three complementary pairs of wrench-joints crossing different buckles. The axial planes and the axes of the buckles shown separately.

B Station 2006

Joints, stress axes, bedding and local fold axis

C Station 2023

Joints, stress axes, bedding and local fold axis

D Station 5012

Joints, stress axes, bedding and local fold axis

E Station 5221

Joints, stress axes, bedding and local fold axis

F Station 9007

Primary and secondary wrench-joints, stress axes, bedding and local fold axis

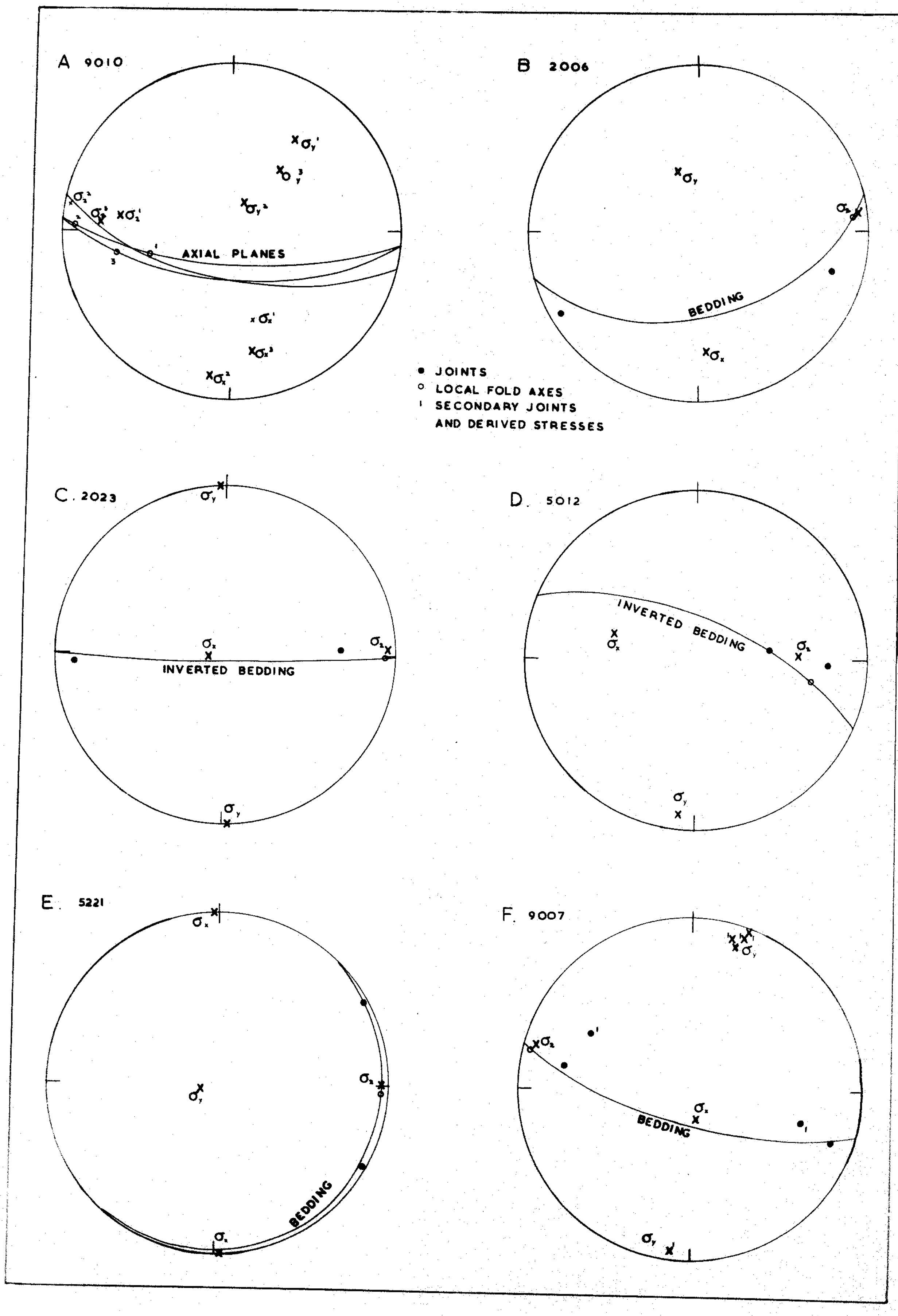
A 9010
AXIAL PLANES
B 2006
BEDDING
JOINTS
LOCAL FOLD AXES
SECONDARY JOINTS
AND DERIVED STRESSES
C. 2023
INVERTED BEDDING
D. 5012
INVERTED BEDDING
E. 5221
BEDDING
F. 9007
BEDDING

Fig. 7.2

Fig. 7.3. REGIONAL STRESS AXIS ORIENTATIONS DURING THE STRIKE SHEAR AND WRENCH JOINT SUB-PHASES

Method of deriving figures described in text.

A All complementary strike shear joints

B Wrench-joints, Lydstep

C Wrench-joints, north Geenala (4001-4008)

D Wrench-joints, Stackpole

E Wrench-joints, south Freshwater West (7015-7070)

F Wrench-joints, West Angle Bay

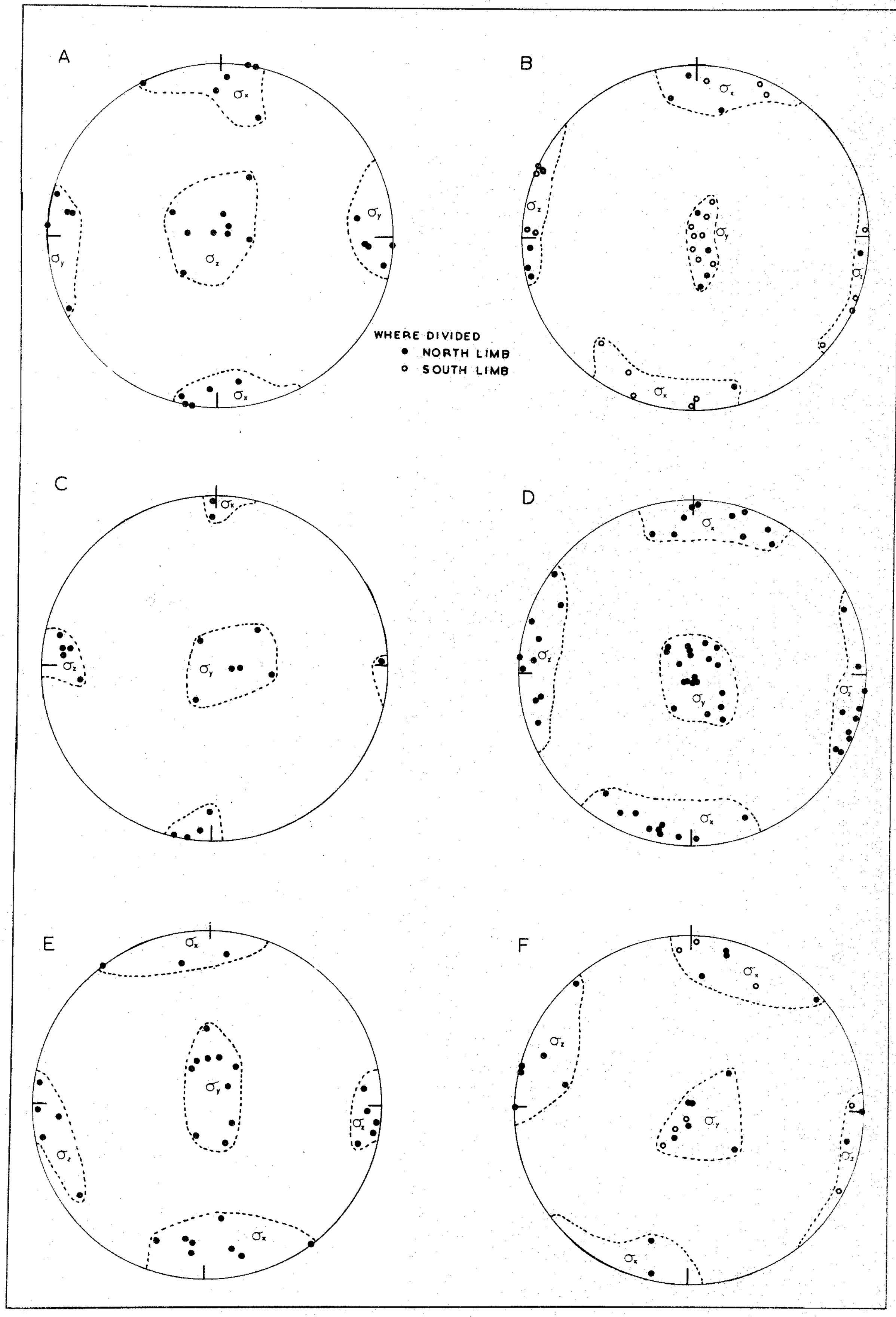
A
B
C
D
E
F
σ_x
σ_y
σ_z
WHERE DIVIDED
• NORTH LIMB
o SOUTH LIMB

Fig. 7.3

Plate 3.1 MURCHISON SYNCLINE Stackpole Quay (5019)
Minor assymetric syncline in C_2S_1 limestones. Axial plane dips north. North limb cut by Thrust parallel to strike shear joints.

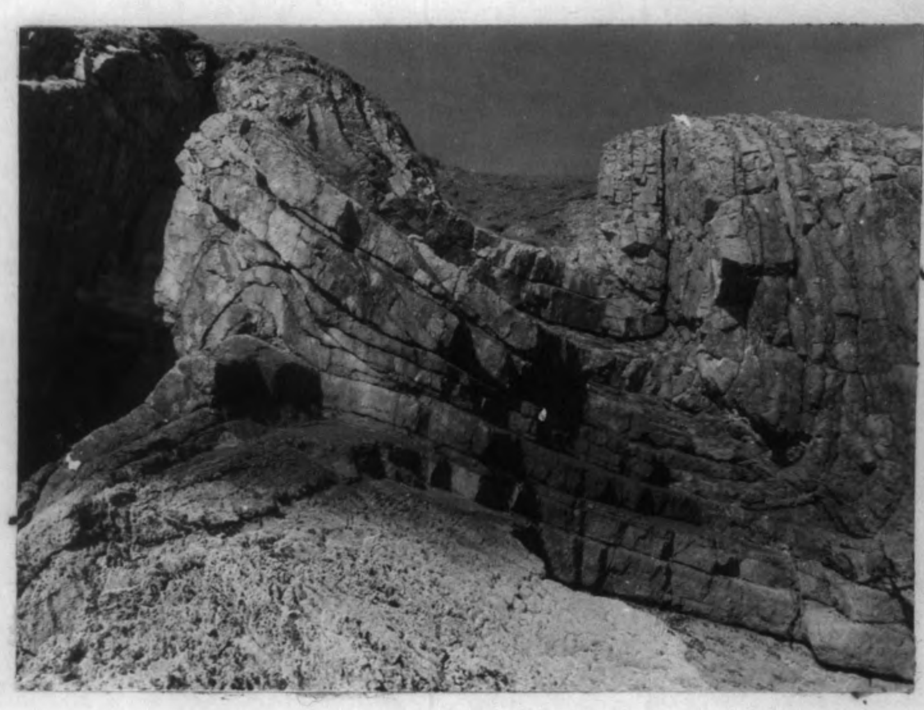

Plate 3.2 LIMB BUCKLE Stackpole Quay (5030)
Assymetric anticline and syncline in C_2S_1 limestones. Axial planes dip north. Strike shear joints cut anticline.

Plate 3.3 LIMB BUCKLE East Bullslaughter Bay
Anticline and syncline with north dipping axial planes in D_1 D_2 limestones.

Plate 3.4 AXIAL BUCKLES West of Greenala Point (4012)
Buckled Castlemartin anticline in Lower Old Red Sandstone. Thrust parallel to strike shears.

Plate 3.5 AXIAL BUCKLES North side West Angle Bay (9010)
Buckles in Z limestones. 'Foreground' syncline rests on scalloped thrust plane. Late wrench joint cuts the steeply plunging fold axis.

Plate 3.6 AXIAL BUCKLES North side West Angle Bay (9008)
Axial buckles in Z limestones dying eastwards (foreground).

Plate 3.7
RIPPLES AND SLATY CLEAVAGE
North side West Angle Bay (100^x W of 9007)
Ripples in sandstone and cleavage in shales. K_2 zone. (Brunton compass for scale)

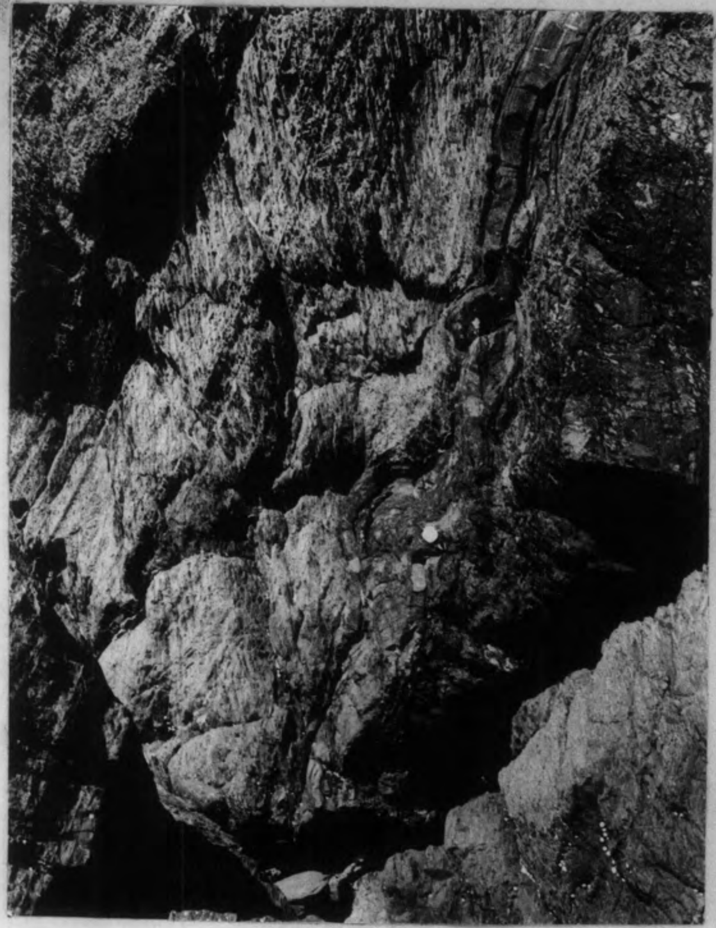

Plate 3.8 FOLD HINGE COMPLICATED BY THRUSTING
South of Babafundle Bay
Buckle and thrust in north dipping D limestones.

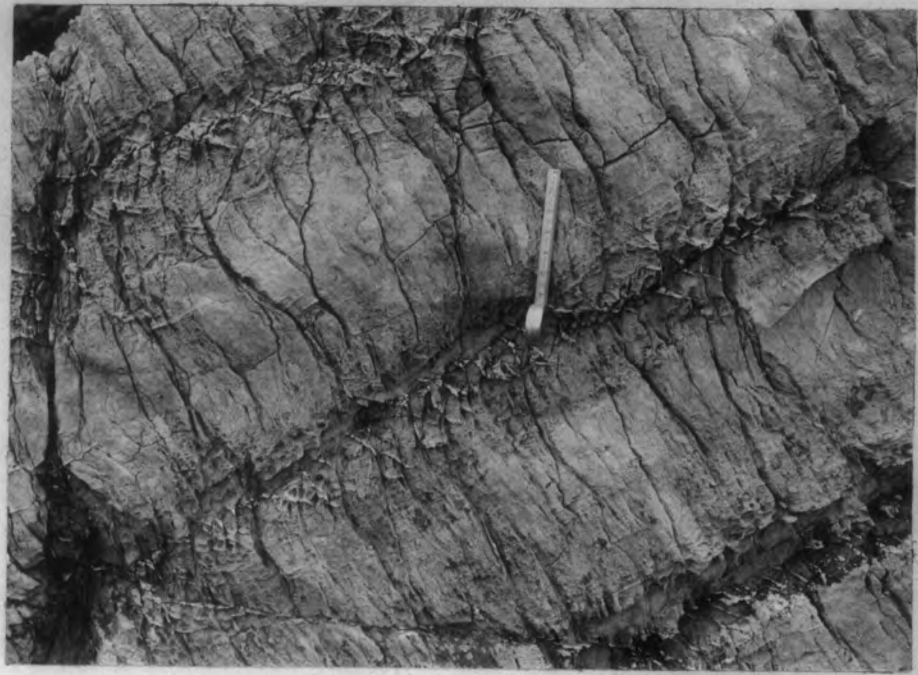

Plate 4.1 FRACTURE CLEAVAGE, TENSION LENSES RELATED TO BEDDING-SLIP AND STRIKE SHEARS N.limb Stackpole Quay anticline (5020)
Deformed cleavage and tension lenses cut by strike shears in C_2S_1 mudstones.

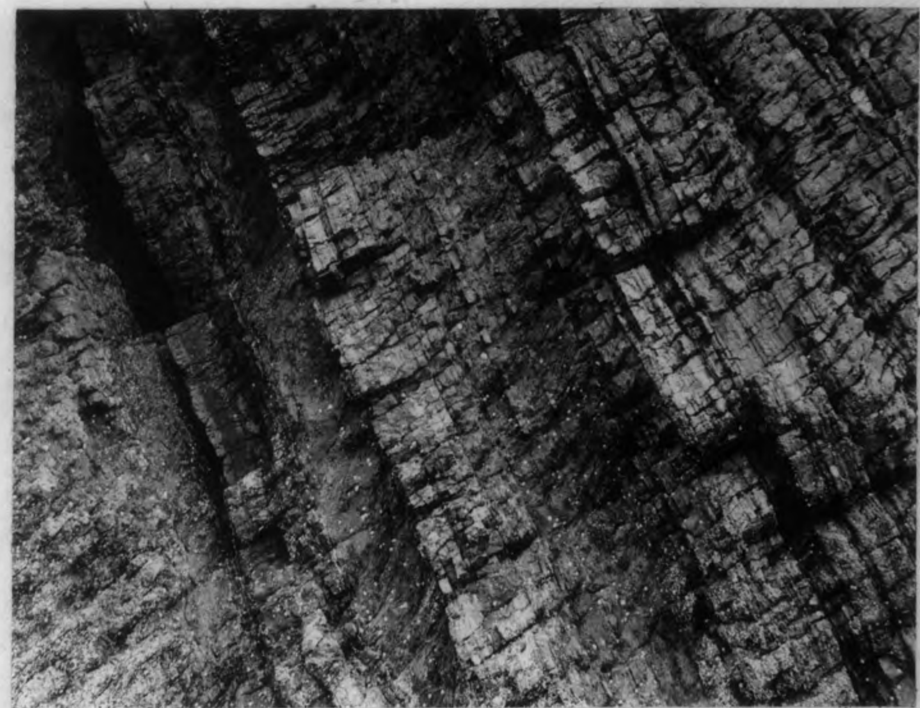

Plate 4.2 ROTATION JOINTS North side, Freshwater East (9003) Rotation joints in sandstones and fracture cleavage in marls. Upper Old Red Sandstone.

Plate 4.3
THRUSTING ON
ROTATION JOINTS
North side, Freshwater East (3016)
Each joint displaces the sandstone band for about one foot. Wide spaced joints in marl. Lower Old Red Sandstone.

Plate 4.4
SLICKENSIDES ON
FRACTURE CLEAVAGE
South limb, Stackpole Quay anticline (5020)
The slickensides are normal to the local fold axis as shown by the bedding-cleavage intersection. C_2S_1 mudstones.

Plate 4.5 FRACTURE CLEAVAGE THRUST AND DOWN DIP DRAG-JOINT Whitedole Bay, Angle cliffs (8013)
Fracture cleavage in Lower Old Red Sandstone marls cut by a down dip drag-joint. One cleavage plane acts as a thrust.

Plate 4.6 INTERSECTION OF BEDDING AND FRACTURE CLEAVAGE Angle cliffs (8002)
Local fold axis trace and two sets of wrench-joints. Lower Old Red Sandstones.

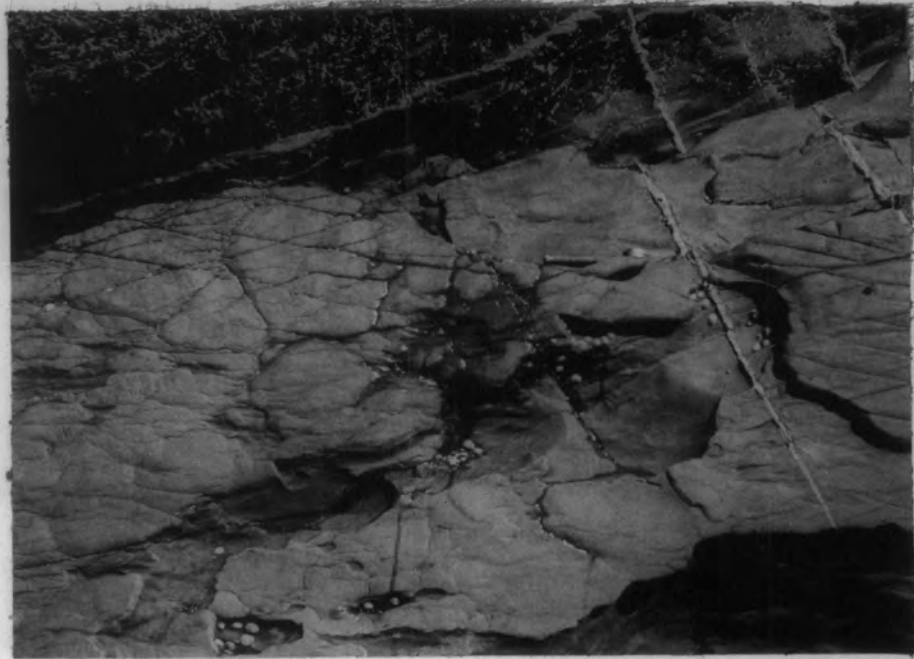

Plate 4.7 ROTATION AND INVERSE ROTATION JOINTS
Castle's Bay, Angle cliffs (8020)
Joints intersect bedding to show local fold axis plunging west (left) and inverse axis plunging east (right). Infilled wrench-joint normal to the fold axis plunge. Lower ORS.

Plate 4.8 TWO SETS OF BEDDING SLICKENSIDES
North of Stackpole Quay (250 yards N.of 5000)
Slickensides in quartz veneers. Lower set related to fold axis, upper set to inverse axis. Lower Old Red Sandstone.

Plate 4.9 'RACE' RODS AND FRACTURE CLEAVAGE CUT BY LOW ANGLE THRUST-JOINTS Little Furzenip (20' E. of 7070) Concretionary rods of limestone in marl parallel to fracture cleavage. Lower Old Red Sandstone.

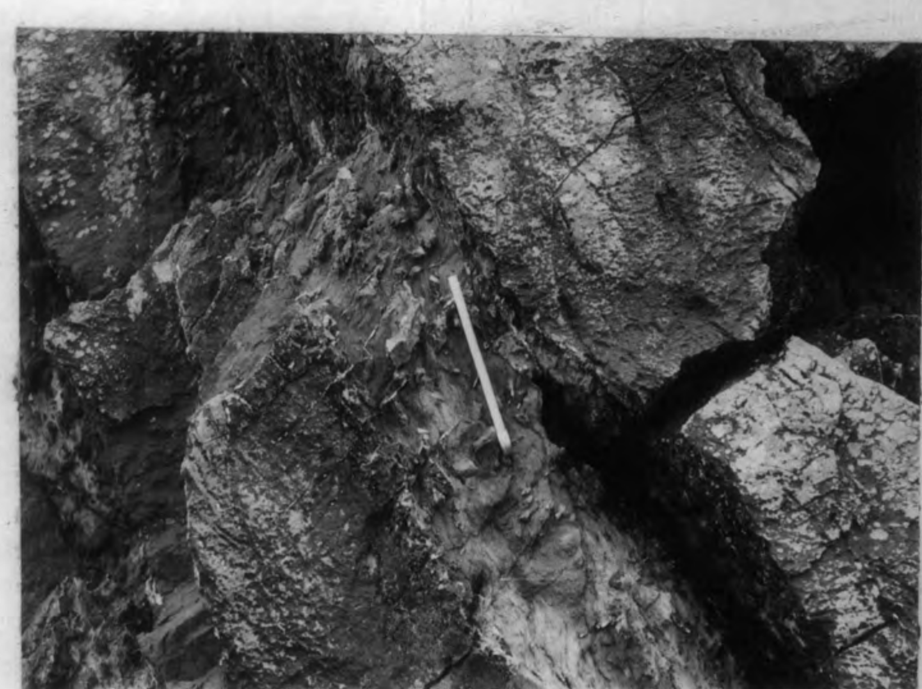

Plate 4.10 LIMESTONE RODS IN MUDSTONE (5019)
C_2S_1 mudstones with limestone rods sub-parallel to the fracture cleavage.

Plate 4.11 DISTORTED 'RACE' RODS North side, Freshwater East (20' W. of 3007)
Concretionary rods sub-horizontal in near vertical Lower Old Red Sandstone marls. (1' rule for scale)

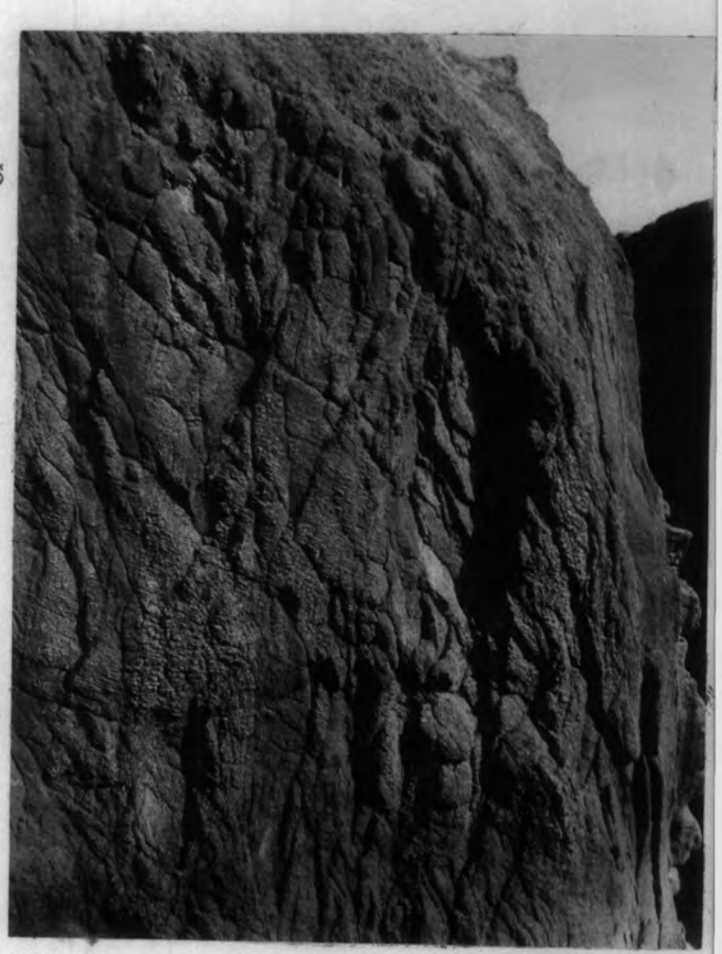

Plate 4.12 CURVING IRREGULAR SHEARS North side, Freshwater East (100' W. of 3013)
Shears cutting 'race' rods and fracture cleavage. Near vertical Lower Old Red Sandstone marls.

Plate 4.13 THRUST North side, West Angle Bay (9012)
K_2 shales thrust over Z limestones, bedding drag below thrust.

Plate 4.14 THRUST Near East Pickard Bay (8001)
Minor thrust displacing a sandstone band 6 feet in the Lower Old Red Sandstone. Thrust cuts fracture cleavage and irregular shears of sub-phase 2.

Plate 4.15 STRIKE SHEAR JOINTS AND ROTATION JOINTS
Freshwater West (7063)
Complementary strike shear joints cutting rotation joints in the Ridgeway Conglomerate.

Plate 4.16 STRIKE SHEAR JOINTS AND A DOWN DIP DRAG ZONE
Freshwater West (7015)
Strike joints and fracture cleavage cut by a low angle down dip drag zone. Z limestones.

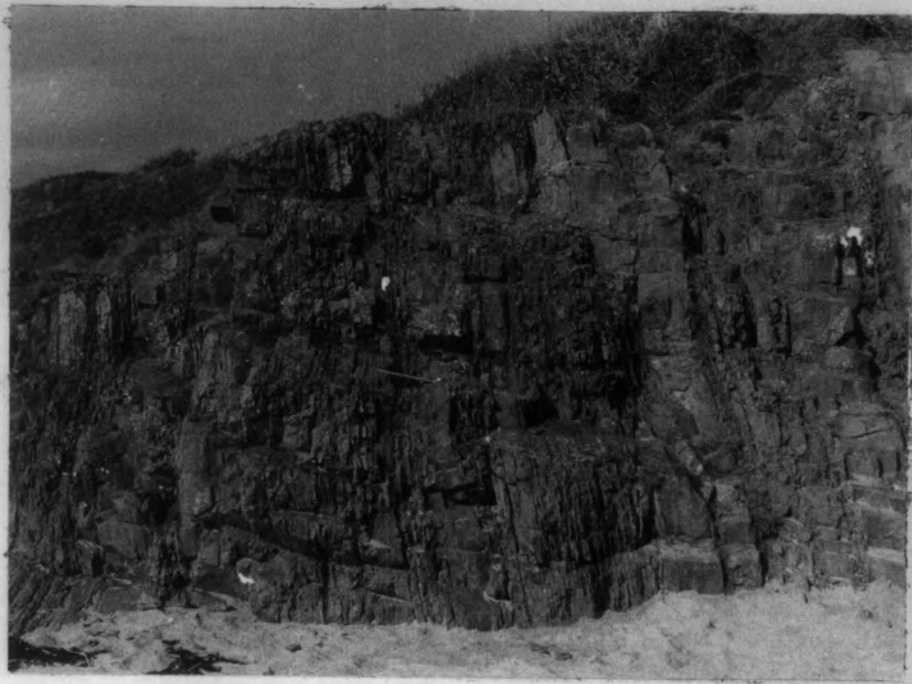

Plate 4.17 THRUST-JOINTS
North side, Freshwater East (3001)
Oblique thrust-joints in Ludlovian mudstones.

Plate 4.18 DOWN DIP DRAG ZONE AND WRENCH-JOINTS
Freshwater West (7016)
Down dip drag flexure crossing Z limestone bedding planes. Near vertical wrench-joints.

Plate 5.1 MINOR WRENCH FAULTS Little Furzenip (7070)
Dextral faults displacing Lower Old Red Sandstone marls and sandstones. Scale.foot rule.

Plate 5.2 FAULT GOUGE AND ANTITHETIC SHEAR JOINTS
Stackpole Quay fault at Stackpole Quay.
To left (west) of fault bedding and fracture cleavage planes are exposed on antithetic shear joints. C_2S_1 mudstones.

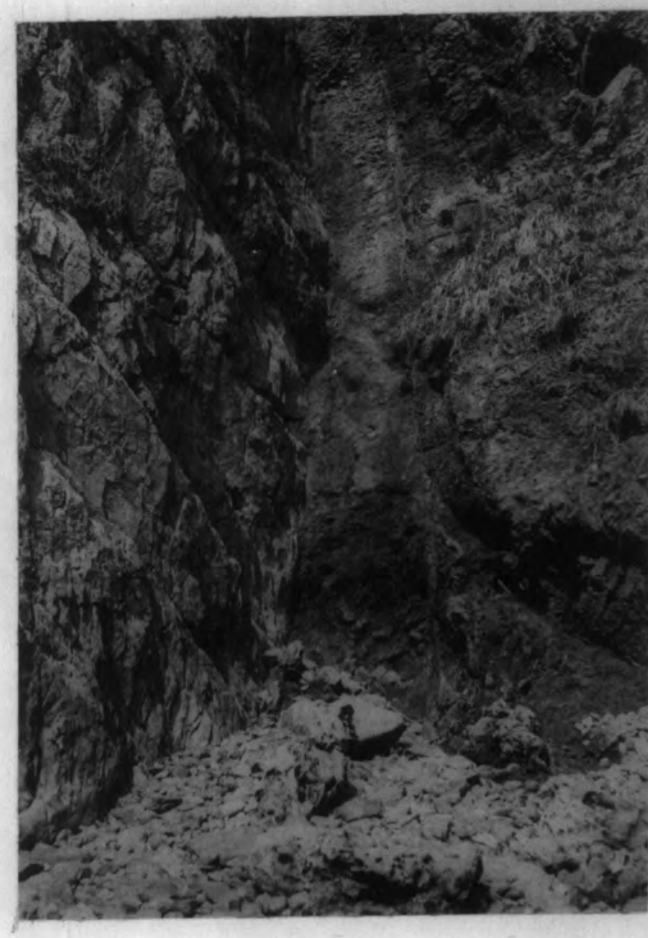

Plate 5.3 DEXTRAL WRENCH FAULT AND A PARALLEL LENS BELT
South side of Lydstep Haven (2017)
Eroded fault cutting overturned D_1 limestones
Lens belt to right (east) of fault.

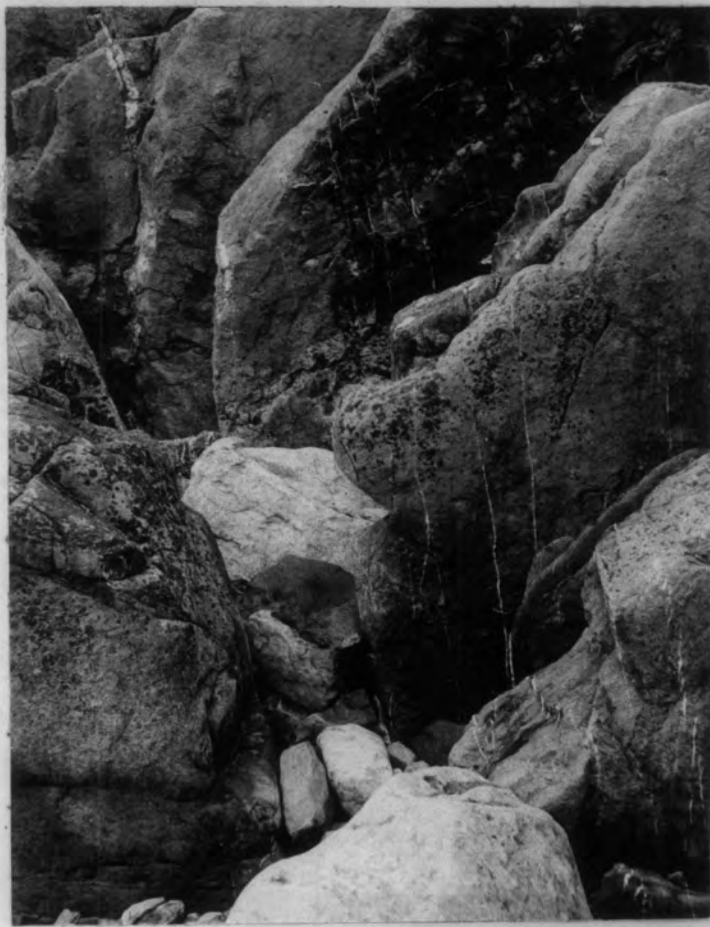

Plate 5.4 THRUST COMPONENT OF A WRENCH FAULT
North side of Freshwater East (3013)
Thrust plane dips north cutting Lower Old Red Sandstone marls with 'race' rods.

Plate 5.5 JOINT-SHEARS Little Furzenip (7070)
Major plane picked out by the trend of the en echelon antithetic joints. Lower Old Red Sandstone. Scale - foot rule

Plate 5.6 PARALLEL JOINT-SHEAR AND WRENCH-JOINT SETS
Greenala Point (4006)
Complementary shear planes cutting near horizontal Lower Old Red Sandstone rocks. Antithetic joints splay off a majot joint in the left middle-ground.

Plate 5.7 JOINT-DRAG CUTTING A THRUST
Angle Cliffs (8001)
Jøint-drag distorts fracture cleavage in Lower Old Red Sandstone marls. Drag continues undisplaced across eroded thrust plane. Scale - foot rule

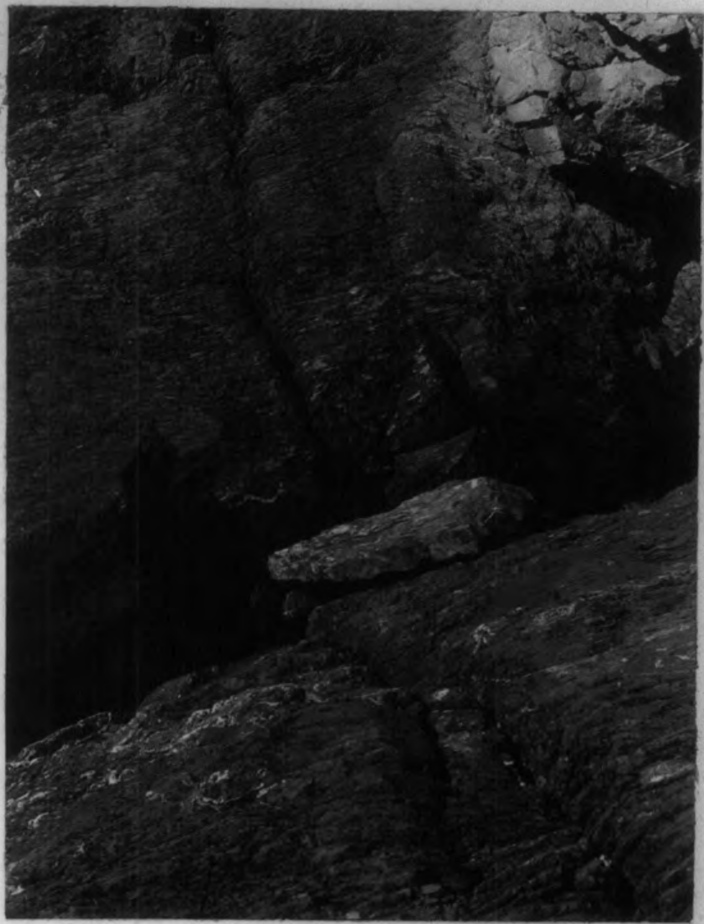

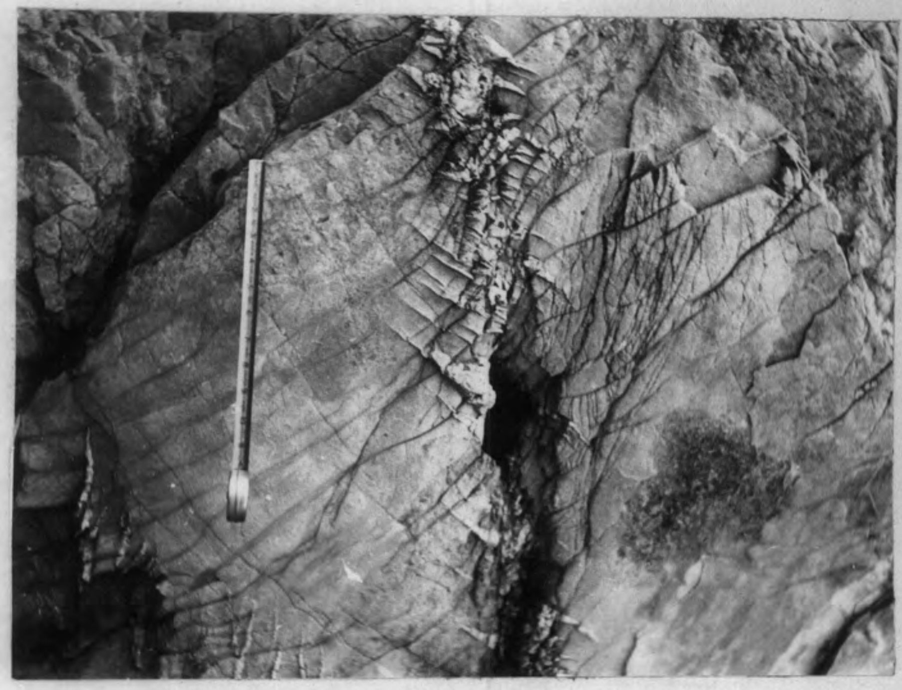

Plate 5.8 TENSION LENSES AND ROTATION JOINTS DISTORTED IN THE SHEAR ZONES OF COMPLEMENTARY LENS BELTS
Great Furzenip (7061)
Structures exposed on a near vertical bedding undersurface of Upper Old Red Sandstone quartzite. Scale - foot rule.

Plate 5.9 COMPLEMENTARY LENS BELTS AND WRENCH-JOINTS
North side of Lydstep Haven (2005)
Structures exposed on a bedding plane of southerly dipping S_2 limestone. The trace of the rotation joints on the bedding is near horizontal.

Plate 5.10 COMPLEMENTARY LENS BELTS SLIGHTLY DISTORTING ROTATION JOINTS
Great Furzenip (7030)
Structures exposed on a steeply dipping bedding plane of Upper Old Red Sandstone. Rotation joints trace as fine near horizontal lines on the bedding surface.

Plate 5.11 COMPLEMENTARY PRIMARY WRENCH-JOINTS
North side of Freshwater East (3003)
Steeply dipping wrench-joints lie symmetrically about the traces of the rotation joints (plunging gently left) on the vertical bedding planes of Lower Old Red Sandstone marls.

Plate 5.12 PRIMARY AND SECONDARY WRENCH-JOINTS
North side of West Angle Bay (9002)
Eroded gap is a fault. The primary joints dip left (west) or are vertical, the secondary joints dip to the right. Lower Old Red Sandstone.

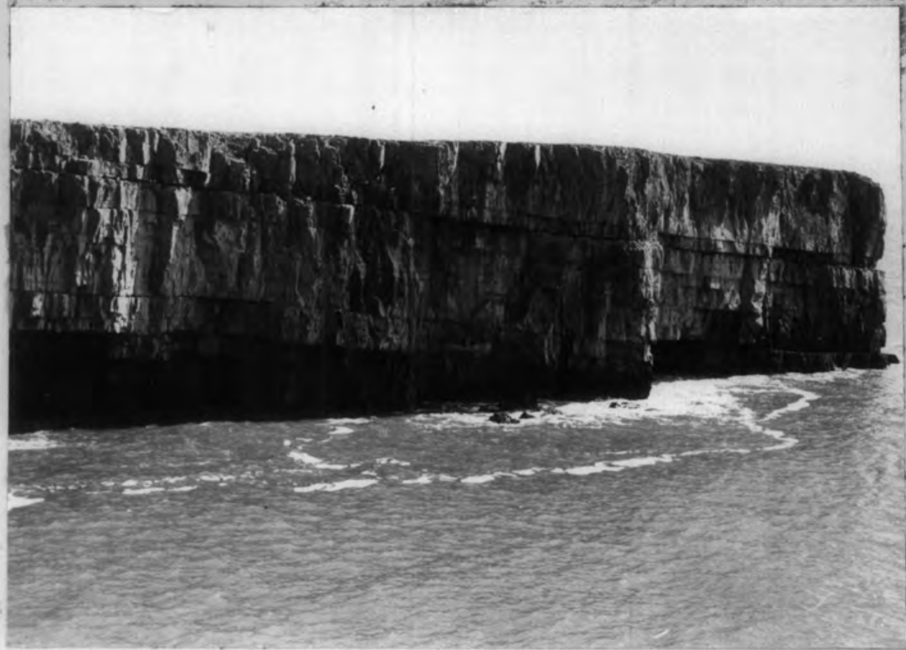

Plate 5.13 NEAR VERTICAL WRENCH-JOINTS AND ROTATION JOINTS IN SHALLOW DIPPING BEDS
Stackpole Head
D_1 limestones. Note structures terminating abruptly at erosion platform.

Plate 5.14 COMPLEMENTARY WRENCH-JOINTS NEAR A FOLD CREST
S.limb, Stackpole Quay anticline.
(5020)
Planes tilted relative to the fold axis (intersection of near vertical bedding with shallow dipping fracture cleavage)
C_2S_1 mudstones.

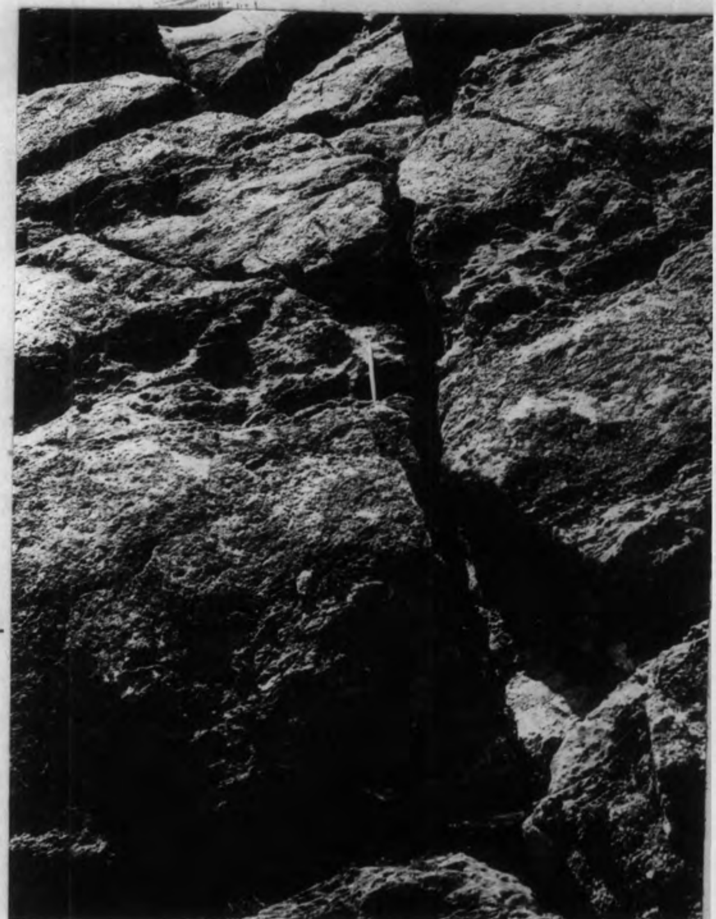

Plate 5.15 'JOINT-SHEAR' OF THE WRENCH-JOINT SUB-PHASE
Angle Cliffs (8004)
Major plane dips into the foreground, antithetic splays dip right, intersecting the cleavage (dipping left) in the plane of the major fracture. Lower Old Red Sandstone. Scale - foot rule.

Plate 5.16 SECONDARY WRENCH-JOINT-DRAG
North side of West Angle Bay (9003)
Drag thrusts near horizontal rotation joints. Other wrench-joints dip left on the bedding plane. Upper Old Red Sandstone. Scale-foot rule.

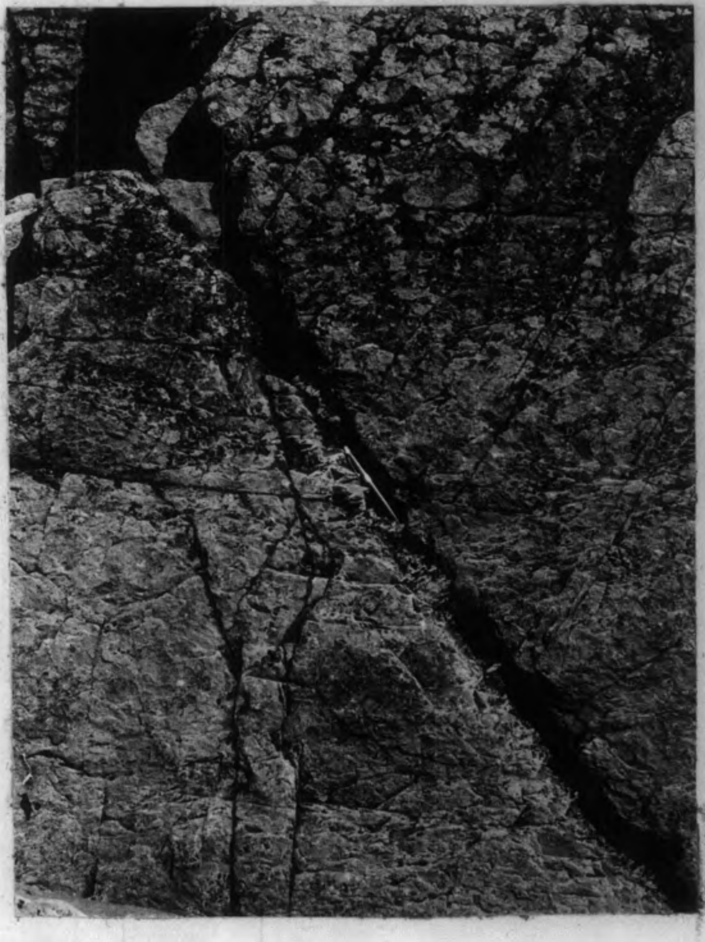

Plate 5.17 VEINED LENS BELT SHEAR PLANE
South Freshwater West (7062)
Infilled shear plane dips left (west), lenses near vertical. Structures exposed on a steeply dipping Upper Old Red Sandstone bedding plane. Scale - florin (bottom right)

Plate 5.18 UNSYSTEMATICALLY DISTORTED VEINS INFILLING WRENCH-JOINT PLANES Little Furzenip (7070)
Large central vein is both thrust and normally faulted along steeply dipping bedding planes. Veins die out in marl (left). Lower Old Red Sandstone. Scale - foot rule.

Plate 6.1 TRIASSIC COLLAPSE BRECCIA Lydstep Point (2022) Large collapsed blocks of S_2 limestone overlain in the foreground by a raised beach deposit breccia.

Plate 6.2 TRIASSIC COLLAPSE BRECCIA Stackpole Warren Chaotic blocks of D_1 limestone set in a red marly matrix.

Plate 6.3
FAULT CUTTING
TRIASSIC BRECCIA
Lydstep Point
(2022)
A fault with its own breccia cutting chaotic blocks of D_1 limestone. The fault dies out lower in the cliff.

Plate 6.4
WRENCH JOINT
INFILLED WITH
TRIASSIC BRECCIA
Saddle Point
(100^x E of 5071)
An infilled N-S joint resembling fault gouge.